Evaluation of Shoreline Changes with Improved One-line Numerical Shoreline Modelling

June 23, 2023

Sonnemans, R.C.

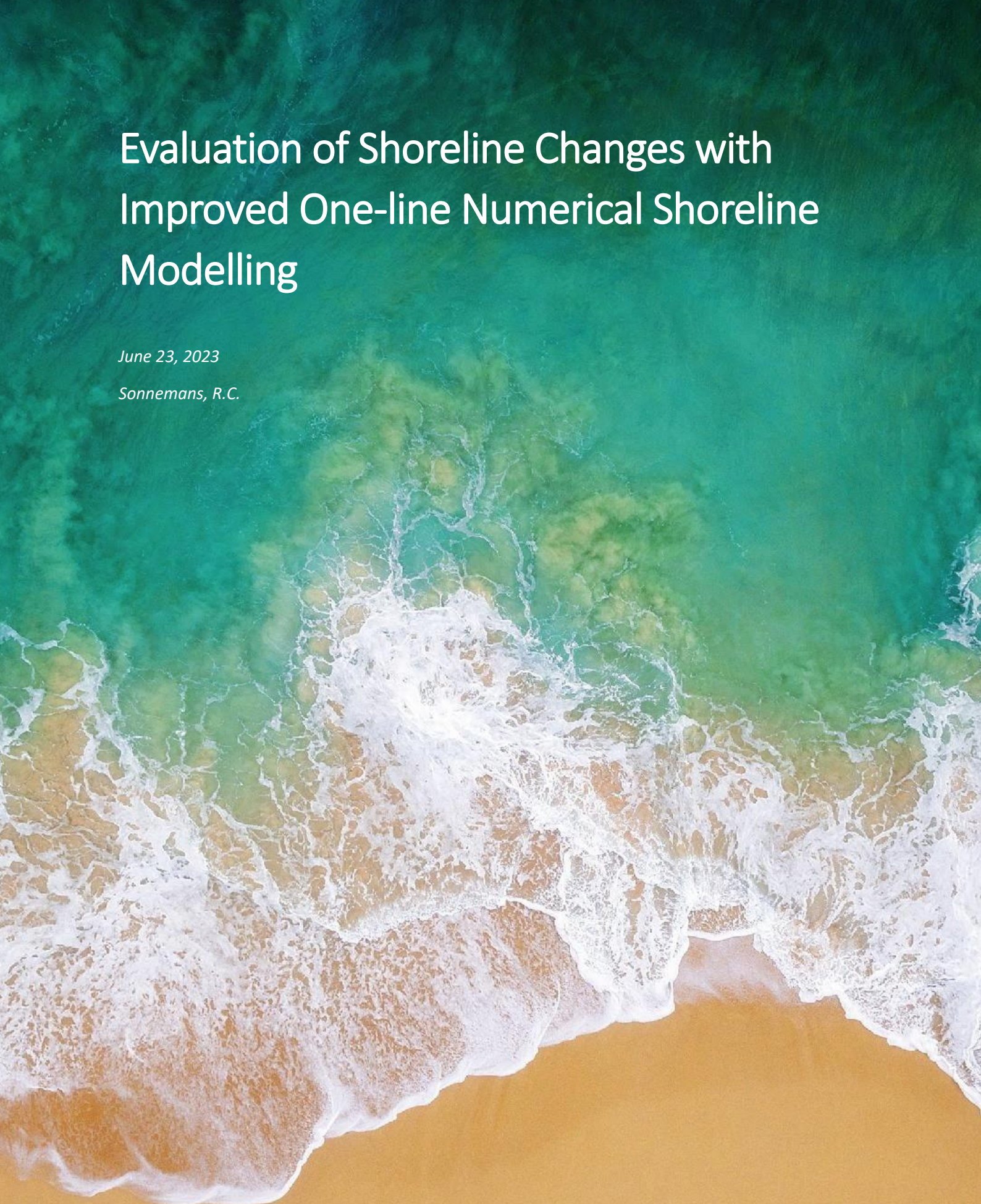

IMDC

UNIVERSITY OF TWENTE.

Colophon

Title	Evaluation of Shoreline Changes with Improved One-line Numerical Shoreline Modelling
Version	Final
Research period	April – June 2023

Author	R.C. (Rowan Ceri) Sonnemans
Student number	S2603322
E-mail	r.c.sonnemans@student.utwente.nl
University supervisor	Ir. Jos Mullers
Second assessor	Drs. Ing. J. Boes
External company	IMDC (International Marine & Dredging Consultants)
Company Supervisors	Dr. Arash Bakhtiari
	Ir. Jaap de Groot

Preface

In this report, I will present the findings of my bachelor thesis “Evaluation of Shoreline Changes with Improved One-Line Numerical Shoreline Modelling”. This thesis is the final part of my Civil Engineering bachelor program at the University of Twente and has been performed in collaboration with International Marine & Dredging Consultants (IMDC).

In the ten weeks that I got to work with IMDC, I learned a lot in the field of coastal processes/engineering. Since I want to pursue my interest and continue my studies in the master field of ‘river and coastal processes’, I thank IMDC for the opportunity to introduce myself to this field of engineering. ShorelineS is a model that is in development and has the capability of becoming a mainstream coastal engineering tool in the near future. I feel lucky to have had the possibility to try this model in its early stages for myself for the purposes of this thesis. IMDC was also kind enough to let me come to the office in Antwerp and experience what a day in the office life is like for them. I talked with some colleagues and I liked how open and accepting they were to a bachelor student suddenly appearing in their office.

I would also like to give my thanks to my external supervisor at IMDC, Arash Bakhtiari who helped me with the research and assisted me during the ten weeks. I would also like to thank Jaap de Groot for keeping in touch with me in the first place after I reached out to him for a possibility to do my bachelor thesis with IMDC. Finally, I would also like to give a thanks to Jos Muller, who was my internal supervisor from the University and was a really inspiring and personal supervisor to me. Because everyone who I have had the opportunity to work with over the ten weeks of my research, were also very busy themselves, I would like to thank all supervisor again for their effort. The effort they put in to supervise me next to their schedules and allow me this opportunity of doing my bachelor thesis in coastal engineering.

To conclude, I hope you will enjoy the reading of my thesis. If you have any questions, you can contact me via the contact info in the colophon.

Rowan Ceri Sonnemans

June 23rd, 2023, Enschede

Abstract

ShorelineS I is a newly developed model that aims at becoming a verified engineering tool that is easy to use and widely applicable for coastal engineers in the near future. By the adaptation of a vector-based grid, and recent improvements that include wave diffraction, ShorelineS has become more accurate in most cases. However, emerged detached breakwaters have remained notoriously difficult for N-line models to simulate properly especially after the case of beaches that connect with the structure.

The objective of this research was to "assess different input parameters impacts on shoreline sensitivity in a detached breakwater case study and suggest improvements for one-line numerical shoreline change models". Therefore, in this thesis, the one-line numerical shoreline change model ShorelineS was first subjected to a sensitivity analysis in for 5 different cases with a detached breakwater where the wave angle and breakwater characteristics were varied. Here, it was found that the use of the Kamphuis longshore transport formulas greatly increased the simulation time. Additionally, the wave height is the most sensitive parameter for the evolution speed of the shoreline. An increase in mean bed slope shifted the shoreline evolution more sideways towards the updrift side. The median grain size showed large differences in sensitivity between the erosion and accretion side of the shoreline.

Second, validation tests were performed and the model equilibrium state was compared with the shoreline equilibrium suggested by a spiral bay solution. The validation tests showed the model to predict the salient parameters accurately while tombolos are generally too wide. Especially, near the breakwater dimensionless length boundary condition between a salient or a tombolo, the model was not able to accurately predict the shoreline shape suggested by analytical solutions. The spiral bay solution also showed that the model severely overestimated the static equilibrium shape while subjected to a wave angle.

Finally, a first effort was made to implement material exchange between the beach berm and the foreshore bars. This implementation has not been finalized and calibrated due to research constraints. However, the initial test results show a little difference with the original model that suggest that it could have some influence in the final result. It is envisioned that this difference may be greater once the model would also be subjected to seasonally changing wave heights and a dynamic boundary for the bar volumes.

Table of Contents

Title page image sourced from Pinterest (starrpictures, 2023).

List of figures

List of tables

List of Symbols

y	Cartesian y-coordinate
t	Time [s]
D_B	Berm height [m]
D_C	Closure depth [m]
Q	Longshore transport [m^3/s]
x	Cartesian x-coordinate
b_1	CERC-coefficient [-]
H	Wave height [m]
φ	Wave angle [°]
K_2	CERC calibration coefficient [-]
T	Wave period [s]
m_b	Mean bed slope in the breaking zone [-]
d_{50}	Median sediment grain size [m]
K_{swell}	Wave period influence parameter [-]
V_{total}	Parameter to account for additional velocities by tide and wide [m/s]
k	Default CERC calibration coefficient according to U.S.A.C.E. [-]
g	Gravitational acceleration [m/s^2]
ρ	Density [kg/m^3]
p	Porosity [-]
γ	Breaker index [-]
p_{swell}	percentage of total wave height with low-period swell wave heights. [-]
V_{wave}	Average wave velocity [m/s]
p_1/p_2	percentage of time in which positive and negative flow respectively are present [-]
V_1/V_2	representative velocities for positive and negative flows respectively [m/s]
n	Cross-shore coordinate
s	Longshore coordinate
β	Mean bed slope [°]
$RSLR$	Relative sea level rise [m/yr]
L_i	Grid element length [m]
K_d	Diffraction coefficient [-]
θ	Angle relative to a control line [°]
A	Equilibrium profile scale factor [-]
h	Water depth [m]
V_B	Bar volume [m^3]
V_{BE}	Equilibrium bar volume [m^3]
λ	Bar volume growth rate coefficient [-]
λ_0	Bar volume growth rate calibration parameter [-]
w	Sediment fall speed [m/s]
L_0	Deepwater wave length [m]
m	Calibration coefficient [-]
L_B	Breakwater length [m]
X	Breakwater offshore distance [m]
X_{80}	Surf-zone width [m]
L_B^*	Dimensionless breakwater length [-]
X^*	Dimensionless breakwater distance [-]
L_G	Length of gap between consecutive breakwaters [m]
R	Length of control line R [m]
R_0	Length of control line R at angle β_R [m]
$C_0/C_1/C_2$	Spiral bay coefficient dependent on β_R [-]
β_R	Angle of control line R_0 relative to the predominant wave crest [°]

1. Introduction

1.1. Study background

This research report is written as a bachelor thesis assignment for the study of Civil Engineering at the University of Twente and performed externally under supervision of IMDC (International Marine and Dredging Consultants), Antwerp.

1.2. Problem statement

A concise problem statement will be defined based on the introduction to the world of coastline change modelling and the context of the research that will be done in collaboration with IMDC.

As a coastline change model, the one-line numerical model 'ShorelineS' provides a promising approach to the efficient modelling of long-term shoreline evolution. The model can account for swells, sea level rise, tidal movements and wave refraction effects to some degree. However, in one-line numerical shoreline models like ShorelineS, so-called bulk longshore transport formulas are used and cross-shore transport is not explicitly accounted for. While recognizing the significant influence of seasonal changes on long-term evolution of shorelines, often, they are not included. An important advancement would be to integrate key attributes of seasonal cross-shore variations into a shoreline response model designed for engineering applications, thereby addressing a limitation of existing one-line models (Hanson & Larson, 1998).

Accurate computation of specific phenomena in cross-shore material exchange requires compatible scales. Consequently, not all cross-shore phenomena are relevant for modelling shoreline evolution on monthly to century scales (Larson & Kraus, 1995). Nevertheless, transport processes operating within corresponding time and space scales should be incorporated in these models.

1.3. Research objective and scope

The research objective aims to solve the problem as stated in the problem statement section 1.2.

The objective of this study is to: "Assess different input parameters impacts on shoreline sensitivity in a detached breakwater case study and suggest improvements for one-line numerical shoreline change models"

Research scope

The research will be limited to ShorelineS as the one-line numerical shoreline change model in which a model improvement will be implemented and a single emerged detached breakwater is assessed. A simple case study model with a single emerged detached breakwater will be made to assess the implementation of transport improvement effects in ShorelineS which will be the spatial scope of the research. The scope of the case study will be limited to two scenarios; a salient and a tombolo detached breakwater. A limited time scale will be used over which the coastline change is modelled in the sensitivity analysis due to available research time and computational constraints. Therefore also, the sensitivity analysis on the input parameters in the case of a detached breakwater will be limited to the most likely sensitive parameters. These parameters will be selected by consultation with a shoreline numerical modelling expert and should also provide a good representation of different types of parameters in the model.

The implemented improvement of the model should conform to be compatible from monthly to centennial time scales and one-line numerical models. Following a storm, the incoming waves may bring deposited sand in the form of bars back to the berm, recovering the damage caused by the

storm on the foreshore and seaward portion of the berm. If the bar develops in deeper water, where the wave action is small during normal conditions, the onshore transport from the bar to the berm occurs at a low rate, implying a slow recovery of the berm. This recovery could take substantial time, or could even cause permanent changes to the system. Therefore, an effort will be made to represent cross-shore transport effects by implementing material exchange between the berm and the bar.

1.4. Research questions

To achieve the research objective within the scope as stated in section 1.3, the study will address the following three research questions;

1. **What is the impact of different parameters in ShorelineS on the shoreline evolutions, particularly in the case of detached breakwater scenarios?**
2. **How does the one-line model perform in predicting shoreline evolution shapes in simple detached breakwater case scenarios?**
3. **How to account for cross-shore sediment transport in a one-line shoreline change model?**

1.5. Research methods

The first research question regarding the impact of different parameters in ShorelineS will be answered by means of a sensitivity analysis on the model output. The model output is quantified in shoreline shape parameters that will be determined in consultation with a modelling expert from IMDC. The output is also drawn as shoreline contours after a set timeframe. These parameters will then be subject to preliminary simulations to determine the parameters that are most sensitive. The most sensitive parameters will then be assessed in more detail. The sensitivity analysis is performed first to set a baseline for future research and testing in the model. Additionally, it will be used to determine the impact of the input parameters on the shape of the shoreline which can then be taken into account in the following research questions if necessary.

The second research question regarding the numerical one-line model performance in detached breakwater scenarios will be answered using several different single detached breakwater setups in the model. For these setups it will first be determined how much simulation time is required to reach a static equilibrium in the model. Then, this static equilibrium will be compared to analytical solutions well-known and accepted by coastal engineers. This can also be used as a baseline test for further developments and different model setups.

The third research question regarding cross-shore transport in a one-line numerical shoreline model will be answered by means of a literature study and an initial model test. This test will indicate whether it would be a viable option to include cross-shore sediment transport in this one-line model and what further improvements to the one-line model could be recommended.

1.6. Report outline

The aim of this proposed research is to evaluate shoreline changes of an improved one-line numerical model for the case of a simple emerged detached breakwater. First, a literature review is presented in chapter two. Chapter three will explain the methodology that will be used to answer the research questions as formulated in section 1.4. Chapter four presents the results of the methodology and answers to the research questions. Then follows the discussion in chapter 5. The conclusion of the report is given in chapter six. Finally, recommendations are given for further research in chapter seven. In the appendix, all other results from the methodology that are not clearly presented in the results are provided.

2. Literature review

In this chapter, the required context to one-line shoreline models is given by means of a literature study. The goal of this literature study is to help to understand where the particular case of ShorelineS as a newly developed one-line shoreline model. This includes where it is currently situated in the context of one-line numerical modelling in general, the differences and innovations it proposes and possible drawbacks of one-line shoreline models. This can then be taken into account when reasoning why the model behaves in a certain manner and to construct suiting recommendations. Additionally, the literature research is used to find analytical solutions to be used to answer research question 2.

2.1. One-line numerical modelling and ShorelineS

The newly developed one-line numerical model of ShorelineS is built slightly different than the commonly found one-line models thus far. In this section, the literature research will focus on common one-line models and how they operate. Then, the ShorelineS model structure and implemented functions will be elaborated upon.

2.1.1. One-line numerical modelling

Engineers have traditionally analysed and predicted long-term shoreline evolution using various methods that include extrapolation and analysis of historical shoreline positions, models based on sediment conservation (also known as one-line models), morphodynamic numerical models and process-based models. Historical analysis is suitable for characterizing change but does not assess potential future changes in a system. Process-based models are more suited for localized analysis due to challenges with scaling from the model to the field. Morphodynamic models on the other hand are not well-suited for large time scales due to their computational requirements. Therefore, when examining long-term changes resulting from natural or human-induced alterations in a beach system, one-line models have remained the preferred option (Thomas & Frey, 2013).

The principle of one-line modelling is that beaches maintain their slope on average over time due to the conservation of sediment, assuming adequate sand-supply. While one-line models recognize that severe storms have the possibility of causing large changes to the shoreline transact, these tend to be temporary and the overall profile remains relatively constant. Similarly, the beach slope experience negligible variation as the shoreline advances or retreats over extended time periods (Frey, et al., 2012; Hanson, 2023). Additional assumptions of one-line models, as noted by Thomas & Frey (2013), include:

- Shoreward and seaward vertical limits of the profile like depth of closure (D_C) are constant
- Breaking waves and longshore currents are the main drivers of sediment transport.
- Detailed nearshore circulation structure like rip currents is ignored
- Long-term trend exists in shoreline evolution

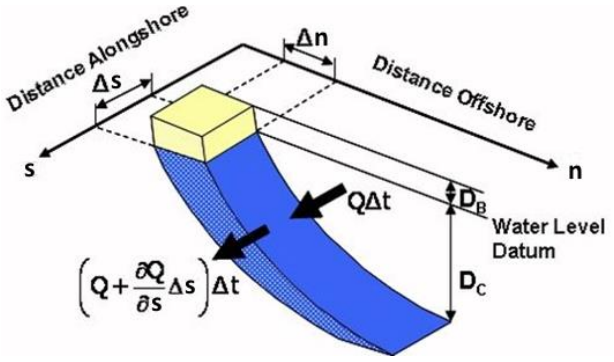

Figure 1: Definition sketch for shoreline change calculation in one-line models (Hanson, 2023).

In one-line models, profile movement and sediment transport is restricted within the active profile height ($D_B + D_C$) as shown in figure 1. This restriction provides the easiest way of computing

shoreline change by evaluating the change of volume within the perimeter. Then, the governing equation (1) for the rate of change for the shoreline as modelled in figure 1 would be:

$$\frac{\Delta \mathrm{n}}{\Delta \mathrm{t}} = \frac{1}{(D_B + D_C)} \frac{\Delta \mathrm{Q}}{\Delta \mathrm{s}} = 0 \quad (1)$$

Limitations of one-line numerical modelling

The assumption of long-term unchanged shore profile up to a constant depth of closure (D_C) becomes invalid when extreme or strong storms change the profile shape which take a long time to recover. Therefore, also influencing the long-term shoreline evolution (Thomas & Frey, 2013).

Additionally, numerical models used in one-line modelling disregard cross-shore sediment transport, both offshore and onshore, and are also limited by numerical instabilities that arise from high wave angles (Mangor *et al.*, 2017 as cited in Ghonim, 2019). Moreover, wave reflection from the structure on the seaward side is neglected and transport rates through the model boundaries are often constant causing no change in the position of the coastline over time at the boundaries. Therefore, sufficient shoreline length is important (Thomas & Frey, 2013). Furthermore, irregular shapes and combinations of structures are subject to restrictions and changes in water levels caused by tides or surges are not represented (Ghonim, 2019). Additionally, Elghandour (2018) also reported some issues with numerical dispersion which is also often a limitation of discretizing continuous differential equations into finite-difference equations in numerical models.

Longshore transport

The common definition for longshore transport, that will also be used in this report: “The movement of water and sediment parallel to the coastline” (Lincoln, Boxshall, & Clark, 1998). Longshore transport occurs due to the combined action of tides, wind, waves and the longshore current caused by those actions.

Forces caused by these actions result in almost constant movement of sediment either in suspension or in bedload flows (mobilized sediment over the seabed), as shown in figure 2 , in a complex pattern varying a lot with time. To actually compute something with this complex pattern, the longshore transport rate is averaged over intervals of waves over longer times. Longshore sediment transport is the main driver of beach morphology at these scales from hours to centuries and spatial scales of several metres to hundreds of kilometres (Larson & Kraus, 1995). Typically, the dominant contribution to the longshore current comes from waves approaching the shoreline at an angle. This can however, be influenced by factors such as wind-driven or tidal currents (Seymour, 2005).

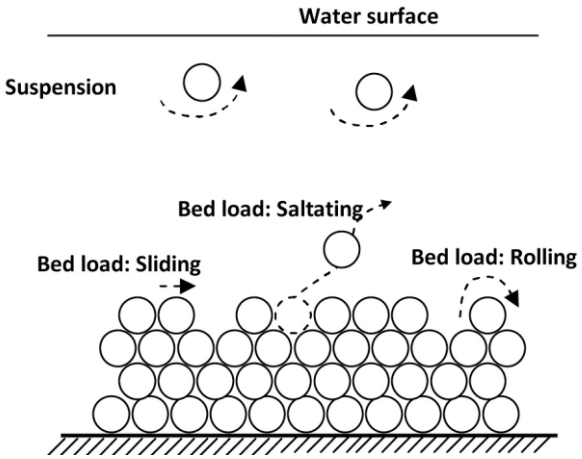

Figure 2: Sketch of typical modes of bed load and suspended load (Gao, 2023)

Longshore transport computation

Due to the large dependence of the longshore current on the breaking wave conditions (Longuet-Higgins, 1970), most used longshore transport formulas are based on properties in the surf zone.

There are two widely used approaches for the computation of longshore transport;

- Bulk transport formulas
- Process-based models

Process-based model include a large number of input parameters and are beyond the scope of this research. Bulk transport formulas are simplified equations based on physical processes and often feature coefficient for calibration. These equations are often used to make a first estimate based on limited information because they offer computations of longshore transport rates with few and easily available parameters. The two most common ones; CERC (U.S.A.C.E., 1984) and Kamphuis (Kamphuis J. W., 1991) formulas are also implemented in ShorelineS. Along with some other longshore transport formulas, these will be further elaborated in section 2.1.5. as they will also be used in the rest of the report.

2.1.2. ShorelineS model goals

The ShorelineS model has already functioned as a research tool for finding driving mechanisms in coastal processes. It has already been used to evaluate salient development behind an offshore breakwater amongst other but it's main strength is it's ability to form and simulate spit formations. The next step in the ShorelineS model development is to make it become a verified engineering tool. The following goals are set for the development of the ShorelineS model (Lenssinck, 2022):

- Quick and easy to apply.
- Computationally efficient.
- Ability to handle complex coastlines that include spit features thus increase applicability.
- Able to deal with nourishments and structures at decadal scales.
- Sufficiently accurate to judge between coastal measure design alternatives.

2.1.3. Model structure

The structure of the basic ShorelineS model consists of three main parts; initialization phase (red area), transport loop (grey area) and a coastline change loop (blue area) as indicated in figure 3. The initialization phase prepares the input data, coastline grid and simulation time. The transport loop calculates the sediment transport and applies boundary conditions to each coastline section. The Coastline change loop translates the calculated sediment transport gradient over the shoreline to a change in the shoreline coordinates.

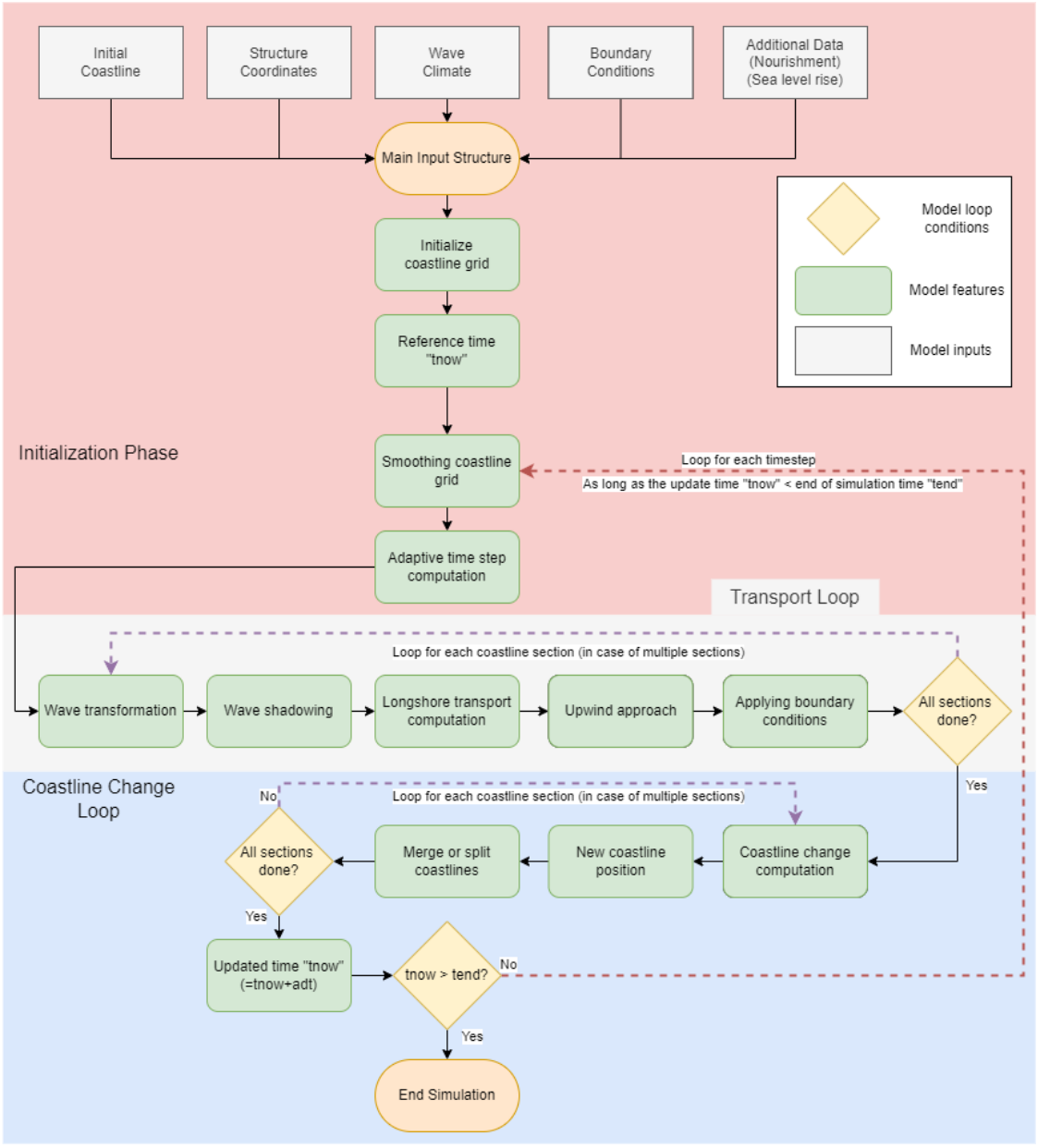

Figure 3: Basic ShorelineS model loop, including loop conditions (in yellow diamond shapes) and a slight adaptation to the model loop structure (Roelvink et al., 2020).

2.1.4. Initialization

The initialization phase of ShorelineS is concerned with the input and preparation of the data to suit the format used by ShorelineS and the input parameters. The initialization phase consists of two main parts; user/model input and model initialization.

Model input

The initial coastline (sections) and structures can be entered as coordinates or drawn manually whenever no coordinates have been provided. The coastline and structure positions, when provided with coordinates, are given in two columns, *x* and *y* in any metric system. Different shoreline sections and structures are seperated by a set of NaN's for *x* and *y* (Roelvink et al., 2020).

For the wave climate, there are two ways of providing the model with the required input; wave conditions time series (1), wave climate characterized by a number of wave conditions (2), and by setting a wave direction and spreading (3). In this research, the third method is used. Wave conditions like the significant wave height, peak period, and mean wave direction are set to a single value. A spreading parameter then randomly distributes the wave direction uniformly around the mean wave direction for each timestep.

Model initialization

In the initialization phase, the coastline grid is prepared first. The input coordinates of the shoreline are interpolated to fit the maximum spacestep as defined by the input model parameter $ds0$. Additionally, shorelines seperated by structures are seperated by NaN's. A reference time $tnow$ is set according to the model input parameter $reftime$. After each timestep, the coastline is smoothed by 3-point smoothing algorithm with a smoothing factor set by the input parameter $smoothfac$. This is done to avoid large variations in grid size but can also lead to overexaggerated straightening of shoreline sections. Therefore, $smoothfac$ should be <0.1 (Roelvink et al., 2020).

2.1.5. Transport

The first loop and second phase of the ShorelineS model is concerned with the computation of the sediment transport between consecutive shoreline nodes. The amount of longshore transport is first calculated for each node before the projection of structures or other coastline sections and boundary conditions change these initial calculated values for longshore transport.

Longshore transport computation

Six bulk longshore transport formulas have been implemented in the model. The one to apply in the simulation can be specified using the $trform$ input parameter and the value indicated by the notation column in table 1.

Table 1: Longshore transport formulas implemented in ShorelineS (Roelvink et al., 2020).

Author	Notation	Formula
(U.S.A.C.E., 1984) (simplified)	$CERC1$	$Q_s = b_1 H_{S0}^{5/2} \sin(2 \cdot \varphi_{loc})$
(Ashton & Murray, 2006)	$CERC2$	$Q_s = K_2 H_{S0}^{12/5} T^{1/5} \cos^{6/5}(\varphi_{loc}) \sin(\varphi_{loc})$
(U.S.A.C.E., 1984)	$CERC3$	$Q_s = b_1 H_b^{5/2} \sin(2 \cdot \varphi_{loc_b})$
(Kamphuis J. W., 1991)	$KAMP$	$Q_s = 2.33 H_b^2 T^{1.5} m_b^{0.75} d_{50}^{-0.25} \sin^{0.6}(2 \cdot \varphi_{loc_b})$
(Mil-Homens, 2013)	$MILH$	$Q_s = 0.15 H_b^{2.75} T^{0.89} m_b^{0.86} d_{50}^{-0.69} \sin^{0.5}(2 \cdot \varphi_{loc_b})$
(van Rijn, 2014)	$VR14$	$Q_s = 0.006 K_{swell} \rho_s H_b^{2.6} m_b^{0.4} d_{50}^{-0.6} V_{total}$

In table 1, b_1 and K_2 are calibration coefficients which are computed as shown in equation 2 and 3 respectively. K_{swell} is a parameter to account for influence of wave period and V_{total} is a parameter to account for additional velocities by tide and wind (van Rijn, 2014):

$$b_1 = \frac{k\rho\sqrt{g/k}}{16(\rho_s - \rho)(1-p)} \tag{2}$$

$$K_2 = \left(\frac{\sqrt{g\gamma}}{2\pi}\right)^{\frac{1}{5}} K_1, \qquad K_1 \sim 0.4 \tag{3}$$

$$K_{swell} = 0.015 p_{swell} + (1 - 0.01 p_{swell}) \tag{4}$$

$$V_{total} = V_{wave} + 0.01 p_1 V_1 + 0.01 p_2 V_2 \tag{5}$$

$$V_{wave} = 0.3(gH_b)^{0.5} \sin(2 \cdot \varphi_{loc_b}) \tag{6}$$

Where;

Q_s	= transport rate [m^3/s].
H_{S0}/H_b	= significant wave height at the offshore location and at point of break respectively [m].
T	= peak wave period [s].
H_b	= wave height at breaking [m].
φ	= the wave angle relative to shoreline normal [°].
m_b	= mean bed slope in the breaking zone [-].
D_{50}	= median grain diameter [m].
k	= default calibration coefficient according to USACE[-].
b	= referring to conditions at the edge of the breaker zone [-].
g	= gravitational acceleration [9.81m/s^2]
p_{swell}	= percentage of total wave height record that consists of low-period swell wave heights.
p_1/p_2	= percentage of time in which positive and negative flow respectively are present.
V_1/V_2	= representative velocities for positive and negative flows respectively.

The default calibration coefficient depends on whether the root-mean-square wave height H_{rms}, or significant wave height H_s is used for the wave height at breaking H_b. Several different values of k have been found for the case that H_{rms} is used and are shown in table 2 (Bosboom & Stive, 2023):

Table 2: Values for coefficient k in literature (Bosboom & Stive, 2023)

Author	Value of $k_{for\ H_{rms}}$
(Komar & Inman, Longshore sand transport on Beaches, 1970)	0.77
(U.S.A.C.E., 1984)	0.92
(Schoonnees & Theron, 1993) and (Schoonnees & Theron, 1996)	~0.5

In the frequent case that H_s is used instead of H_{rms}, the value of k is smaller and can be translated using equation 7 (Bosboom & Stive, 2023):

$$k_{for\ H_s} = \left(\frac{1}{\sqrt{2}}\right)^{5/2} \cdot k_{for\ H_{rms}} \approx 0.4 k_{for\ H_{rms}} \tag{7}$$

Concerning the choice between the CERC and KAMP formulas, each has its own advantages and disadvantages. CERC1 is the simplest and meant for illustrating principle behaviour. CERC2 is derived from the general CERC formula and includes effects of refracting and shoaling. CERC3 and KAMP are also used in GENESIS and UNIBEST one-line models. The CERC options have a single calibration whereas KAMP requires uncertain extra inputs like slope and grain size but can be more accurate.

Wave shadowing

In ShorelineS, structures and other coastal sections produce a region shadowed from waves called the "shadow zone" as shown in figure 4. Inside these shadow zones the wave height is set to zero, thus no longshore transport occurs here. Note that, this does only mean that in the model, no longshore transport actually occurs when wave diffraction is not enabled (see section 2.1.7).

Figure 4: Areas affected by wave shadowing the case of a hard structure or coast section

Boundary conditions

For shoreline sections that are non-cyclic, boundary conditions in the model control the sediment transport rate at the edges of the shoreline in the model. These boundary conditions can be set by the parameters $boundary\_condition\_start$ and $boundary\_condition\_end$ respectively indicating the boundary conditions at the left and right side of non-cyclic the shoreline section. Boundary conditions included in the model are shown in table 3:

Table 3: Shoreline endpoint boundary conditions in ShorelineS

Boundary condition	Definition	Notes
"$Neumann$"	Fixed shoreline position by matching the transport through the boundary with the transport in front of the boundary.	
"$Function$"	Transport rate across the boundary can be input as a timeseries in m^3	
"$CTAN$"	Set a single value as a constant transport through the boundary.	Only used as start boundary condition.
"$constant$"	Use the first calculated transport value according to Neumann as a constant transport through the boundary.	
"$periodic$"	Match the transport in the start boundary with the transport out the right boundary.	
"$closed$"	Pretend the model is a closed box. No transport through boundaries.	

2.1.6. Coastline Change

The coastline change loop in the ShorelineS model consists of a few steps. It starts with computing displacement distance of each node and translating the change to new coordinates in the cartesian system by using the average angle between the two neighbour nodes.
Then, the coastline is checked against locations where coastlines intersect for possible merging or splitting of the coastline and the merging/splitting is translated to the coordinate sequence.

Coastline change computation

ShorelineS does not use a grid-based approach but instead, is built like a string of arbitrary points with longshore nodes s with cartesian coordinates x and y that can move freely. A representation of this is schematically shown in figure 5 along with the definition of the angles.

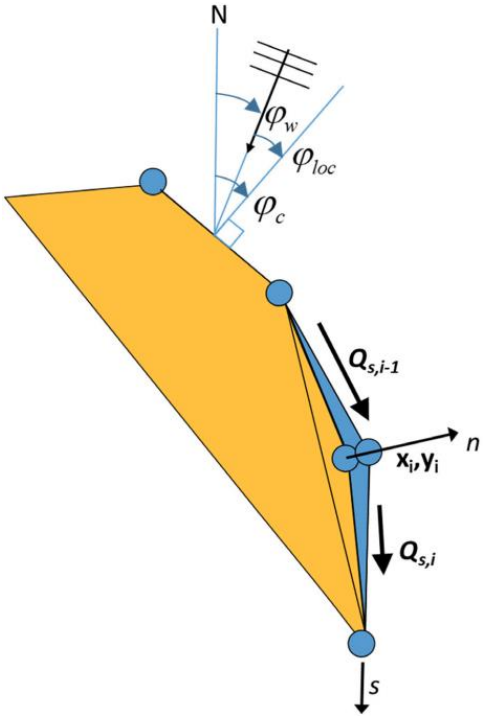

Figure 5: Coastline-following coordinate system and definition of wave and coast angles (Roelvink et al., 2020).

The coastline positions in ShorelineS are represented by two column vectors (X_{mc} and Y_{mc}). Different coast sections are seperated by "NaN". When following the coastline position coordinates (Cartesian) in the order of the input, the sea will be located to the left of the line. (Roelvink et al., 2020).

The basic equation used for calculating the new coastline position is based on a sediment conservation equation as shown in equation 8 (Roelvink et al., 2020).

$$\frac{\partial n}{\partial t} = -\frac{1}{D_c}\frac{\partial Q_s}{\partial s} - \frac{RSLR}{\tan\beta} + \frac{1}{D_c}\sum q_i \qquad (8)$$

Where;

t = time [yr].
D_c = the active profile height [m].
Q_s = longshore transport [m^3/yr]. (see section 3.3)
β = profile slope between the dune and depth of closure (average).

$RSLR$ = relative sea level rise [m/yr].
q_i = source/sink term [m^3/m/yr].

In terms of ShorelineS, the vector n in figure 5 is a normal displacement to the shore. It follows then that the change in node coordinates (Δx_i^j and Δy_i^j) caused by a gradient of longshore transport over coastline length, and the new position of the node coordinates (x_i^{j+1} and y_i^{j+1}) are computed as shown in equations 9 and 10.

$$\begin{aligned} \Delta n_i^j &= -\frac{1}{D_c}\frac{2(Q_{s.i}^j - Q_{s.i-1}^j)}{L_i}\Delta t \\ \Delta x_i^j &= -\Delta n_i^j (y_{i+1} - y_{i-1})/L_i \\ \Delta y_i^j &= \Delta n_i^j (x_{i+1} - x_{i-1})/L_i \\ x_i^{j+1} &= x_i^j + \Delta x_i^j \\ y_i^{j+1} &= y_i^j + \Delta y_i^j \end{aligned} \tag{9}$$

Where;
i = point/node index [-].
j = timestep index [-].
L_i = length of grid element calculated as shown in equation 6 [m].

$$L_i = \sqrt{(x_{i+1} - x_{i-1})^2 + (y_{i+1} - y_{i-1})^2} \tag{10}$$

Merging or splitting coastlines

One of the advantages/strengths of ShorelineS compared to 'regular' one-line models is the ability to simulate multiple coastal sections simultaneously. However, this can also cause shorelines to touch each other. The merging or splitting of coastlines in ShorelineS is performed with a simple principle computation as shown in figure 6.

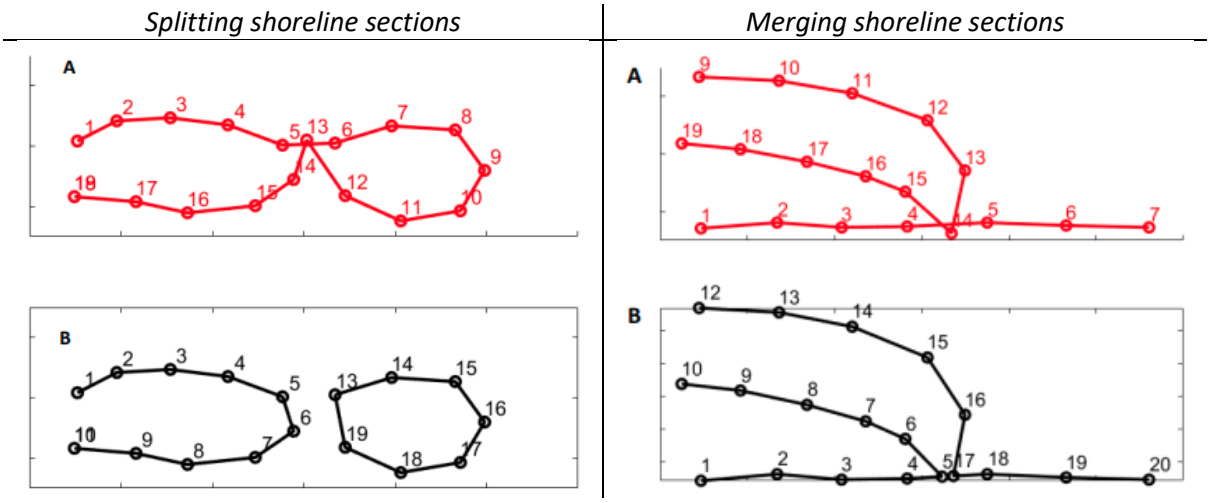

Figure 6: Illustration of splitting and merging process where numbers indicate the grid cell connection change after the process. A is the schematic situation before the splitting or merging process and B is the situation after splitting/merging. (Roelvink, Huisman, Elghandour, Ghonim, & Reyns, 2020)

2.1.7. Recent improvements

Several improvements have been made to the model of ShorelineS since its release. However, improvements like *sand bypassing* and *transmission around structures, and dune foot evaluation* are less important for this research and will not be further elaborated as they will not be used. Other improvements have been made to the model that will be used and these include: *adaptive timestep*, *improved upwind approach,* and *wave diffraction*.

Adaptive timestep

One of the advantages of using a one-line numerical model over other types of shoreline evolution models is the low computational time required for a simulation over a long time. However, using too small timesteps will lead to long calculation times negating this specific advantage. On the other hand, using too large timesteps will lead to instability in the numerical model. Therefore, Elghandour (2018) introduced the adaptive timestep to ShorelineS that restricts the timestep size by physical conditions. It was shown that it prevents numerical instabilities except for the shoreline response behind an offshore breakwater.

Improved upwind approach

The upwind approach part of the model takes care of the so-called high-angle instability which on one hand allows spits to develop but on the other hand can lead to instable behaviour. Where the local angle exceeds the critical angle (angle at which the computed longshore transport equals the maximum transport) at the updrift side, the transport downdrift is set to the maximum transport (transport computed with critical angle). Elghandour (2018) slightly changed this approach such that the critical angle is dependent on the transport formula used.

Wave diffraction

While breakwaters can shield harbours from direct wave impacts, wave diffraction occurs around the end of breakwaters causing wave fronts to curve into the sheltered zone as shown in figure 7. Taking into account the effect of wave diffraction is typically crucial when planning and assessing design options. It is significant in determining harbour layouts and specifying the location and length of coastline that needs to feature wave absorbing material (Briggs, Thompson, & Vincent, 1995).

The common definition of wave diffraction is “a process by which wave energy is transmitted and radiated when the wave is bending around an obstacle such as an island or structure in order to propagate into the sheltered region” .

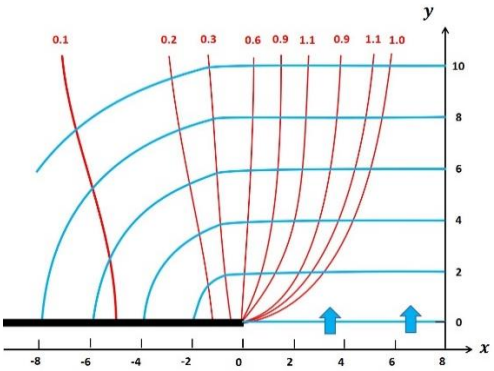

A: analytical solution of diffraction of a linear wave. Blue lines are wavefronts and red lines are lines of equal wave height (Penney & Price, 1952).

B: Wave diffraction around the tip of a breakwater.

Figure 7: Images of wave diffraction where. (a): analytical solution of wave diffraction, and (b): wave diffraction in reality

In ShorelineS, the diffracted breaking wave height inside the sheltered zone as shown in figure 7 is calculated by multiplying the wave height at the tip of the structure (H_{tip}) with a diffraction coefficient (K_d) as shown in the following equation (11):

$$H_{diff,br} = H_{tip} * K_d \tag{11}$$

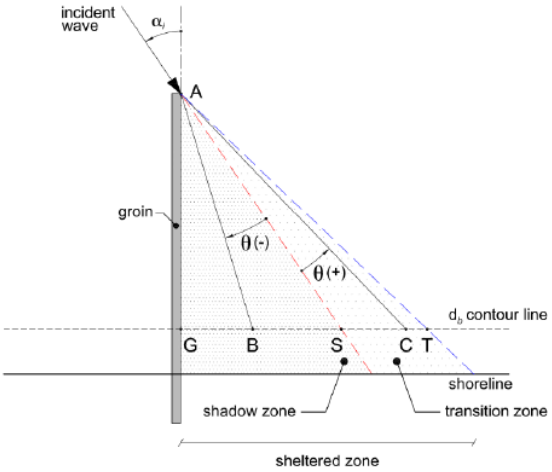

Figure 8: sketch of wave diffraction near a groyne (Baykal, 2006)

For this research, the ShorelineS model as used by IMDC will use the Kamphuis method for diffraction. Therefore, this method will only be discussed here.

Overgaauw (2021) implemented the derivations by Kamphuis (1992) in equation 12 for the diffraction coefficient in equation 11 in ShorelineS where the angle $\theta < 0°$ indicates a location in the shadow zone as shown in figure 8. In the transition zone, the angle θ is positive and the diffraction coefficient K_d approaches to 1 at the edge of the transition zone where $\theta = 90°$.

$$\begin{aligned} K_d &= 0.69 + 0.008\theta \;\; for \;\; 0 \geq \theta > -90 \\ K_d &= 0.71 + 0.37\theta \;\; for \;\; 40 \geq \theta > 0 \\ K_d &= 0.83 + 0.17\theta \;\; for \;\; 90 \geq \theta > 40 \end{aligned} \tag{12}$$

Kamphuis (1992) also provided the derivation for the diffracted breaking wave angles in the sheltered zone as shown in equation 13 used by Overgaauw (2021) and implemented in ShorelineS.

$$\varphi_{br,diff} = \varphi_{br,undiff} K_d^{0.375} \tag{13}$$

2.1.8. One-line numerical modelling and ShorelineS conclusion

To conclude, in contrast to most one-line numerical models, ShorelineS uses a vector-based grid instead of a cell-based grid. This allows ShorelineS to be applicable in a wider variety of cases since multiple coastal sections are able to split and merge. Bulk longshore transport formulas are used to calculate longshore transport gradients on the shore that are translated to shore normal movement of the coastline nodes. Originally, the model used only a wave shadowing algorithm where shadowed coastline sections would experience no wave action at all. A recent wave diffraction improvement has enabled some wave action to be possible in shadowed zones.

2.2. Cross-shore processes modelling

2.2.1. Cross-shore transport

Cross-shore transport occurs in the perpendicular direction to longshore transport and refers to the sediment movement perpendicular to the shore caused by forces generated due to tides, wind, waves and shore-perpendicular currents (Seymour, 2005).

Unlike longshore transport, cross-shore transport is easier to observe and can introduce large and visible changes to the beach configuration in a short timespan. Since it's easier to observe than longshore transport and important for beach erosion, cross-shore transport has been well studied. However, due to its complex nature, the magnitude is usually derived from changes in beach elevation and ocean floors (Seymour, 2005).

Equilibrium profile

The cross-short transport studies by Bruun (1954) resulted in the first coastal engineers to introduce an empirical equation for the dynamic equilibrium profile (14). This profile equation assumes that when a shoreface is subject to a constant incident wave, it will evolve to a particular profile shape. This incident wave can then be generalized to include all seasonal variations.

$$h(y) = Ay^m \tag{14}$$

Where;

h = Water depth [m].
A = Scale factor related to grain size distribution of sediment at the shore [-].
y = Cross-shore distance [m].
m = Empirical exponent equal to 2/3.

The dynamic equilibrium shoreface profile may never be actually reached. However, it provides a tool for coastal engineers to make predictions about the expected profile after land reclamation. It is also useful for engineers and scientists concerned with natural variability of beaches and does not include any contour complexities like bars and seasonal variation as shown in figure 9 (Bosboom & Stive, 2023; Seymour, 2005).

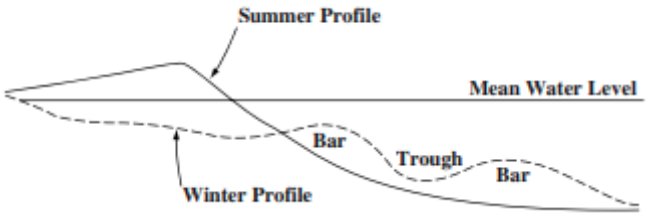

Figure 9: How seasonal changes in wave climate affect beach profiles and the forming of one or more offshore bars (Seymour, 2005).

Cross-shore material exchange occurs on many scales, where not all are relevant for modelling regional coastal evolution (Larson and Kraus, 1995). Transport processes that act over compatible time and space scales should be included in shoreline evolution models. An example of these processes is the slow recovery of bars that formed after a severe storm transported berm material to the offshore.

2.2.2. Equilibrium bars

A storm or prevailing large waves in the winter transport material from the berm to the offshore (q_B), where it may be deposited in one or more longshore bars, with a specific volume V_B as shown in figure 10.

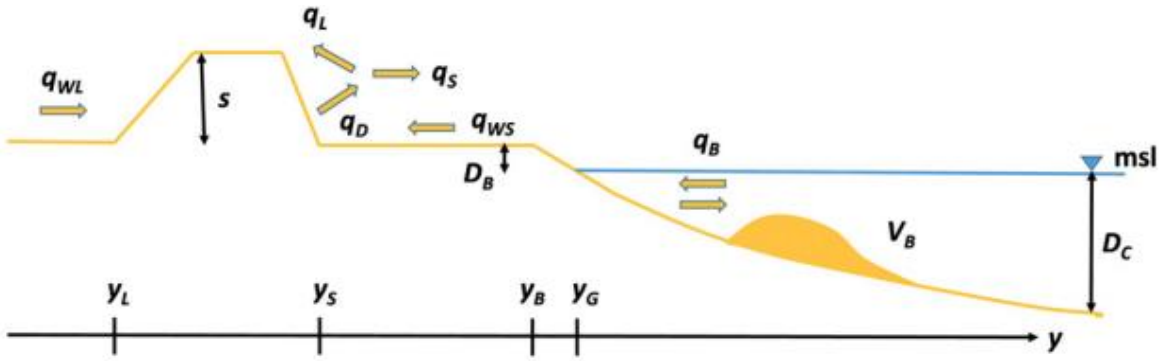

Figure 10: Definition sketch of cross-shore transport parameters and beach profile evolution. (Larson, Palalane, Fredriksson, & Hanson, 2016).

After a storm, or even during its declining phase, the waves may bring the sand back from the bar to the berm (q_B), recovering the damage caused by the storm on the foreshore and seaward portion of the berm. The larger the waves, the bigger the closure depth (D_C) and the further from the shoreline, bars will be formed. So, when a heavier storm has caused a bar to have been formed in deeper waters, the wave activity interacting with it is smaller in the normal circumstances after the storm. Therefore, the transfer of material from the bar to the berm can also occur at a slower rate. Incorporating this exchange described by equation 15, 16, and 17 by Larson et. al. (2016) between the berm and the bar into a monthly to centennial one-line numerical model like ShorelineS would be beneficial as it encompasses scales that can align with the overall evolution process.

$$\frac{dV_B}{dt} = \lambda(V_{BE} - V_B) \tag{15}$$

$$\frac{V_{BE}}{L_0^2} = C_B \left(\frac{H_0}{wT}\right)^{4/3} \frac{H_0}{L_0} \tag{16}$$

$$\lambda = \lambda_0 (\frac{H_0}{wT})^m \tag{17}$$

Where;

V_B = Current bar volume [m^3]
V_{BE} = Equilibrium bar volume [m^3]
t = time [s]
λ = rate coefficient for bar volume approaching equilibrium [-]
L_0 = deepwater wavelength [m]
C_B = dimensionless coefficient [-]
H_0 = deepwater wave height [m]
w = sediment fall speed [m/s]
T = wave period [s]
m = calibration coefficient [-]

Field data suggested that $m = -0.5$, $C_B = 0.08$, and $\lambda_0 = 0.002h^{-1}$ (Larson, Palalane, Fredriksson, & Hanson, 2016).

Growth or decay of bar volume (V_B) is linked to the evolution of the beach berm; sediment brought back from the bar increases berm width (Komar, 1998 as cited in Larson *et. al.*, 2016). In some countries the width of the beach is an important measure; a beach that is too narrow is bad for flood safety measures and provides less space for potential visitors. A beach that is too wide is less convenient and therefore, also less attractive to potential visitors for other reasons (Larson, Palalane, Fredriksson, & Hanson, 2016).

2.2.3. Cross-shore processes modelling conclusion

To conclude section 2.2, cross-shore sediment transport is not explicitly taken into account by ShorelineS. Material exchange formulas as presented by Larson et al. (2016) between the bar and berm has been identified as a possible solution. Under circumstances, the material exchange between the bar and the berm occurs at timescales compatible with the purpose of the ShorelineS model and has the ability to significantly influence or even permanently change the shape of the beach.

2.3. Detached breakwaters

In general, a detached breakwater is a structure situated parallel to the coast inside or close to the surf zone that has the purpose of protecting a coast or activities on the coast by modifying wave action (Dally & Pope, 1986; Mangor K., 2023). In this research, as also mentioned in the scope of the research in section 1.3, detached breakwaters will be limited to single emerged detached breakwaters. Therefore, segmented detached breakwaters or submerged/floating detached breakwaters will not be considered.

2.3.1. Characteristic breakwater parameters

A detached breakwater can be characterized by the following parameters as also shown in figure 11;

L_B = breakwater length [m].
X = offshore distance [m].
X_{80} = width of surf-zone [m].
L_B^* = dimensionless breakwater length [-].
X^* = dimensionless breakwater offshore distance [-].
L_G = length of gap between breakwaters (segmented breakwaters) [m]

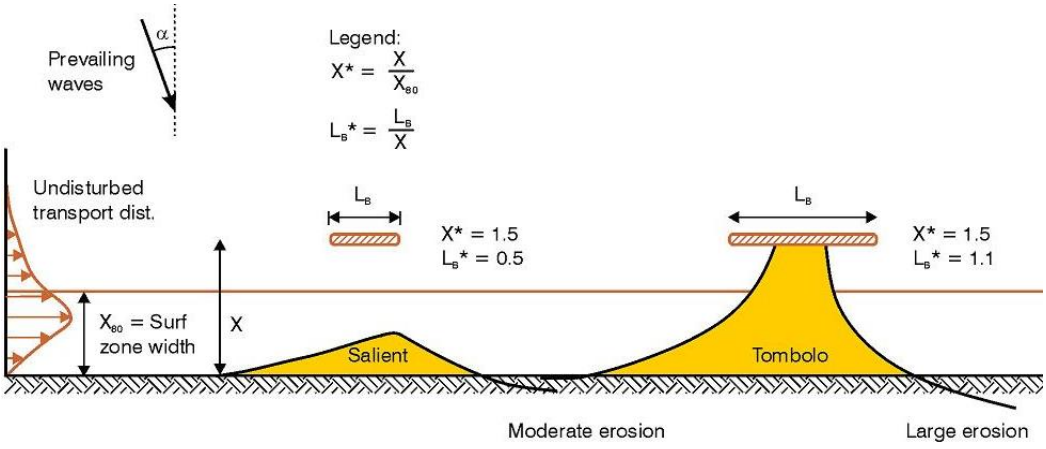

Figure 11: definition sketch of detached breakwater parameters and accumulation forms (Mangor K. , Detached breakwaters, 2023).

As also shown in figure 11, the dimensionless breakwater length $L_B^* = L_B/X$ and the dimensionless breakwater offshore distance $X^* = X/X_{80}$. These dimensionless parameters are mainly used for the classification of detached breakwaters and prediction of accumulation forms as will be further elaborated in section 2.3.3.

2.3.2. Applicability

Some disadvantages of groynes also affect breakwater schemes. In contrast to groynes, a breakwater is better suitable for trapping sediment on a coastline subject to perpendicular wave angles. Types of coasts can be defined by wave angle of incidence and wave exposure as shown in table 4.

Table 4: Classification of coastlines (Mangor K. , 2021).

Classification	Wave angle incidence (°)
Type 1	0
Type 2	$1 - 10$
Type 3	$10 - 50$
Type 4	$50 - 85$
Type 5	> 85

Classification subdivision	12 hours per year exceeded wave height
P	$H_{12h/y} < 1m$
M	$1m < H_{12h/y} < 3m$
E	$H_{12h/y} > 3m$

A (single) detached breakwater structure parallel to the coast is not effective in type 4 and type 5 shorelines where the wave approach exceed 50° relative to the shore normal. However, breakwaters are applicable on coasts of type 1, type 2 and low type 3 with subdivision M or E, where the angle of incidence is between 0° and 20° and the once per year wave height event is larger then 1 meter (Mangor K. , 2021).

2.3.3. Accumulation forms

There are generally two types of accumulation forms (excluding "no response") in the lee of a detached breakwater as also shown in figure 11; *salient* or *tombolo.* Several studies have shown a relationship between the dimensionless breakwater length (L_B^*) and the type of accumulation form that will develop over time. The accumulation form is not only dependent on the characteristic dimensions of the breakwater but also by surf-zone properties like wave angle. However, the accumulation will usually result in a salient form under the condition that the dimensionless breakwater length (L_B^*) is less then 0.7. The accumulation in the lee side of the breakwater will usually connect the breach and breakwater to form a tombolo over time when the breakwater length (L_B^*) is greater than 1.0 (Hsu & Silvester, 1990; Mangor et al., 2017; Suh & Dalrymple, 1987).

$$\begin{aligned} L_B^* &\geq 0.9 - 1.0 \rightarrow tombolo \\ L_B^* &\leq 0.6 - 0.7 \rightarrow \ salient \end{aligned} \tag{18}$$

2.3.4. Accumulation analytical solutions

Several studies have been conducted in the past, concerned with the shoreline response behind an offshore structure. In this section, three studies will be presented that aimed at developing a relationship for shape parameters of the accumulation form in the lee side of the detached breakwater structure which can be used to verify the model.

Hsu and Silvester

Hsu and Silvester (1990) provided a relation based on prototypes for the formation of a salient between the breakwater length (L_B), original offshore distance (X_0) and the distance between the new shoreline and the breakwater (X) as shown in equation 19. Since a static equilibrium is assumed

here, this relationship is independent on wave characteristics. Therefore, sufficient wave duration should be provided when modelling to reach the predicted static equilibrium shape.

$$\frac{X}{L_B} = 0.6784\left(\frac{L_B}{X_0}\right)^{-1.1248} \tag{19}$$

Khuong

Khuong (2016) recently expanded on the study by Hsu and Silvester (1990) by using data of 93 projects with 1114 structures and included their physical conditions. He provided a similar equation for the relation regarding salient formation as shown in equation 20 but also provided a linear relation for tombolo formation between tombolo formation width (T), original offshore distance (X_0) and breakwater length (L_B) as shown in equation 21.

$$for\ salient: \frac{X}{L_B} = 0.62\left(\frac{L_B}{X_0}\right)^{-1.15} \tag{20}$$

$$for\ tombolo: \frac{T}{X_0} = 0.85\left(\frac{L_B}{X_0}\right) - 0.5 \tag{21}$$

Spiral bay geometry

Using shoreline position data from prototype bays that were considered to be in static equilibrium, Hsu, Silvester and Xia (1989) proposed a logarithmic and a polynomial expression for the shoreline in the lee of headland features. The polynomial expression is shown in equation 22.The parabolic shape performs better for beaches with one headland but it is more difficult to fit and is sensitive to the choice of the control line (R_0) (Moreno & Kraus, 1999). Moreno and Kraus (1999) also provide a hyperbolic tangent beach that fits well for one-headland beaches and is more convenient to apply which could also be used.

$$\frac{R}{R_0} = C_0 + C_1\left(\frac{\beta_R}{\theta}\right) + C_2\left(\frac{\beta_R}{\theta}\right)^2 \tag{22}$$

Where;

R	= shoreline distance measured from the end of the upcoast headland at angle θ. [m]
R_0	= length of control line drawn [m]
$C_0/C_1/C_2$	= coefficient dependent on angle β. [-]
β_R	= angle between predominant wave crest and control line R_0. [°]
θ	= angle to control line R. [°]

In the case of a single detached breakwater, the control line (R_0) is drawn from the end of the headland to the nearest point on the downcoast shoreline at which the shore is parallel with the predominant wave crest. This can also be seen in figure 12.

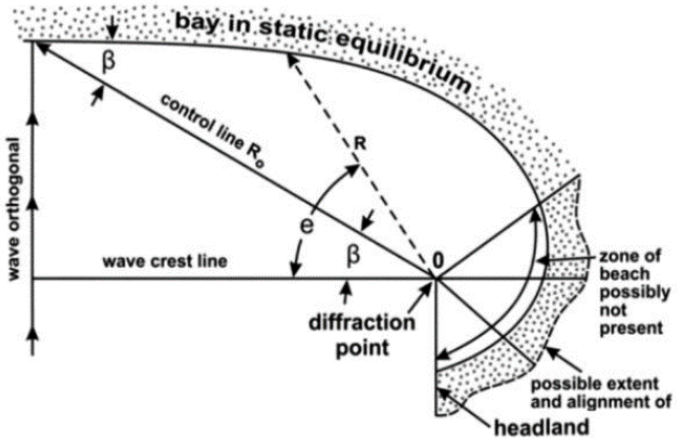

Figure 12: definition sketch of static equilibrium bay showing variables involved in the spiral bay geometry analytical solution (Hsu, R., & Xia, 1989).

The coefficients (C_0, C_1,and C_2) in equation 22 are dependent on the wave crest angle (β_R) to the control line (R_0) and are shown in figure 13. The wave crest angle to the control line (β_R) should be limited to $22° < \beta_R < 80°$.

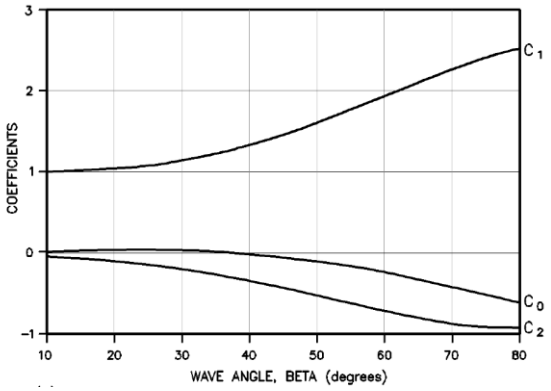

Figure 13: Coefficients in parabolic spiral bay geometry against wave angle θ (Evans & Hsu, 1989).

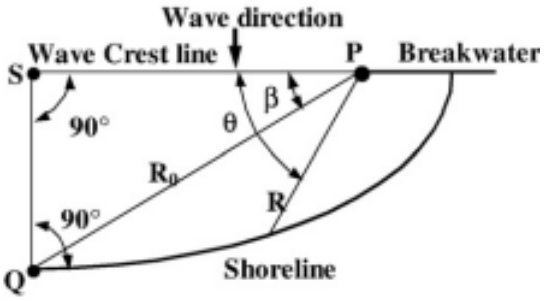

Figure 14: definition of coordinate system (Tan & Chiew, 1994).

The relations obtained by Tan and Chiew (1994) can be used to simplify determining the correct coefficient and parameters of the spiral bay geometry. At the nearest point on the shore where the wave crest is parallel to the shoreline defined as point Q in figure 14, $R = R_0$ and $\theta = \beta_R$. Additionally, the length $SQ = R \sin\theta$ which leads to the following relations for the coefficients:

$$C_0 + C_1 + C_2 = 1 \tag{23}$$

$$C_1 + 2C_2 = \beta_R / \tan\beta_R \tag{24}$$

Now, if one of the coefficients for example C_0 is determined, the other two can be easily determined via these conditions as shown in equations 25 and 26;

$$C_1 = -2C_0 - \frac{\beta_R}{\tan\beta_R} + 2 \tag{25}$$

$$C_2 = C_0 + \frac{\beta_R}{\tan\beta_R} - 1 \tag{26}$$

Here, also for simplicity, C_0 if often expressed as a function of β where $0° < \beta < 80°$;

$$C_0 = A_0 + A_1\beta_R + A_2{\beta_R}^2 + A_3{\beta_R}^3 + A_4{\beta_R}^4 \tag{27}$$

Where;

β_R = angle between predominant wave crest and control line (R_0) in radians.
A_0 = -0.0116
A_1 = 0.376
A_2 = -0.451
A_3 = 0.276
A_4 = -0.331

2.3.5. Recent detached breakwater ShorelineS study

A recent ShorelineS modelling study by Elghandour (2018) also featured a detached breakwater case to validate his implemented model improvements. For the chosen set of wave conditions and other input parameters, the model showed acceptable results. They were compared with the earlier discussed analytical solutions (in section 2.3.4.) by Khuong (2016) and Hsu & Silvester (1989) and the ability to form a tombolo as shown in figure 15. Note that the model currently only features the "Kd" approach for calculating diffraction wave heights.

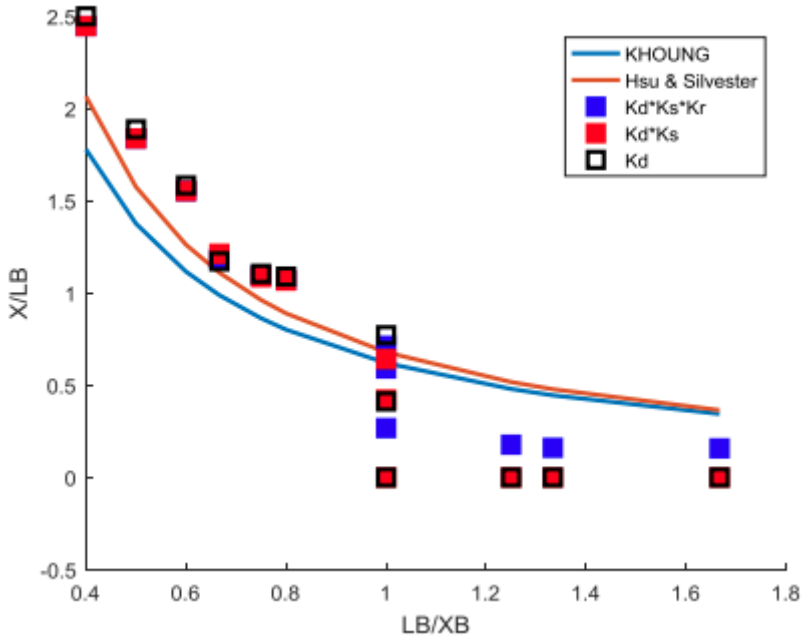

Figure 15: Verification test by Elghandour for to test ShorelineS under different expected response for different breakwater configurations. (Elghandour, 2018)

2.3.6. Detached breakwaters conclusion

To conclude section 2.3, detached breakwaters can form two types of accumulation forms in their lee side depending on their dimensionless length (L_B^*).The first one is a salient, where the beach is does not connect to the structure. For this case, the structure is expected to have a dimensionless length $L_B^* < 0.7$. The second one is a tombolo, where the beach connects to the structure. For this case, the structure is expected to have a dimensionless length $L_B^* > 1.0$. Detached breakwaters are usually applied for cases where the wave height is larger than 1 meter and the wave angle is at most 20°. ShorelineS can be validated in the case of a simple detached breakwater by using salient and tombolo shape parameters for a beach in static equilibrium as presented by Khuong (2016) and Hsu & Silvester (1990). Research question 2 can then be answered by using the spiral bay geometry (Hsu, R., & Xia, 1989). Elghandour (2018) has already tested and concluded that ShorelineS is already able to predict salient shapes well.

3. Methodology

In this section, the methodology that will be used to answer the research questions will be elaborated. First, section 3.1 elaborates upon the output parameters that will be used to quantify the shape of the resulting shoreline. Section 3.2. discusses the methodology of the sensitivity analysis to answer research question 1 regarding the impact of different parameters in ShorelineS. Section 3.3 elaborates upon the methodology to answer research question 2 regarding the model performance. Section 3.4. elaborates the methodology to answer research question 3 regarding the implementation of cross-shore transport implementation

3.1. Output parameters

It will first be determined what the interesting shoreline shape parameters are that will be used to assess the of the model. After consultation with a coastal modelling expert from IMDC, the following parameters will be used to quantify the change in shoreline shape from the model results, these can also be seen in the figure (16) below;

- *Effected shoreline length* = length of shoreline that has been affected by the placement of a single detached breakwater, shoreline shifted at least 1.5m.
- *Erosion distance* = distance that the shoreline has eroded land inwards.
- *Accretion distance* = distance that the shoreline has accreted towards the sea.
- *Erosion volume* = volume of sediment that has eroded in the shoreline.

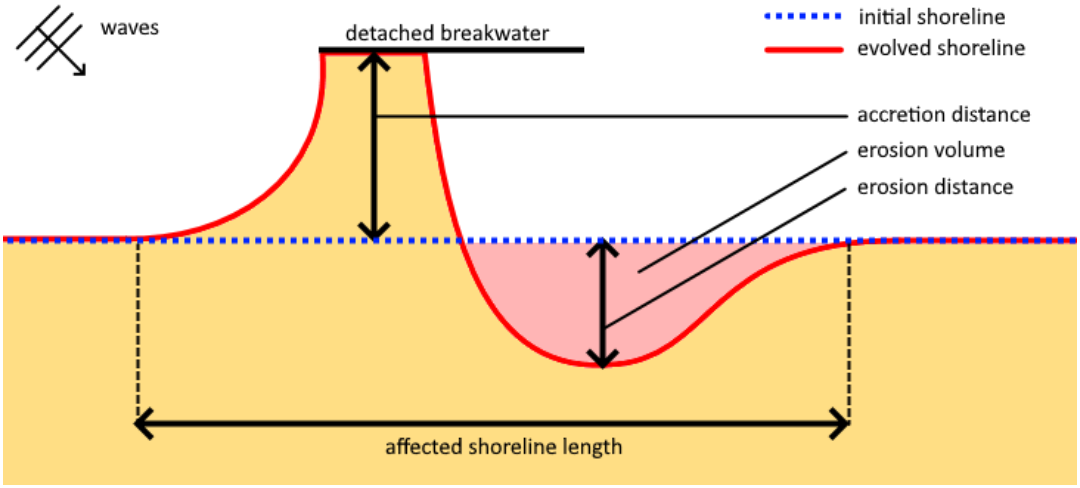

Figure 16: Shoreline evolution quantification parameters schematized

Additionally, the sensitivity on the required actual simulation time is also assessed by the model output. This is the elapsed time it took in seconds for the model to simulate the time period from 2023-01-01 until the end of the simulation with the current input parameter setup. As one of the goals of the ShorelineS model is to be used as a quick and efficient engineering tool (Lenssinck, 2022), effects on simulation time might also be useful to consider.

3.2. Sensitivity analysis (RQ1)

Preliminary simulations will be used to determine boundary conditions for a relatively stable model and what the most likely sensitive and interesting parameters are to assess in the sensitivity analysis. Then, based on the preliminary simulations, a final setup is determined for the sensitivity analysis.

3.2.1. Preliminary simulations

Since ShorelineS is still in development, preliminary simulations in the form of a small sensitivity analysis will be performed first. As a sensitivity analysis is time consuming, the goal of the preliminary simulations is to address instability issues and unforeseen circumstances. Based on the preliminary simulations, a final setup of the model sensitivity analysis will be determined that should be relatively stable and assess the likely most sensitive parameters. The results of these preliminary simulation runs are expressed in figure 17 as a maximum change in preliminary simulations. A realistic range of values has been used for each input parameter in consultation with IMDC. The setup for these preliminary simulations can also be found in Appendix A.1.

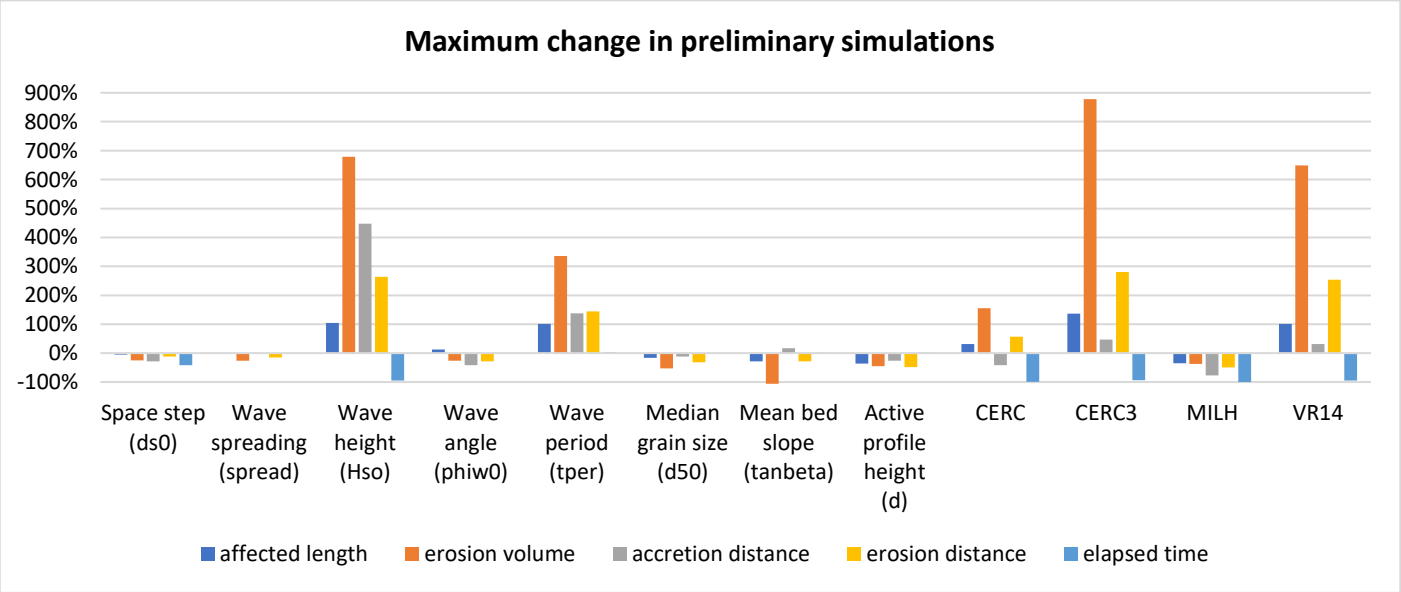

Figure 17: Preliminary simulation runs result

3.2.2. Boundary conditions

The boundary conditions of the model setup that will be used across all 5 sensitivity scenarios are shown in table 5 below. These have all been determined in consultation with IMDC and/or changed based on the results of the preliminary simulations.

Wave spreading

In the preliminary simulations, it was found that enabling the wave spreading resulted in less stable behaviour of the model. Especially in the case of tombolo, after the shoreline connected to the structure and formed the tombolo in the model, spreading would cause large instabilities. Therefore, no spreading will be used in the sensitivity analysis. This issue is elaborated in the discussion in section 5.

Simulation time

To give the shoreline more time to develop, the simulation time is adjusted for all scenarios such that the model will definitely develop a tombolo in the 'tombolo scenarios' within the chosen

simulation time. The simulation time will be increased from 3 months to 5 months. Such that realistic values for other input parameters can also be maintained.

Table 5: Boundary conditions sensitivity analysis

PARAMETER	SETTING	MODEL PARAMETER	VALUE
BOUNDARY CONDITIONS	Neumann	$boundary\_condition\_start/boundary\_condition\_end$	$"Neumann"$
SHORELINE LENGTH	3km	x_mc	$[0\ 3000]$
ACTIVE PROFILE HEIGHT	6 meters	d	6
ADAPTIVE TIMESTEP CFL	4	tc	0.9
TRANSPORT SCALING PARAMETER	1	$qscal$	1
SMOOTHING FACTOR	0.03	$smoothfac$	0.03
START TIME	1st January 2023	$reftime$	$2023-01-01$
END TIME	1st June 2023	$endofsimulation$	$2023-06-01$
WAVE SPREAD	0 degrees	$spread$	0
SPACE STEP	25 metres	$ds0$	25
TRANSPORT FORMULA	Kamphuis	$trform$	$'KAMP'$

Increase in smoothing factor

Due to included randomness in wave height and spreading, equal setups could result in different shoreline evolutions. Occasionally, unrealistic behaviour could be seen in the shoreline evolution as can be seen in figure 18 where narrow indentations and spikes have resulted from initially small deviations. ShorelineS includes a 3-point smoothing algorithm set by the parameter $smoothfac$ that aims at resolving these situations and make the sediment beach act more aggregated.

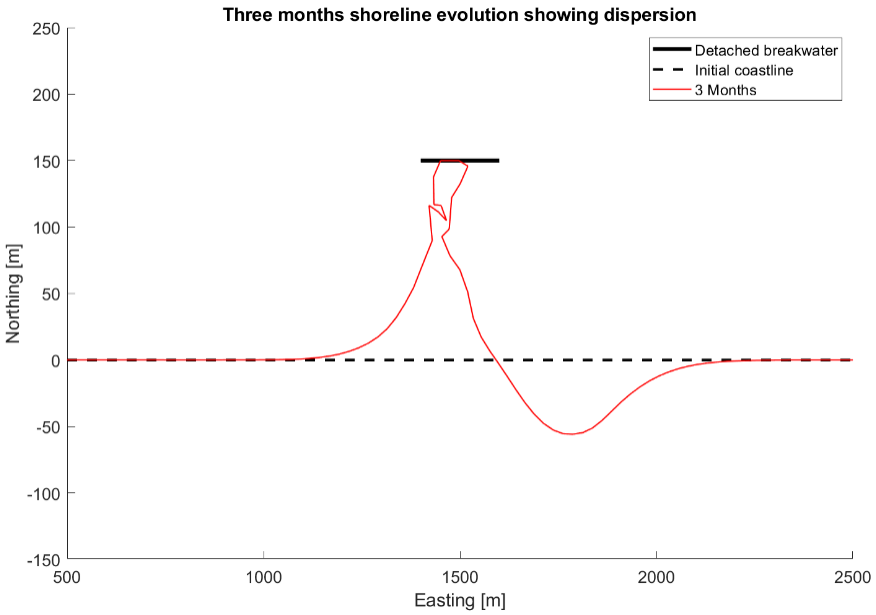

Figure 18: Example of consequence of low smoothing factor in the shoreline model after 3 months of evolution.

Adaptive timestep multiplier

From the preliminary simulation results as presented in section 3.2.1., it became evident that the use of the Kamphuis longshore transport formulas had resulted in significantly longer simulation times as shown in the tables below. The use of any other transport formula would result in at least a 94% decrease of simulation time. CERC formulas are also used by IMDC for their shoreline simulations in ShorelineS and are well recognized in the field of coastal engineering. However, these formulas do not contain the wave period and median grain size parameters making it unviable to use CERC instead of Kamphuis to continue the simulations. Additionally, CERC and Kamphuis showed big differences in calculated longshore transport volumes likely changing the results. Instead it was chosen to increase the multiplier of the adaptive timestep restriction in order to save time and stay within the timeframe limitations of this research.

3.2.3. Model setup

The detached breakwater characteristics and wave angle setup for the 5 sensitivity analysis scenarios that will be assessed in are shown in figure 19-23.

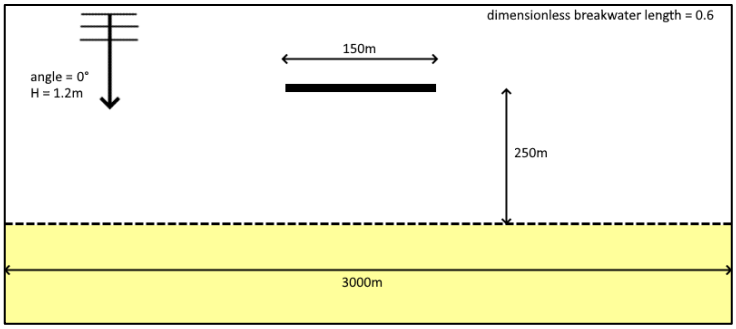

Figure 19: ShorelineS coastline and structure setup for the second salient scenario (wave angle=0°).

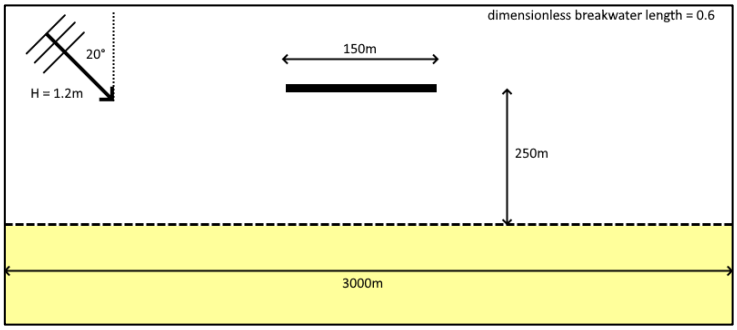

Figure 20: ShorelineS coastline and structure setup for the second salient scenario (wave angle=20°).

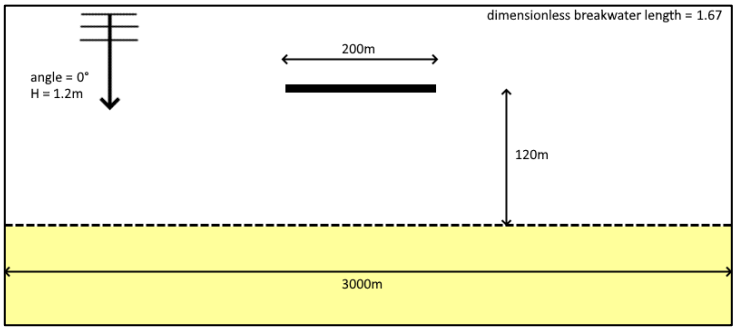

Figure 21: ShorelineS coastline and structure setup for the second tombolo scenario (wave angle=0°).

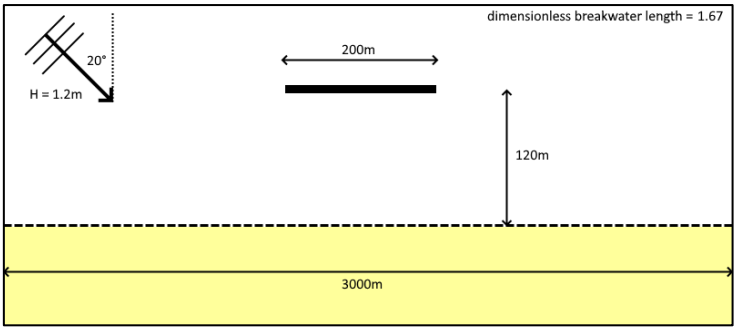

Figure 22: ShorelineS coastline and structure setup for the second tombolo scenario (wave angle=20°).

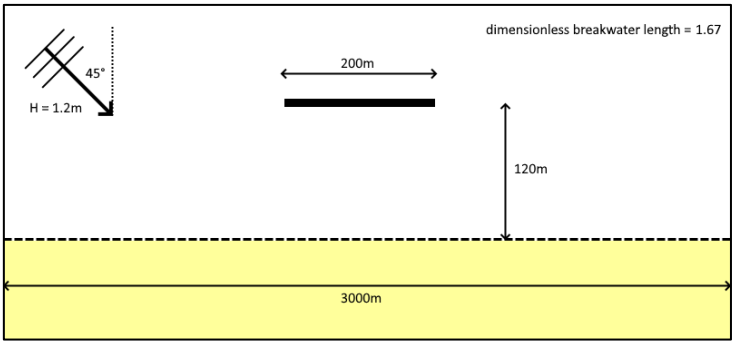

Figure 23: ShorelineS coastline and structure setup for the third tombolo scenario (wave angle=45°).

Adjusted breakwater offshore distance

From the preliminary simulations, it became apparent that in the case of a "tombolo" configuration, the model would not actually form a tombolo within the simulation time of 3 months and the default set of parameters used in these preliminary simulations (table 11, Appendix A.1.). Therefore, the breakwater offshore distance is adjusted in the case of the 'tombolo' breakwaters. This is done such that the model will develop a tombolo within new simulation time of 5 months while maintaining realistic values for the other input parameters.

Salient and Tombolo wave angle

In the literature research in section 2.3.2. it was found that the applicability of detached breakwaters is normally between 0° and 20° wave angle approach. However, in the preliminary simulations, a default wave angle of 45° had been used. Therefore, this will be reduced to a default wave angle of 20° with respect to the initial shore normal.

Despite this, in the case of the tombolo structure, the wave angle will also be set to 45° with respect to the shore normal. This can be an interesting result to find nevertheless, because this wave angle should cause a maximum longshore transport within the simulation time.

3.2.4. Input parameters

The preliminary simulations as described in section 3.2.1. suggested the four most influential parameters to be; *wave height* (Hso)*, wave period* (*tper*)*, median grain size* ($d50$), and *mean bed slope* ($tanbeta$). For the sensitivity analysis, these will be varied between -40% and +40% of their default values.

Table 6: Sensitivity analysis parameters and values (green values are default setup).

PARAMETER VALUE	WAVE PERIOD [S]	WAVE HEIGHT [M]	MEAN BED SLOPE (TAN(B))	MEDIAN GRAIN SIZE DIAMETER [MM]
60%	4.8	0.72	0.012	0.12
70%	5.6	0.84	0.014	0.14
80%	6.4	0.96	0.016	0.16
90%	7.2	1.08	0.018	0.18
DEFAULT	8	1.2	0.02	0.2
110%	8.8	1.32	0.022	0.22
120%	9.6	1.44	0.024	0.24
130%	10.4	1.56	0.026	0.26
140%	12.8	1.92	0.032	0.32

Increase in wave height

From the preliminary simulations, it was noted that tombolos were not formed in the simulation time of 3 months. Therefore, the detached breakwater in the tombolo scenarios has already been moved closer to the shore to increase the dimensionless length of the breakwater and the simulation time was increased. Additionally, the default wave height has also been increased by 20% compared to the preliminary simulations for the same purpose to reach a tombolo quicker within the simulation time while maintaining realistic values for the input parameters.

3.2.5. Sensitivity expectations

Considering Kamphuis will be used for the setup of the sensitivity analysis, some expectations can already be made regarding the sensitivity of the model parameters. Longshore transport is calculated using equation 28 as seen before in section 2.1.5.

$$Q_s = 2.33 H_b^2 T^{1.5} m_b^{0.75} d_{50}^{-0.25} \sin^{0.6}(2 \cdot \varphi_{loc_b}) \quad (28)$$

Where;

Q_s = longshore sediment transport rate [m^3/s]
H_b = breaking wave height [m]
T = wave period [s]
m_b = mean bed slope in the breaking zone [-].
d_{50} = median grain size [m].
φ_{loc_b} = wave angle at point of breaking relative to shore normal [°]

Based on the exponents in equation 28, it is expected that the *wave height* (Hso) is the most sensitive parameters followed by the *wave period* ($tper$), *bed slope* ($tanbeta$). The least sensitive parameter is expected to be the *median grain size* ($d50$).

3.3. Model validation and performance (RQ2)

A scenario is developed and compared with analytical solutions to validate the model ShorelineS and assess its performance in predicting shoreline evolution shapes in simple detached breakwater case scenarios. This will be done by a comparison with analytical solutions, commonly accepted by coastal engineers. These solutions are based on static equilibrium beaches. Therefore, some preliminary simulations have to be done prior to comparing with analytical solutions to determine the simulation time that is required to reach a static equilibrium in the model. This is done by varying the wave angle and wave spread for the same tombolo and salient setups used in the sensitivity analysis. For all other input parameters, the default set of input parameters shown in green in table 6 of section 3.2.4. above and the boundary conditions as shown in table 5 of section 3.2.2. will be used unless otherwise stated.

3.3.1. Preliminary simulations

The purpose of the preliminary simulations here, is to determine the simulation time that the model takes for a particular setup to reach an equilibrium state. The adaptive timestep multiplier has been increased to a factor 11 due to the use of relatively slow Kamphuis formulas and the long simulation time needed to find the static equilibrium. It was found that at this adaptive timestep multiplier, the ShorelineS model would simulate 3 months roughly as quick as the CERC3 formulas. Additionally, to compensate for any unwanted numerical instabilities as a result of this, the smoothing factor has also been increased to 0.05. This is still significantly below the recommended maximum of 0.1 by Roelvink et. al. (2020). From the results of the simulation time tests it became apparent that the updrift shoreline is in equilibrium long before the downdrift erosion side as can be seen in the figure 32 below. While the accretion distance has settled after 2-3 years, the erosion distance only settles after approximately 9 years.

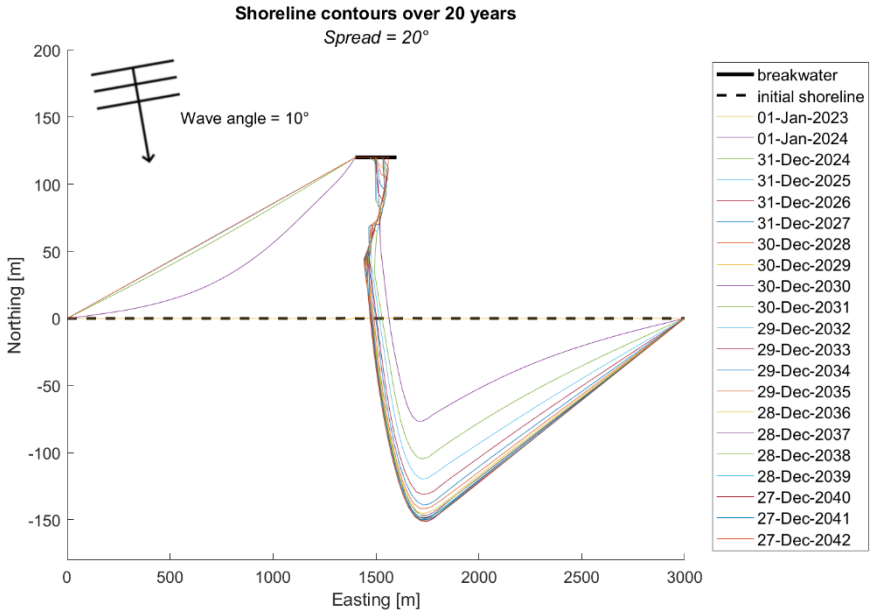

Figure 24: Shoreline contours over 20 years with a wave angle of 10° and a spread of 20°. Xb=120m, Lb=200m

On average, with these tested wave angles, spreads and structure characteristics, the model takes 2-3 years to reach a static equilibrium for cases where the wave angle is perpendicular. This then increases based on wave angle and wave spread. The full results for equilibrium time for the tested setups can be read in table 7 and the shoreline contours can all be found in Appendix B.1.

Table 7: Static equilibrium time simulation setups and determined equilibrium time

SIMULATION	WAVE ANGLE [°]	WAVE SPREAD [°]	OFFSHORE DISTANCE [M]	BREAKWATER LENGTH [M]	EXPECTED RESPONSE	EQUILIBRIUM TIME
1	0	0	120	200	Tombolo	2 years
2	0	40	120	200	Tombolo	error
3	0	20	120	200	Tombolo	3 years
4	10	20	120	200	Tombolo	7 years
5	20	40	120	200	Tombolo	10 years
6	20	0	120	200	Tombolo	error
7	0	20	200	150	Salient	2-3 years
8	0	0	200	150	Salient	2 years
9	10	20	250	150	Salient	error

3.3.2. Model validation approach

In section 2.3.4. of the literature research, several different analytical solutions for the shoreline formation behind a single detached breakwater have been presented. The Salient and Tombolo parameter relations for static equilibrium beaches as presented by Khuong (2016) and Hsu & Silvester (1990) will be used to validate the model. From the results of the static equilibrium simulation time tests, it became apparent how much simulation time will be used to simulate the model to reach a static equilibrium in the end

Salient parameters

A recent study by Elghandour (2018), just after the first release of ShorelineS, has already explored the ShorelineS model performance for salient configuration behind a single detached breakwater and compared it to the analytical solutions by Khuong (2016) and Hsu & Silvester (1990) which are only valid with a perpendicular wave angle. Therefore, there is no need to do this extensively anymore. However, several other functions and changes in the model have been implemented after the study by Elghandour (2018), so a simple check will still be performed using the parameters in table 8 (run 1 and 2).

Tombolo parameters

In the recent study by Elghandour (2018), it is mentioned that a comparison of the ShorelineS model results with the tombolo width parameter described by Khuong (2016) would be valuable. In this research, this comparison will be made to reflect upon the accuracy of the tombolo width resulted from the ShorelineS model. This solution only describes tombolos as a result of perpendicular waves in the form of a ratio of tombolo width (T) and offshore distance (X_0).

3.3.3. Model validation setup

For the validation of the model, the setup will be varied in breakwater length and offshore distance to create several different dimensionless length ratios to be tested as shown in table 8 below.

Table 8: ShorelineS model configurations for comparison with tombolo and salient parameters suggested by analytical solutions

RUN	BREAKWATER LENGTH (LB)	OFFSHORE DISTANCE (X0)	WAVE ANGLE	WAVE SPREAD	EXPECTED RESPONSE	T/X_0 (KHUONG, 2016)	X/L_B (HSU & SILVESTER, 1990)	X/L_B (KHUONG, 2016)
1	150m	200m	0°	0°	Salient	0.138	0.938	0.863
2	150m	200m	0°	40°	Salient	0.138	0.938	0.863
3	200m	120m	0°	0°	Tombolo	0.92	0.382	0.345
4	200m	150m	0°	0°	Tombolo	0.63	0.491	0.445
5	150m	150m	0°	0°	Mixed	0.35	0.678	0.62
6	250m	150m	0°	0°	Tombolo	0.92	0.382	0.345
7	250m	250m	0°	0°	Mixed	0.35	0.678	0.62
8	150m	120m	0°	0°	Tombolo	0.56	0.528	0.48
9	120m	120m	0°	0°	Mixed	0.35	0.678	0.62
10	350m	250m	0°	0°	Tombolo	0.69	0.465	0.421

3.3.4. Model performance approach

The performance of the model to predict the shoreline shape behind detached breakwaters (RQ2) will be assessed by comparing the model with spiral bay geometry solutions as presented in section 2.3.4.

Spiral bay geometry

The spiral bay geometry analytical solution (Hsu, R., & Xia, 1989) as elaborated upon in section 2.3.4. is an analytical solution for connected beaches to structures and provides a solution for beaches in static equilibrium. In contrast to the previous two analytical solutions, the spiral bay geometry can also be used to check the model performance from the static equilibrium beach that was subject to a wave angle, not necessarily perpendicular to the shore. Therefore, the following simulation configurations in table 9 will be made to check against the spiral bay geometry solution. Additionally, it was decided that it would also be interesting to see how the CERC3 transport formulas that are frequently used by IMDC would compare to the KAMP formulas in the case detached breakwater tombolos. The simulation setup for the performance tests are shown in table 9 below;

Table 9: ShorelineS model configurations for comparison with analytical solutions by spiral bay geometry.

RUN	BREAKWATER LENGTH [M]	OFFSHORE DISTANCE [M]	WAVE ANGLE [°]	WAVE SPREAD [°]	TRANSPORT FORMULA	SIMULATION TIME [YEARS]
1	200	120	0	0	KAMP	5
2	200	120	0	0	CERC3	5
3	200	120	10	10	KAMP	7
4	200	120	10	10	CERC3	7

3.4. Implementation of cross-shore sediment transport (RQ3)

The bar-berm material exchange functions as made by Larson et. al. (2016), are in a format that could easily be used in a one-line numerical shoreline model like ShorelineS. Adding formulations for cross-shore sediment transport to longshore transport one-line numerical model may increase the accuracy of the model predictions without too much effect. In this section, a possible implementation is explored by first identifying where the bar-berm exchange functions could be implemented in the model and second, how these functions can be adapted to ShorelineS parameters.

3.4.1. Cross-shore formulations in the model structure

The current model structure as shown in figure 3 in section 2.1.3. can be used to identify a possible location for cross-shore functions to be implemented. Considering the cross-sediment should be added or subtracted from the longshore transport, equation 8 in section 2.1.6 can be rewritten as shown in equation 28. Therefore, the cross-shore effects of longshore transport should be implemented directly after the longshore transport computation and before any of the boundary conditions are applied.

$$\frac{\partial n}{\partial t} = -\frac{1}{D_c}\left(\frac{\partial Q_s}{\partial s} - q_B\right) - \frac{RSLR}{\tan\beta} + \frac{1}{D_c}\sum q_i \tag{28}$$

Where;

t = time [yr].
D_c = the active profile height [m].
Q_s = longshore transport [m^3/yr]. (see section 3.3)
β = profile slope between the dune and depth of closure (average).
$RSLR$ = relative sea level rise [m/yr].
q_i = source/sink term [m^3/m/yr].
q_B = transport rate towards the bar [m^3/m/yr]

3.4.2. Cross-shore formulations implementation

In section 2.2.2., equations 15, 16 and 17 have been gathered from the literature research that could potentially be used to implement cross-shore effects in a one-line numerical shoreline change model. Here, the first step will be made towards the implementation of these functions. First, unknown variables need to be defined in the model and existing model parameters are linked to the function variables.

$$\frac{dV_B}{dt} = \lambda(V_{BE} - V_B) \tag{15}$$

$$\frac{V_{BE}}{L_0^2} = C_B\left(\frac{H_0}{wT}\right)^{4/3}\frac{H_0}{L_0} \tag{16}$$

$$\lambda = \lambda_0(\frac{H_0}{wT})^m \tag{17}$$

Where;

V_B = Current bar volume [m^3]
V_{BE} = Equilibrium bar volume [m^3]
t = time
λ = rate coefficient for bar volume approaching equilibrium [-]
L_0 = deepwater wavelength [m]
C_B = dimensionless coefficient
H_0 = deepwater wave height
w = sediment fall speed
T = wave period
m = calibration coefficient

For the implementation of equations 15, 16 and 17, field data from Duck, North Carolina suggested that $m = -0.5$, $C_B = 0.08$, and $\lambda_0 = 0.002h^{-1}$ (Larson, Palalane, Fredriksson, & Hanson, 2016).

The ShorelineS model does not currently calculate any sediment fall velocity (constant) or wave length values. Sediment fall velocity as a constant in the model and wave length can be calculated as shown in equations 29 and 30 respectively;

$$w = \frac{(s-1)gd}{18v} \quad (29)$$

$$L_0 = \frac{g * T^2}{2\pi} \quad (30)$$

Where;

w = sediment fall velocity [m/s]
s = length of control line drawn [m]
g = gravitational acceleration [9.81m/s^2]
d = median grain size [m]
v = kinematic viscosity [m^2/s]
T = wave period [s]

Now, it is checked whether every variable that is needed to implement bar-berm exchange, exists in the model or can be calculated easily. Table 10 shows the relation between function variables and ShorelineS model parameters.

Table 10: definition of necessary variables for bar-berm exchange in ShorelineS

DEFINITION	FUNCTION VARIABLE	SHORELINES PARAMETER	UNIT
DEEPWATER WAVE HEIGHT	H_0	$WAVE.hstdp$	Metres
WAVE PERIOD	T	$WAVE.tp$	Seconds
RELATIVE DENSITY	s	$TRANSP.rhos/TRANSP.rhow$	-
GRAVITATIONAL ACCELERATION	g	9.81	Metres/second^2
MEDIAN GRAIN SIZE	d	$TRANSP.d50$	Metres
KINEMATIC VISCOSITY	v	$1.271 * 10^{-6}$	Metres^2/second

3.4.3. Implementation testing

After implementation of cross-shore effects, the model will be tested to compare the differences. The model setup for this test is equal to the tombolo cases in the sensitivity analysis for a wave angle of 45°. For this model test, the same boundary conditions will be used as used in the sensitivity analysis shown in table 5 in section 3.2.1.. Other input parameters regarding the wave climate and beach characteristics will be set to their default sensitivity analysis values, as shown in table 6 in section 3.2.4. in green.

Since the implementation of cross-shore bar-berm material exchange requires the user to set the starting volume of the bars, two options will be tested. One where the bar volume at the start $V_{B0} = 0m^3$ and one scenario where the bar volume at the start of the simulation is equal to the expected equilibrium bar volume for the straight beach $V_{B0} = V_{BE0}$ which can be calculated using equation 16 and the average wave climate.

4. Results

4.1. Sensitivity analysis results

All the sensitivity analysis results can be found in appendix A. Here, the most important results will be presented. The results reflect the expectation as described in section 3.2.5. very well.

Most sensitive parameter

From the sensitivity analysis results, the wave height seemed to be the parameter that had the most influence on the shoreline evolution. This could best be seen in the case for the salient scenario where a 40% increase in wave height resulted in a 250% increase in erosion volume and roughly 100% increase in erosion distance. An example of this can be seen in the result of the sensitivity of wave height in the case of the salient configuration with a wave angle of 20° as can be seen in the figures below.

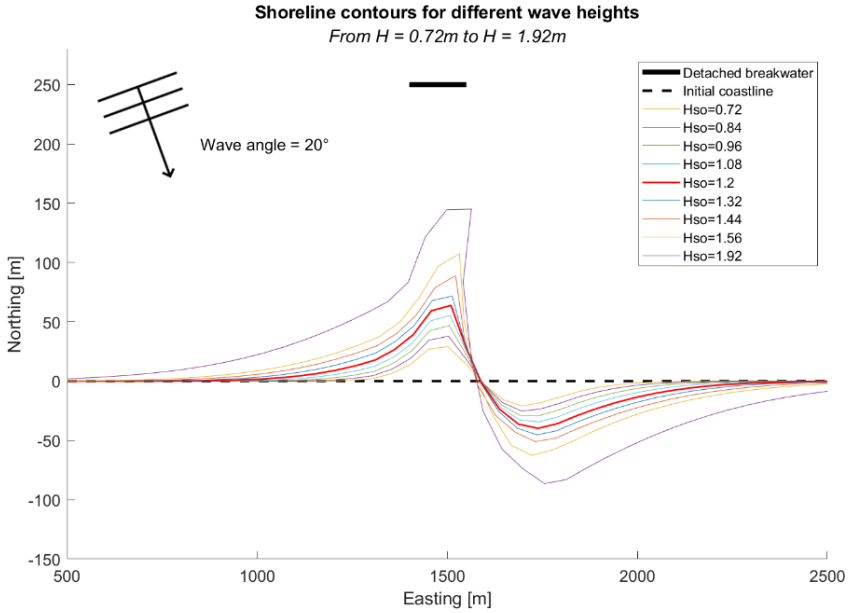

Figure 25: Shoreline contours for different wave height in the case of a single salient detached breakwater (red line is the default value).

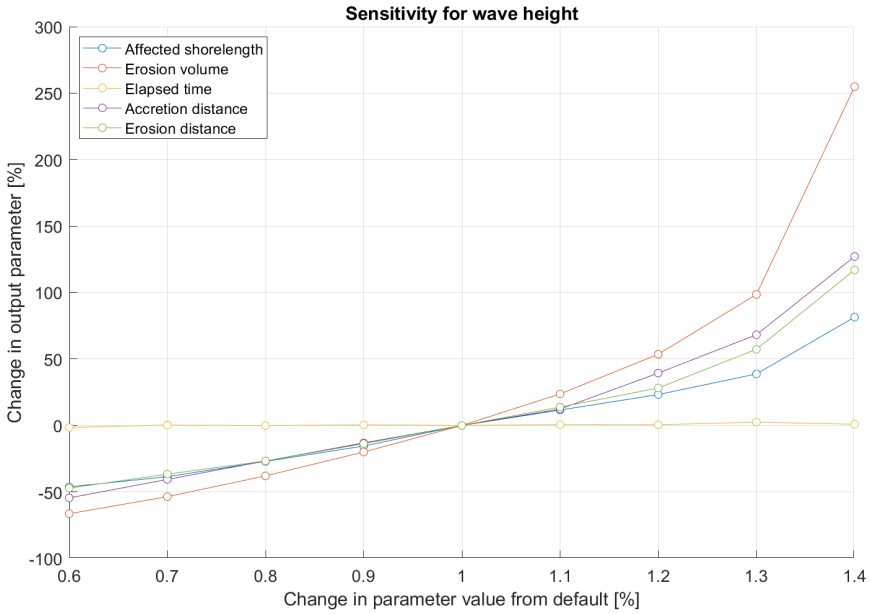

Figure 26: Sensitivity of shoreline quantification parameters for a change in wave height (x-axis) in the case of a single detached breakwater and a wave angle of 20°.

Impact of mean bed slope

The sensitivity of the shoreline for a change in bed slope is low relative to the wave height or wave period sensitivity, where a 40% increase in mean bed slope would only result in a 20% increase in affected shoreline length for each scenario and depending on the scenario, 10% to 40% increase in erosion volume. However, a change in mean bed slope would result in a shift in shoreline position evolution sideways towards the updrift side with increasing mean bed slope, in addition to an increase or decrease of shoreline volume shoreward/landward. An example of this can be seen in the result of the sensitivity of wave height in the case of the salient configuration with a wave angle of 20° as can be seen in the figures below. Also, the mean bed slope tended to follow a positive relationship for larger wave angles and a negative relationship for lower wave angles.

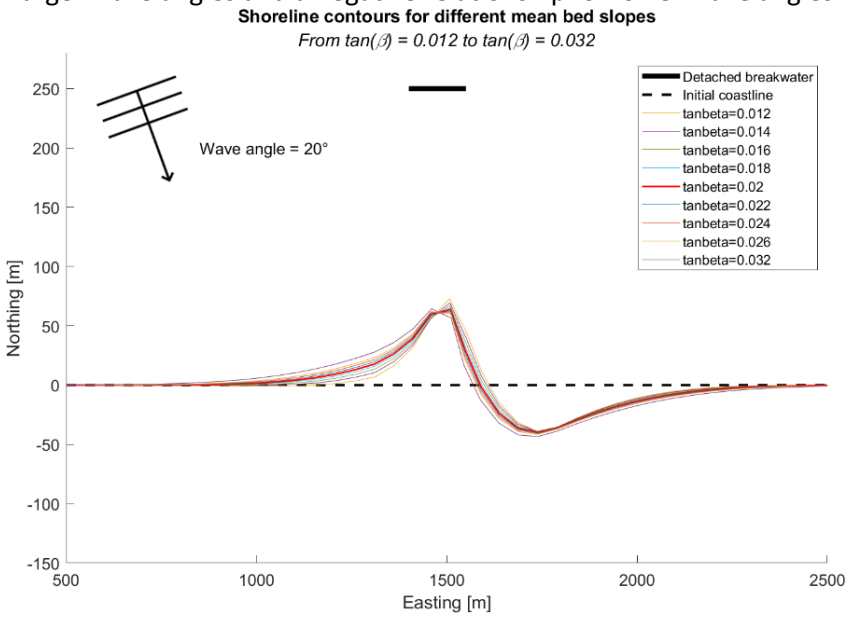

Figure 27: Shoreline contours for different mean bed slope in the case of a single salient detached breakwater (red line is the default value).

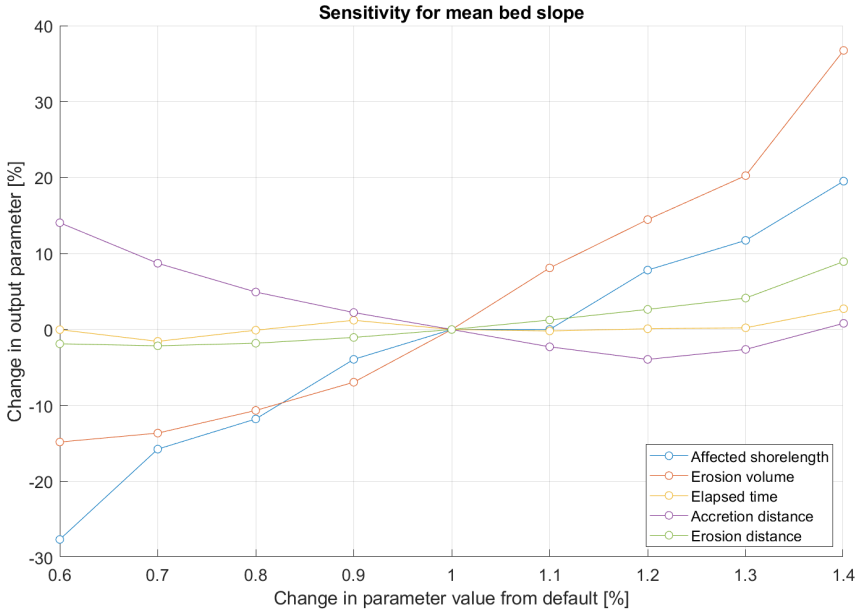

Figure 28: Sensitivity of shoreline quantification parameters for a change in mean bed slope (x-axis) in the case of a single detached breakwater where the wave angle is 20 degrees for the salient scenario

Difference between Salient and Tombolo structure parameters

The sensitivity of the shoreline erosion volume is significantly larger in the case of the salient structure configuration. Where the erosion volume in the case of the tombolo would not exceed a 100% increase for a 40% increase in wave period, in the case of a salient structure, the erosion volume increased by roughly 200%. The other quantification parameters showed less significant differences across scenarios but still, the salient scenario is for almost each parameter and each shoreline quantification measure, more sensitive. An example of this can be seen in the result of the sensitivity of wave height in the case of the salient configuration with a wave angle of 20° as can be seen in the figures below.

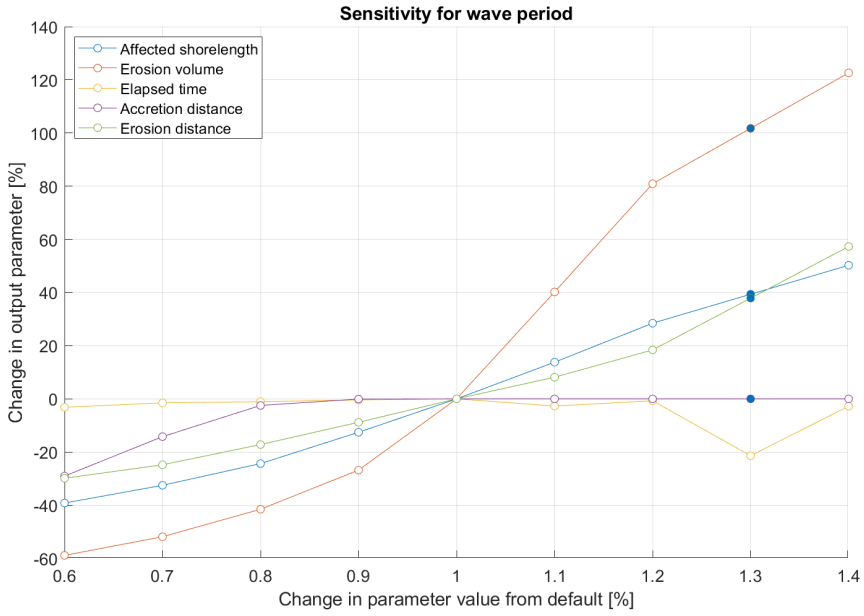

Figure 29: Sensitivity of shoreline quantification parameters for a change in wave period (x-axis) in the case of a single detached breakwater where the wave angle is 20 degrees for the tombolo scenario. (markers are interpolated value for errors.)

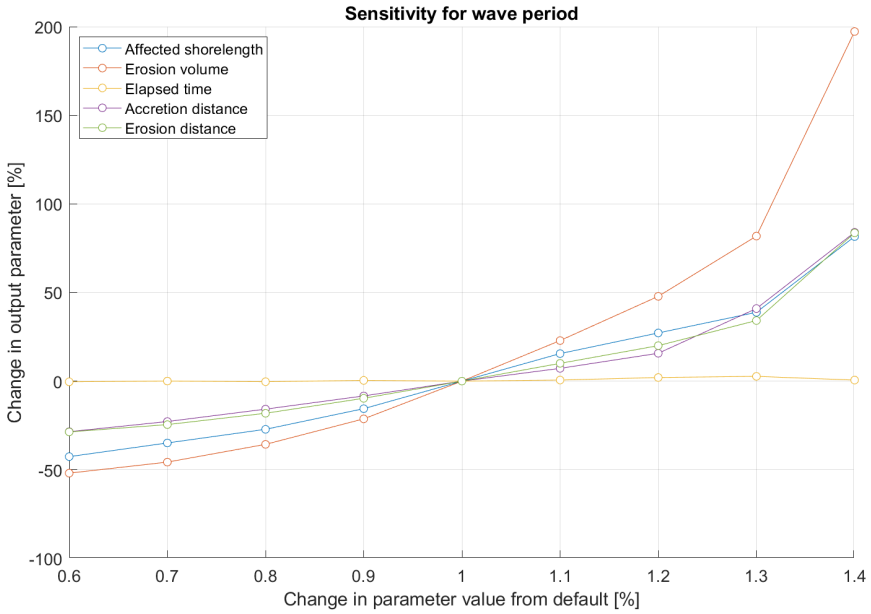

Figure 30: Sensitivity of shoreline quantification parameters for a change in wave period (x-axis) in the case of a single detached breakwater where the wave angle is 20 degrees for the salient scenario.

Differences between shoreline quantification parameters

For the salient scenarios, the erosion volume is almost always the most sensitive shoreline quantification parameter. However, in the tombolo scenarios, especially for changes in the mean bed slope, the affected length and erosion distance are approximately as sensitive as the erosion volume. In the tombolo scenarios, the accretion distance changes are almost negligible. This can all also be seen in the example in figure 30, for the salient and tombolo scenarios where the wave angle is set to 20° and the change in input parameters is +40%. The comparison for all other cases can also be found in appendix A.7.

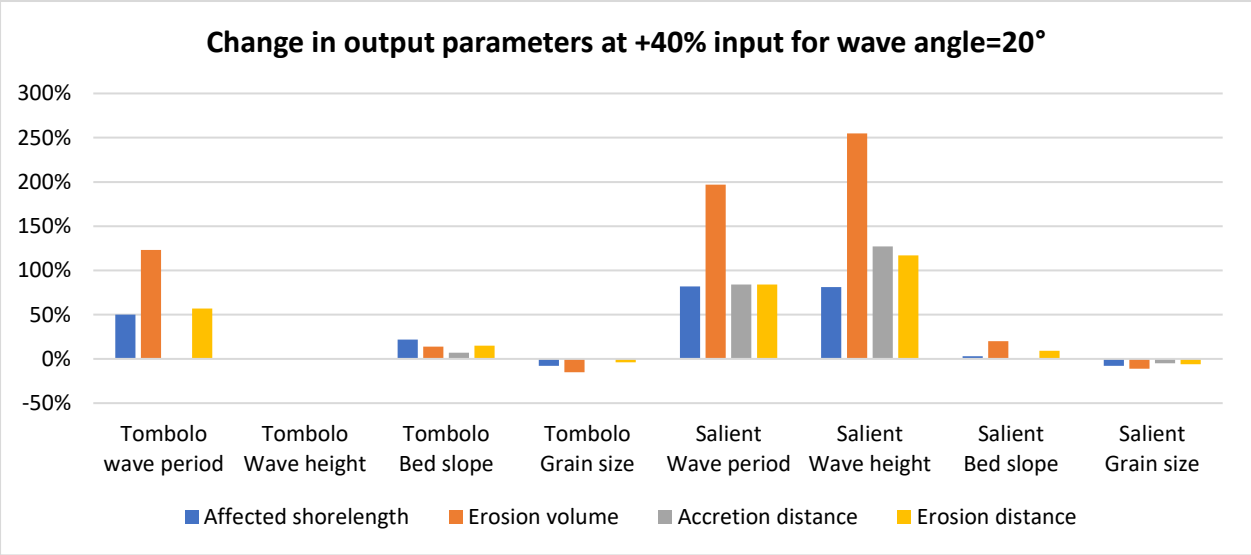

Figure 31: Change in output parameters at +40% input for case in the x-axis and wave angle=20°.

Impact of median grain diameter

In contrast to the other tested parameters of wave height, wave period, and mean bed slope, the median grain diameter shows a negative relationship with the shoreline quantification parameters, where an increase in median grain diameter would mostly lead to a decrease in measured effects. Additionally, the median grain diameter was deemed the least sensitive in most scenarios. However, a change in median grain diameter showed larger variability in shoreline shape in the accretion zone in compared to the erosion zone. The most extreme example of this is shown in the figure below from the tombolo case where the wave angle was 20°.

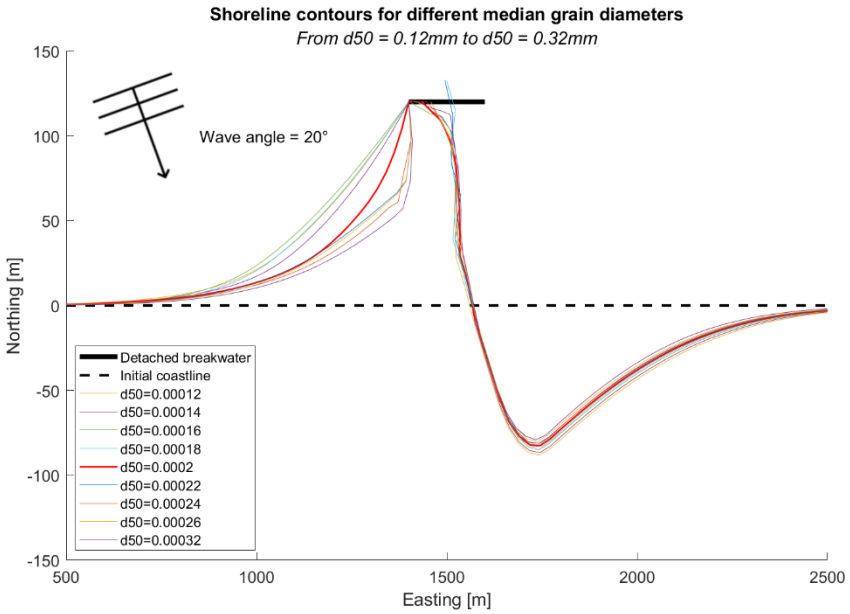

Figure 32: Shoreline contours for different median grain sizes in the case of a single tombolo detached breakwater (red line is the default value).

Wave angle versus perpendicular wave sensitivity

More extreme values for the tested input parameters seemed to have the tendency to form wider tombolos. This is likely because the longshore transport is so large that there is no time for the model to slowly develop the proper tombolo shape as you might expect.

Elapsed time

No significant results have been gathered from the inclusion of the elapsed time in the sensitivity analysis. By a change of input parameter, the elapsed time rarely changed by a value larger than 1%. Therefore, from the elapsed time, it can be deducted though, which simulations have resulted in an error and ended prior to the specified end of simulation time. This may also be useful in further applications.

4.2. Model validation and performance results

In this section, the results of the model validation will be presented. Additionally, the comparison with an analytical spiral bay solution according to the methodology of section 3.3.4. will be presented. With this result, an answer should be provided to research question 2: ”How does the one-line model perform in predicting shoreline evolution shapes in simple detached breakwater case scenarios?”.

4.2.1. Validation results

Tombolo parameters

In this test, the static equilibrium shoreline that results from different structure setups in ShorelineS are compared to the analytical solution provided by Khuong, (2016), which has been elaborated in section 2.3.4. of the literature research. The ShorelineS model has been simulated for different configuration of breakwater structure shown in table 8 of section 3.3.3. The model results compared to the solution provided by Khuong is shown in the figure below.

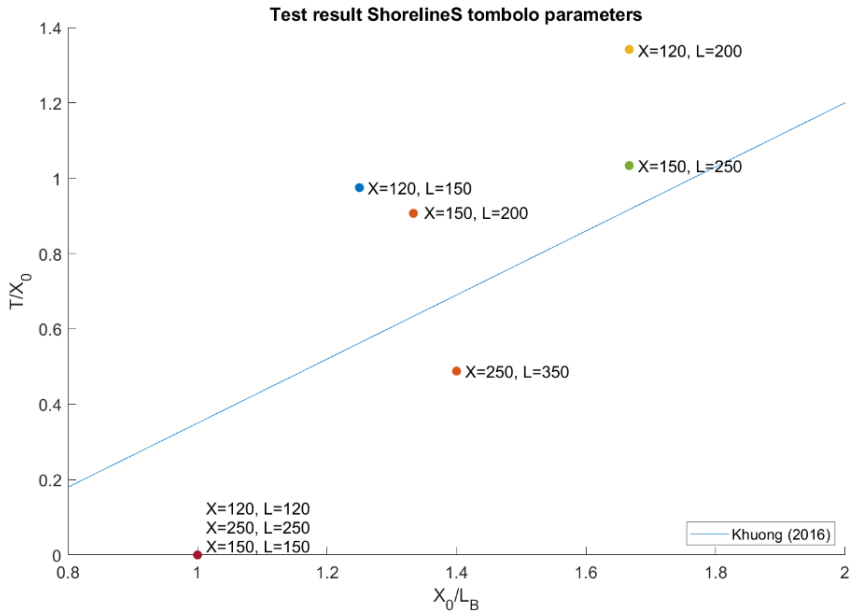

Figure 33: ShorelineS model results for tombolo parameters compared to the analytical solution by Khuong, (2016).

The model does not seem to develop a tombolo in the cases where the dimensionless breakwater length (L_B^*) is close to the boundary condition for tombolo formation as suggested by Hsu & Silvester (1990) and Khuong (2016). Other than this, the model seems to perform okay and is able to predict some sort of tombolo formation that does not deviate much from the analytical solution. All output shoreline contours used for the construction of figure 33 can also be found in Appendix B.3. Since some of the expected tombolo configurations actually resulted in salient static equilibrium shorelines, these will also be included in the salient parameter results.

Salient parameters

The tombolo test resulted in a few salient formations that have thus, also been included in this test. The result of this test is shown in figure below. The resulting shoreline contours for the two salient configuration setups can be found in Appendix B.2.

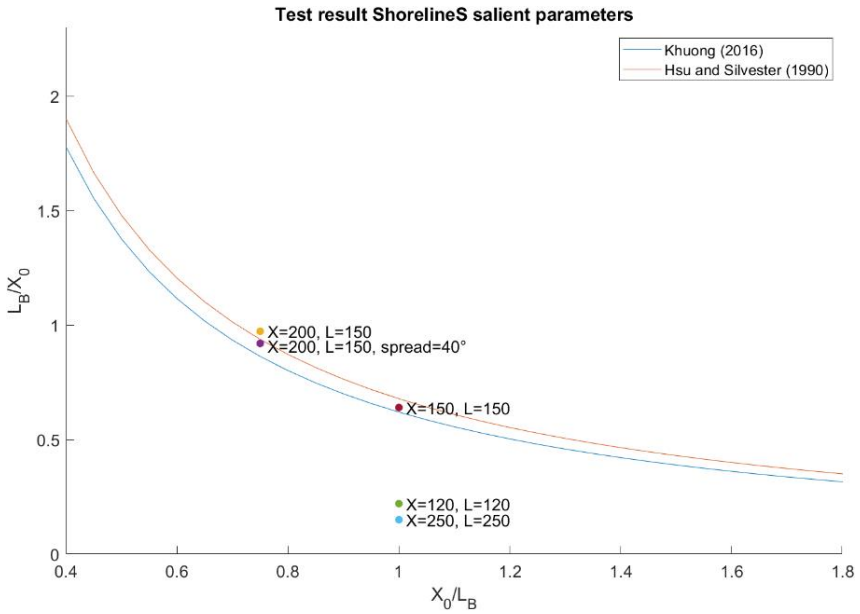

Figure 34: ShorelineS model results for salient parameters compared to the analytical solutions provided by Khuong (2016) and Hsu & Silvester (1990).

For the salient configurations that are not close to the boundary condition for salient formation the model is deemed accurate. The salient formations that are close to the boundary resulted in more inaccurate results but this was also the case for Elghandour (2018). The model settings were able to reproduce the findings from Elghandour (2018), supporting the validation of the current model setup.

4.2.2. Model performance results

The results of the spiral bay geometry comparison for the simulations setups as elaborated in table 9 of section 3.3.4. can be seen in figure 35 and figure 36.

Perpendicular wave angle

For the perpendicular wave angle in figure 35, the developed tombolo by the model is approximately 70 meters too wide compared to the solution suggested by the spiral bay geometry. This is an overestimation in tombolo width of roughly 60% which is in correspondence with the earlier observed results from the tombolo parameters in figure 33 for this case. The CERC3 transport formula would not even develop a tombolo and instead, developed a small salient within the simulation time. This was further tested and is elaborated in the discussion section 5.6.

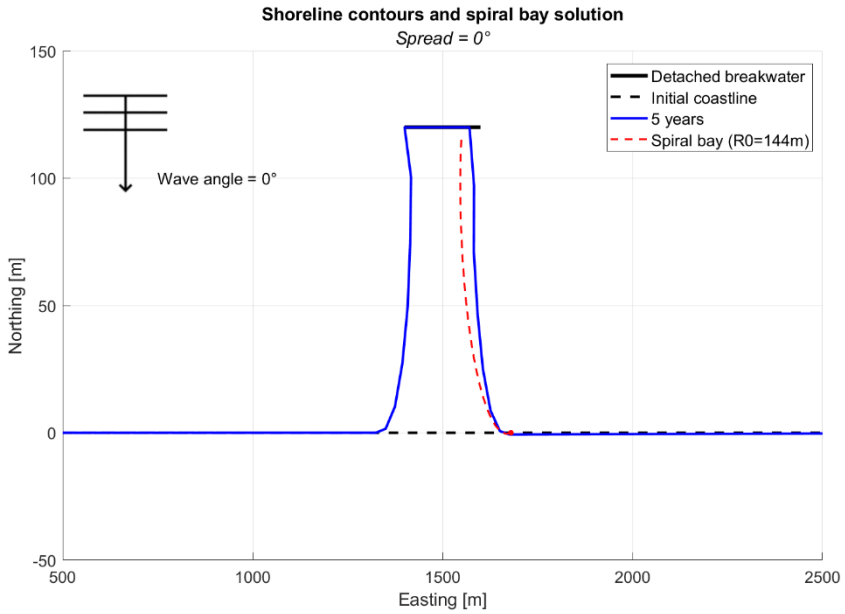

Figure 35: ShorelineS tombolo result in the case of perpendicular wave angle compared to spiral bay geometry solution.

Persistent angled wave

For the scenario with a persistent angled wave of 10°, it can be seen that ShorelineS severely overestimates the static equilibrium shape. The static equilibrium in the model is already reached after 3 months for KAMP and 1 month for CERC3. There are some inconsistencies in the shoreline near the structure but these can be simply ignored. The scenario tested for CERC3 formulas seems to represent the shape of the spiral bay geometry better than KAMP. For the case of KAMP transport, the model overpredicts the erosion distance and the beach recovers too quick. However, CERC3 does show some numerical dispersion after some time in the form of tooth like shapes as can be seen in figure 32 on the right and would not reach the 7 years of simulation time.

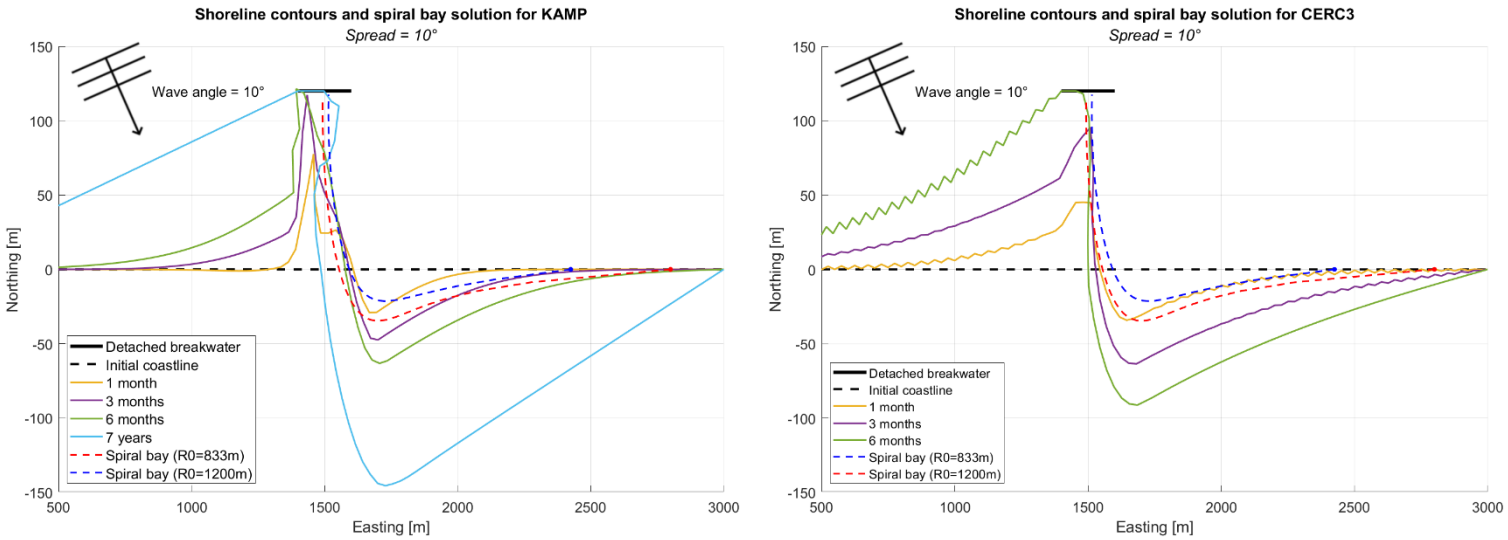

Figure 36: ShorelineS tombolo results in the case of a wave angle of 10° and CERC3/KAMP transport compared to spiral bay geometry solutions with varying scaling radii (R0).

4.3. Implementation of cross-shore effects

As of writing this report, the implementation of cross-shore effects has not been finalized due to time constraints. The coordinate system of the bar material at any point along the coast is not able to convert when the shoreline grid changes. 1 month of simulation has eventually been used since the shoreline grid has not changed within this timeframe. The largest deviation compared to the original model occurs in the tip of accretion zone, where the difference is approximately 1m as can be seen in figure 37. This means that after 12 months simulation time, there is a possibility for the model to develop a 12 meter difference. However, this is highly unlikely since by this time it will have reached the structure already and with the results as shown in figure 33, no further expectation can be drawn. The rest of the shoreline shows negligible differences between the model with implemented bar-berm material transport function and the original model where the deviation does not exceed 0.1m anywhere on the shore. After reaching a static equilibrium in 5 years, this deviation is expected to only be roughly 5m at maximum which might not be worth the additional simulation complications like additional parameters.

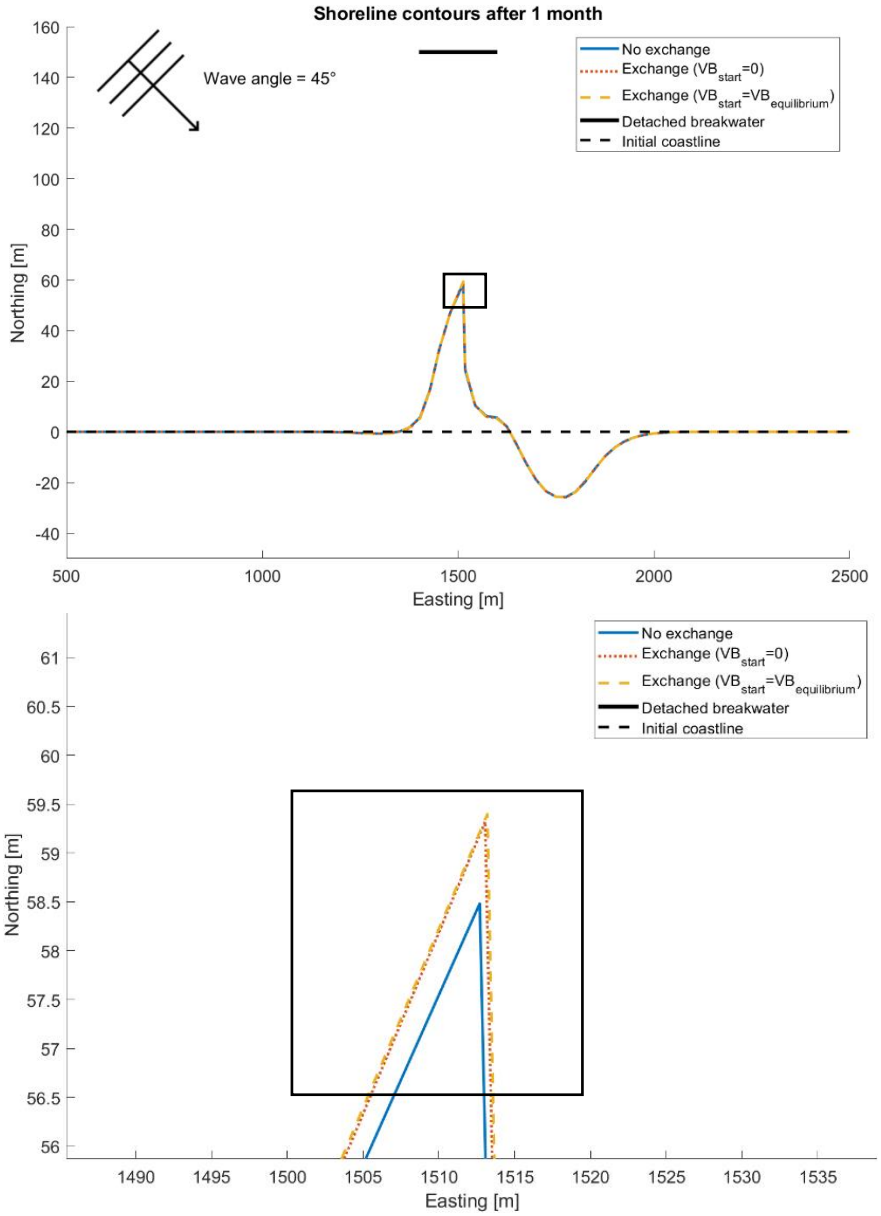

Figure 37: ShorelineS model result after 1 month of simulation with bar-berm exchange implementation

5. Discussion

Overall, the model has its limitations regarding the simulation of detached breakwaters. Expected salient formations should be limited to small angles. Tombolo formations for relatively normal wave angles are too wide. Tombolos at a wave angle are surprisingly accurate compared to analytical solutions but should still be assessed by coastal engineering experts due to numerical instabilities. These numerical instabilities, like shoreline gaps or spikes, are mainly caused by wave angle spread and non-resolved spike formations. Additionally, this research has not taken into account a seasonal variation in wave height and the influence of the scaling parameter for longshore transport. Bar-berm exchange has been chosen to implement but this also comes with its limitations and assumptions that were made.

5.1. Sensitivity analysis

The change in accretion distance in the tombolo cases are caused by numerical instabilities in the model where the shoreline either moves through the structure or the shoreline creates a gap. This gap will be elaborated upon in the discussion section 5.6. For the case of tombolos structure characteristics and 0° wave angle, the accretion distance actually does change since the accumulation form does not reach the structure in all cases. Therefore, part of these results are actually salient cases.

5.2. Seasonal variation in wave height

Seasonal variation in wave height has not been taken into account for these simulations. This is not needed when only considering longshore transport but after a possible implementation of some cross-shore effects, these seasonal variation play a larger role. This could also be an important factor why the difference between the original model and the model with implemented bar-berm exchange is so small.

5.3. Scaling parameter

No consideration has went to the scaling parameter for longshore transport. Therefore, the impact of this parameter is unknown. This is a parameter that is normally used to scale the speed of the shoreline evolution in the model to the real world scenario using historical data. The simulations have all been performed with the scaling parameter set to $qscal = 1$. Scaling this parameter would result in the need to scale sensitivity and static equilibrium simulation time accordingly.

5.4. Bar-berm exchange

According to Larson et al. (2016), the bar-berm exchange is a process that occurs with annual changes and can also occur event-based. By implementing it in ShorelineS, it has been assumed that it could also be used naturally for monthly to centennial timescales. It has also not been tested for an event-based occurrence. Additionally, the implementation has not been finalised yet and no calibration has been performed on the evolution speed of bars in the model. Therefore, this leaves a lot of uncertainty to be questioned about the results of the bar-berm exchange. So far, it showed at least a little effect.

The calibration coefficients C_B, λ_0 and m in equations 16 and 17 have not been calibrated against data but were set equal to the calibration coefficients used by Larson et al. (2016) which was calibrated against beach in Duck, North Carolina. In their research, the field site showed a large difference in time scales with the large wave tank which indicated that the field site would grow bars larger and the response would be slower. Additionally, they also introduced a multiplier that has not been introduced in this model yet. This multiplier made sure to reduce the rate of transport only when onshore transport occurred.

Currenlty, the bar volume is located on the coastline itself. Ideally, a dynamic boundary at a distance from the shoreline would be created where the bar volume is accounted for. This would however, add another degree of complexity while this current implementation has not even been finalized yet. Though, this would avoid the cases where narrower parts of the coast or indentations where the same bar volume is spread over more length of the coastline.

5.5. Validation tests

For the tombolo parameters, it was concluded that ShorelineS did not accurately predict the width of a tombolo. Mostly, the width of the tombolo was overestimated by as much as 50%. This could be due to the usage of a fixed cross-shore profile and active profile height. However, the depth of closure is dependent on the wave height (Hallermeier R. J., 1978). The wave height is adjusted in the zones of wave diffraction but the depth of closure is not. Not adjusting the depth of closure could lead to different results since the transformation of the beach is also dependent on the closure depth. What is also noted is that from the simulations performed by Elghandour (2018), it seemed that the tombolos in his simulations for formed significantly less wide than the tombolos in this research. The cause of this is due to different boundary conditions (closed) and a shorter shoreline. Despite this, in this research, the boundary conditions were kept at 'Neumann' boundary conditions and a longer shoreline in consultation with IMDC.

In the validation test for salient parameters, it has been concluded that the salient parameters are still similar to the ones by Elghandour (2018). The same dimensionless length (L_B^*), resulted in both cases in a good fit with the empirical solutions by Khuong and Hsu & Silvester. However, they are not equal. Using the same approach, this research salient parameters were slightly lower by approximately 10%. This difference could have been caused by a difference in model setup. Elghandour (2018) uses a different peak wave period and closure depth than this research. Additionally it is not explicitly stated how much simulation time was taken before his results were gathered. A longer simulation time in his research could have lead to a little more growth of the salient compared to this research.

5.6. Model instability issues

Tombolo formation

During the simulations that have been carried out in ShorelineS, it has also been noted that a model configuration using the CERC transport formulas, is unable to form a tombolo after any arbitrary time when the wave angle is set close to zero as shown in figure 38.

For the final sensitivity analysis, the simulation time had been increased to 5 months, to be able to generate some tombolos during the simulation. However, with a perpendicular wave angle, the longshore transport remained too small for a tombolo to form within 5 months for the default settings as well. The purpose was to be able to compare a default set that would generate a tombolo to a default set that would generate a salient. For this, a longer simulation time would have to be used. Also, the simulation time of 5 months was not reached by the Salient case where the wave angle was 20° and the tombolo case where the wave angle was 45° due to prematurely occuring errors in the simulation.

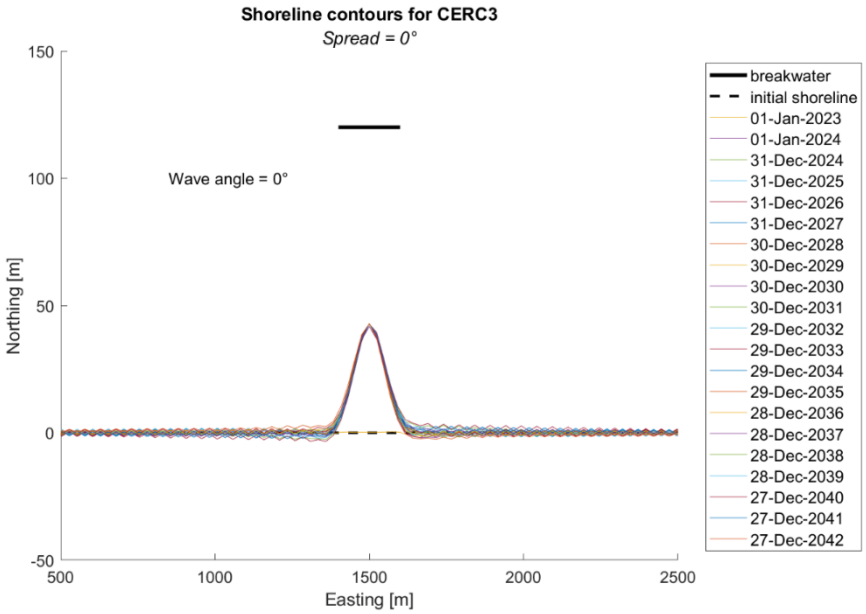

Figure 38: Salient instead of Tombolo formation for CERC3 transport of wave angles

Frequent occuring errors in the tombolo cases

In the case of the formation of a tombolo, one error frequently occurred above all others. The message of the error being:" Array indices must be positive integers or logical values." The location of this error was identified to be at Line 81 of the "transport_boundary_condition.m" function.

This appeared to happen whenever a very small spit would split of the coastline that is not sufficiently able to calculate the transport on it due to the limited amount of nodes of two, where it needs at least three nodes to calculate some type of transport. This also results in the formed spit the have the shape of a line instead of being a closed polygon. This would therefore mean that either the "get_spikesremoved.m" function is not working properly for removing all spikes or that the splitting of coastlines need some type of constraint when to split that would not allow for these types of cases to happen. Ultimately, this is not an error in either of these as spikes should not be able to develop in the first place. The smoothing factor could be increased for this but this would also result in straightening of the coastline and a significant, non-negligible loss of transport.

Despite the fact that an error catch loop was built around the ShorelineS script which would be able to log an error and continue simulating if it occurred, MATLAB stopped working as well sometimes. The cause of this is not clear and this happened throughout all simulations performed for this research. Sometimes this was solved by just trying to run the simulation again and hoping for a better result and sometimes, a small change in adaptive time step multiplier, smoothing factor or space step would solve this issue. Other times, no result was gathered as it would repeat the crash. This was also the case for the sensitivity analysis where the salient setup of 20° wave angle and tombolo setup of 45° could not be simulated whole the way to 5 months. Therefore, these results are from a simulation time of 3 months instead.

Shoreline gaps

Since the sensitivity analysis is uni-variable, the model has simulated the same set of input parameters four times, which was the default setup. If the result of the sensitivity analysis is used to compare the 4 identical default model setups, the results between the sensitivity analysis result show a peculiar result. In one case, when doing the sensitivity for the mean bed slope, it can be seen

that a gap has occurred where the shoreline is not attached to the structure anymore as shown in the figure below. This also happened more often for different configuration and is not case specific. However, it was noted that it happened significantly more frequent when wave spreading was enabled and even more frequent when the wave spreading was larger than twice the wave angle with respect to the shore normal.

Whenever one of the two detached shorelines sections (green in figure 39) grows back towards the structure again, the model crashes in an attempt to find a second intersection between the structure and the shoreline that does not exist in “merge_coastlines”.

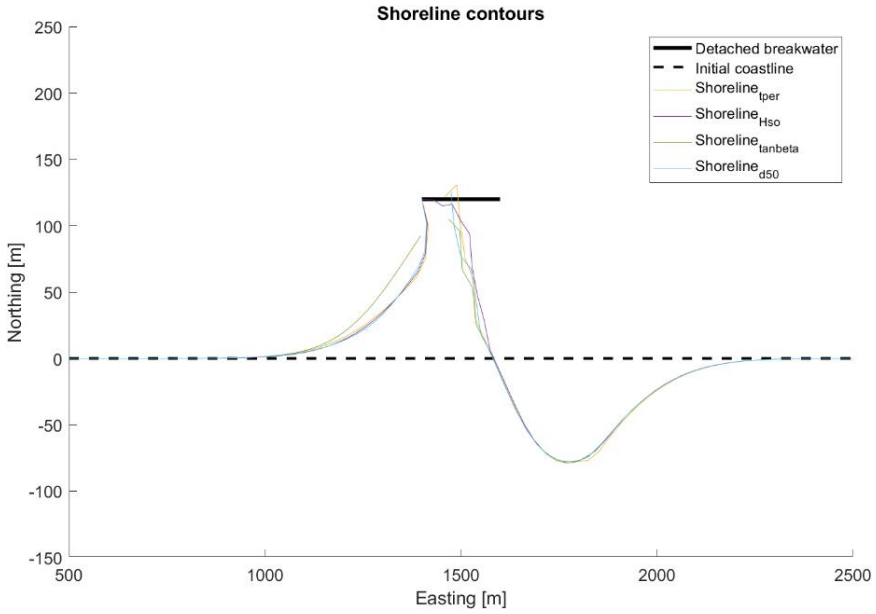

Figure 39: four shoreline contours for four equal input parameters with wave spreading enabled. Green shoreline is a shoreline with a gap.

Wave diffraction angle

If the angle to the wave crest exceeds 180 degrees, this resulted in no diffraction effects on that part of the shore close to the structure, where big lumps of non-smooth shoreline sediment was located in the shadow zone. The diffraction functions have been implemented in the case of perpendicular groynes, where an angle greater than 180 degrees does not occur.

6. Conclusion

The objective of this research was to "assess different input parameters impacts on shoreline sensitivity in a detached breakwater case study and suggest improvements for one-line numerical shoreline change models". Therefore, in this thesis, the one-line numerical shoreline change model 'ShorelineS' was subjected to a sensitivity analysis, validation tests, and a spiral bay geometry comparison. Additionally, a first effort was made for the implementation of material exchange between the bar and berm. This has all been done in the scope of a simple, emerged, detached breakwater scenario.

The first research question stated: "What is the impact of different parameters in ShorelineS on the shoreline evolutions, particularly in the case of detached breakwater scenarios?". This has been answered by means of a uni-variable sensitivity analysis. The use of Kamphuis for longshore transport took significantly more time to simulate. The second slowest transport formula (CERC3) already decreased the simulation time by ~95%. The wave height is the most sensitive parameter of the model which was expected from the Kamphuis transport formula. The magnitude of the sensitivity varied greatly over the different cases but a change of 40% in wave height resulted in a change of 240% in erosion volume over the same timeframe of 3 months. In contrast to the other tested parameters; *wave height, wave period* and *median grain size,* the mean bed slope also shifted the shoreline evolution sideways. The eroding part of the shore was not sensitive to changes in median grain size in contrast to the shape of the accretion zone in the same case. The initial method was to test each sensitivity for 5 months of simulation time. However, due to re occuring model issues, the case of a salient and a tombolo breakwater with a 20° and 45° wave angle respectively have been simulated for 3 months evolution instead.

The second research question stated: "How does the one-line model perform in simple detached breakwater scenarios?". The comparison with analytical solutions showed that in cases where the wave angle is perpendicular, the ShorelineS model can accurately represent salient formations as long as the dimensionless breakwater length $L_B^* \leq 0.9$. For the used boundary conditions, ShorelineS was not able to accurately predict tombolo width. For the used setup the model was also not able to form tombolos when expected using CERC formulas or when the dimensionless breakwater length (L_B^*) is close to one. When the wave angle is increased towards the applicable limit of detached breakwaters, ShorelineS severely overestimates the shape of the shoreline in equilibrium. However, this could also be due to the use of a persistent wave angle instead of a wave angle that changes over the course of the year. The wave diffraction implemented in the model has also been purposed for groynes that do not experience diffraction in angles greater than 180°. However, this case does occur when tombolos are formed with detached breakwaters making the shoreline close to the structure unstable and not accurate.

The third research question stated: "How to account for cross-shore sediment transport in a one-line shoreline change model?". This has partially been answered by providing a start to implementing bar-berm exchange in the ShorelineS model. This was not fully completed due to time constraints. The preliminary results did not show any significant results. After 1 month of evolution, the new shoreline was still almost exactly equal to the original shoreline with a maximum deviation of 0.1m everywhere expect for the tip of the accretion zone. Here, the difference was approximately 1m. When forming a tombolo, the maximum deviation is expected to not exceed 5m from the original model. Some assumptions have been made by implementing bar-berm exchange. It consists of empirical formulas developed for decadal timescales and it is unknown how these would scale to monthly or centennial timescales. Due to research time constraints, the calibration coefficients have also not been calibrated but were set equal to the ones found for a beach in Duck, North Carolina.

7. Recommendations

7.1. Complete bar-berm material exchange

The results of the bar-berm material exchange are presented after 1 month of simulation since it has not been finalised. The bar volume (V_B) does not change along with a regridding of the coastline. To implement and calibrate this would be the first recommendation for future research. For this, the bar volume at any point on that gets regridded could be interpolated while taking sediment conservation into account. Optimally, the volume of the bars at any given time could be tracked on a dynamic boundary line parallel to the coastline. However, this would take more complex computations. Though, this would solve the issue where there is a narrow space, there would also be less volume in the bars per length of coastline.

Then after this, the bar-berm material exchange could be coupled to the dune evolution module by Ghonim (2019). As transport from the berm to the bar is also dependent on the available sediment in the berm, this could be a valuable addition to the model.

7.2. More effort towards solving numerical instabilities for detached breakwaters in one-line modelling

One-line models have proven to be an efficient method of determining viable options for coastline management schemes. Detached breakwaters are frequently used coastal management solutions that are not well represented by the model currently. More effort should therefore go to fixing specifically these frequently used coastal management schemes.

7.3. Check the accuracy for other coastal structures as well

The spiral bay geometry solution already exists as a recognized engineering tool for coastal engineers. Since the ShorelineS model aims to develop a model that can be used in the same manner, it can be useful to check more cases in which the spiral bay geometry could be applied. For example shorelines between multiple headlands, segmented detached breakwater or more complex shorelines that include several different types of structures (groynes and detached breakwaters in a single setup).

7.4. Purpose of the one-line model

The purpose of one-line models is to be able to quickly and easily make decisions about viable solutions for coastal management schemes. The persistent adding of functions, options, input variables etc. into Shorelines over the past 1.5 years has kind of lost this purpose in my opinion. Clearer and more transparent assessment of the consequences of additions in usability should be considered and communicated more. The same goes for continuing with bar-berm/cross-shore material exchange. There should be considered if it would be worth adding this complexity to the model.

References

Ashton, A. D., & Murray, A. B. (2006). High-angle wave instability and emergnet shoreline shapes: 1.Modeling of sand waves, flying spits and capes. *Journal of Geophysical Research: Earth Surface, 111*(F04011), 1-19. doi:https://doi.org/10.1029/2005JF000422

Baykal, C. (2006). *Numerical modeling of wave diffraction in one-dimensional shoreline change model.* Master Thesis, Middle East Technical University, Graduate School of Natural and Applied Sciences. Retrieved from https://hdl.handle.net/11511/16451

Bosboom, J., & Stive, M. J. (2023). *Coastal Dynamics* (1.2 ed.). Delft: TU Delft Open. doi:https://doi.org/10.5074/T.2021.001

Briggs, M. J., Thompson, E. F., & Vincent, C. L. (1995). Wave Diffraction around Breakwater. *Journal of Waterway, Port, Coastal and Ocean Engineering, 121*, 23-35. doi:https://doi.org/10.1061/(ASCE)0733-950X(1995)121:1(23)

Bruun, P. (1954). *Coast Erosion and the Development of Beach Profiles.* Technical University of Denmark; U.S.A.C.E. United States, Beach Erosion Board. Retrieved from http://hdl.handle.net/11681/3426

Buijsman, M. C., Ruggiero, P., & Kaminsky, G. M. (2001). Sensitivity of Shoreline Change Predictions to Wave Climate Variability along the Southwest Washington Coast, USA. *Fourth Conference on Coastal Dynamics.* Lund: American Society of Civil Engineers. doi:https://doi.org/10.1061/40566(260)63

Dally, W. R., & Pope, J. (1986). *Detached Breakwaters for Shore Protection.* Technical report, Coastal Engineering Research Center, US Army Corps of Engineers. doi:https://apps.dtic.mil/sti/citations/ADA171183

Elghandour, A. M. (2018). *Efficient modelling of coastal evolution.* Delft: UNESCO-IHE Institute for Water Eduction. doi:https://doi.org/10.25831/vh82-7w82

Evans, C., & Hsu, J. (1989). Parabolic bay shapes and applications. *Proceedings of the Institution of Civil Engineers, 87*, 557-570. doi:https://doi.org/10.1680/iicep.1989.3778

Frey, A. E., Thomas, R. C., Connell, K. J., Hanson, H., Larson, M., Munger, S., & Zundel, A. (2012). *GenCade Version 1: Model Theory and User's Guide.* Lund University, Department of Water Resources Engineering. Lund: Coastal and Hydraulics Laboratory, Engineer Research and Development Center. Retrieved from https://hdl.handle.net/11681/7333

Gao, P. (2023). *A general bedload transport equation for homogeneous grains.* Retrieved May 30, 2023, from Vignettes: Key Concepts in Geomorphology: https://serc.carleton.edu/48147

Ghonim, M. E. (2019). *Recent Development in Numerical Modelling of Coastline Evolution.* Delft: TUDelft.

Hallermeier, R. (1983). Sand Transport Limits in Coastal Structure Design. *Coastal Structures '83* (pp. 703-716). American Society of Civil Engineers. Retrieved from https://cedb.asce.org/CEDBsearch/record.jsp?dockey=0037946

Hallermeier, R. J. (1978). Uses for a calculated limit depth to beach erosion. *Coastal Engineering Proceedings*, *1*, p. 88. doi:https://doi.org/10.9753/icce.v16.88

Hanson, H. (2023). *Littoral drift and shoreline modelling*. Retrieved May 22, 2023, from Coastalwiki: http://www.coastalwiki.org/wiki/Littoral_drift_and_shoreline_modelling

Hanson, H., & Larson, M. (1998). Seasonal Shoreline Variations by Cross-Shore Transport in a One-Line Model under Random Waves. *26th International Conference on Coastal Engineering* (pp. 2682-2695). Copenhagen: American Society of Civil Engineers. doi:https://doi.org/10.1061/9780784404119.203

Hsu, J. R., & Silvester, R. (1990). Accretion Behind Single Offshore Breakwater. *Journal of Waterway, Port, Coastal, and Ocean Engineering, 116*(3), 362-380. doi:https://doi.org/10.1061/(ASCE)0733-950X(1990)116:3(362)

Hsu, J., R., S., & Xia, Y. (1989). Generalities on static equilibrium bays. *Coastal Engineering, 12*(4), 353-369. doi:https://doi.org/10.1016/0378-3839(89)90012-4

Kamphuis, J. (1992). *Computation of Coastal Morphology.* Delft: ICCE 1992 local organising committee. doi:http://resolver.tudelft.nl/uuid:042607fc-46eb-46c9-b8f1-bffc426510fe

Kamphuis, J. W. (1991). Alongshore Sediment Transport Rate. *Journal of Waterway, Port, Coastal and Ocean Engineering, 117*(6), 624-640. doi:https://doi.org/10.1061/(ASCE)0733-950X(1991)117:6(624)

Khuong, C. (2016). *Shoreline response to detached breakwaters in prototype.* Delft University of Technology, TU Delft Hydraulic Structures and Flood Risk. doi:https://doi.org/10.4233/uuid:cdae6a2f-78dc-45fe-af01-43ed39c02ccc

Komar, P. (1998). *Beach Processes and Sedimentation.* New Jersey, USA: Prentice Hall.

Komar, P., & Inman, D. (1970, October). Longshore sand transport on Beaches. *Journal of Geophysical Research, 75*, 5914-5927. doi:https://doi.org/10.1029/JC075i030p05914

Larson, M., & Kraus, N. C. (1989). *Sbeach: Numerical Model for Simulating Storm-Induced Beach Change. Report 1. Empirical Foundation and Model Development.* Science and Technology University of Lund, Water Resources Engineering. Vicksburg: Coastal Engineering and Research Center. doi:https://apps.dtic.mil/sti/citations/ADA212212

Larson, M., & Kraus, N. C. (1995). Prediction of cross-shore sediment transport at different spatial and temporal scales. *Marine Geology, 126*(1-4), 111-127. doi:https://doi.org/10.1016/0025-3227(95)00068-A.

Larson, M., Palalane, J., Fredriksson, C., & Hanson, H. (2016, October). Simulating cross-shore material exchange at decadal scale. Theory and model component validation. *Coastal Engineering, 116*, 57-66. doi:https://doi.org/10.1016/j.coastaleng.2016.05.009

Lenssinck, L. (2022, March 30). *DEL148 - ShorelineS research & development*. (B. Huisman, Editor) Retrieved June 08, 2023, from Publicwiki Deltares: https://publicwiki.deltares.nl/pages/viewpage.action?pageId=210371793

Lincoln, R., Boxshall, G., & Clark, P. (1998). *A dictionary of Ecology, Evolution and Systematics* (2nd ed.). Cambridge: Cambridge University Press.

Longuet-Higgins, M. (1970). Longshore Currents Generated by Obliquely Incident Sea Waves. *Journal of Geophysical Research, 75*(33), 6778-6789. doi:https://doi.org/10.1029/JC075i033p06778

Mangor, K. (2021). *Applicability of detached breakwaters*. Retrieved June 1, 2023, from Coastalwiki: https://www.coastalwiki.org/wiki/Applicability_of_detached_breakwaters

Mangor, K. (2023). *Detached breakwaters*. Retrieved April 20, 2023, from Coastalwiki: http://www.coastalwiki.org/wiki/Detached_breakwaters

Mangor, K., Drønen, N., Kærgaard, K., & Kristensen, S. (2017). *Shoreline management guidelines.* DHI Water and Environment.

Mil-Homens, J. (2013). Re-evaluation and improvement of three commonly used bulk longshore sediment transport formulas. *Coastal Engineering, 75*, 29-39. doi:https://doi.org/10.1016/j.coastaleng.2013.01.004.

Moreno, L. J., & Kraus, N. C. (1999). Equilibrium shape of headland-bay beaches for engineering design. *Coastal sediments '99*, (pp. 860-875). New York. doi:https://apps.dtic.mil/sti/citations/ADA483142

Overgaauw, T. S. (2021). *Modeling shoreline evolution in the vicinity of shore normal structures.* Delft: TUDelft.

Penney, W., & Price, A. (1952). Part I. The Diffraction Theory of Sea Waves and the Shelter Afforded by Breakwaters. *Philosophical Transaction of the Royal Society of London. Series A, Mathematical and Physical Sciences, 244*, 236-253. Retrieved from http://www.jstor.org/stable/91516

Roelvink, D., Huisman, B., Elghandour, A., Ghonim, M., & Reyns, J. (2020). Efficient Modeling of Complex Sandy Coastal Evolution at Monthly to Centurty Time Scales. *Fronties in Marine Science, 7*. doi:https://doi.org/10.3389/fmars.2020.00535

Roelvink, D., Huisman, B., Elghandour, A., Ghonim, M., & Reyns, J. (2020). Efficient Modeling of Complex Sandy Coastal Evolution at Monthly to Centurty Time Scales. *Fronties in Marine Science, 7*, 1-20. doi:https://doi.org/10.3389/fmars.2020.00535

Schoonnees, J., & Theron, A. (1993). Review of the field-data base for the longshore sediment transport. *Coastal Engineering, 19*(1-2), 1-25. doi:https://doi.org/10.1016/0378-3839(93)90017-3

Schoonnees, J., & Theron, A. (1996). Improvement of the most accurate longshore transport formula. *25th International Conference on Coastal Engineering* (pp. 3652-3665). Orlando: American Society of Civil Engineers. doi:https://doi.org/10.1061/9780784402429.282

Seymour, R. J. (2005). Cross-Shore Sediment Transport. In M. L. Schwartz, *Encyclopedia of Coastal Science* (pp. 352-353). Dordrecht: Springer Netherlands. doi:https://doi.org/10.1007/1-4020-3880-1_104

Seymour, R. J. (2005). Longshore Sediment Transport. In M. L. Schwartz, *Encyclopedia of Coastal Science* (p. 600). Dordrecht: Springer Netherlands. doi:https://doi.org/10.1007/1-4020-3880-1_199

starrpictures. (2023). *Oceaan achtergrond*. Retrieved from Pinterest: https://nl.pinterest.com/pin/648025833860015485/

Suh, K.-D., & Dalrymple, R. (1987). Offshore Breakwaters in Laboratory and Field. *Journal of Waterway, Port, Coastal, and Ocean Engineering, 113*. doi:https://doi.org/10.1061/(ASCE)0733-950X(1987)113:2(105)

Tan, S.-K., & Chiew, Y.-M. (1994). Analysis of Bayed Beaches in Static Equilibrium. *Journal of Waterway, Port, Coastal, and Ocean Engineering, 120*(2), 145-153. doi:https://doi.org/10.1061/(ASCE)0733-950X(1994)120:2(145)

Thomas, R. C., & Frey, A. E. (2013, December 01). Shoreline Change Modeling Using One- Line Models: General Model Comparison and Literature Review. Fort Belvoir, Virginia, United States of America: Defense Technical Information Center.

U.S.A.C.E. (1984). *Shore Protection Manual.* Department of the Army. Vicksburg: Coastal Engineering Research Center. Retrieved from https://www.academia.edu/download/60169868/shoreprotectionm01unit20190731-80620-sqg8y6.pdf

van Rijn, L. C. (2014). A simple and general expression for longshore transport of sand, gravel and shingle. *Coastal Engineering, 90*, 23-39. doi:https://doi.org/10.1016/j.coastaleng.2014.04.008

Appendix A – Sensitivity analysis

A.1. Preliminary parameter choice

Table 11: Preliminary sensitivity analysis parameter values (green values are default).

DS0	SPREAD	AW	HSO	PHIW0	TPER	TRFORM	D50	TANBETA	D
5	0	0	0.5	330	6	CERC	0.0001	0.025	4
10	10	2.5	1	315	8	CERC3	0.0002	0.02	6
25	20	5	2	300	10	KAMP	0.0004	0.0167	10
50	40		3		12	MILH		0.0125	
						VR14			

Table 12: Single detached breakwater characteristic parameter values for preliminary sensitivity analysis

SALIENT		TOMBOLO	
$X =$	250m	$X =$	150m
$L =$	150m	$L =$	200m
$L_B^* =$	0.6	$L_B^* =$	1.34

Tombolo results

	ds0 [m]	spread [°]	spread [°]	spread [°]	Aw [-]	Hso [m]	phiw0 [°N]	phiw0 [°N]	phiw0 [°N]	tper [s]	d50 [mm]	tanbeta [1/slope]	d [m]
[from]-[to]	25-50	20-0	20-40	0-40	0-5	0.5-1	45-30	45-60	30-60	6-12	0.1-0.4	0.025-0.0125	4-10
AffectedLength	-5.05%	-0.12%	0.32%	0.43%	0.02%	104.24%	12.60%	-10.60%	-20.65%	101.17%	-15.76%	-26.07%	-36.19%
ErosionVolume	-18.66%	7.67%	-13.22%	-19.40%	-0.16%	679.20%	-10.28%	-25.26%	-16.70%	336.44%	-40.34%	-76.43%	-44.57%
AccretionVolume	-18.66%	7.67%	-13.22%	-19.40%	-0.16%	679.21%	-10.28%	-25.26%	-16.70%	336.44%	-40.34%	-76.43%	-44.57%
ErosionDistance	-2.48%	0.26%	-4.90%	-5.17%	0.04%	219.53%	-2.51%	-19.20%	-17.13%	143.50%	-20.59%	-24.55%	-47.74%
AccretionDistance	-28.21%	0.42%	-1.59%	-2.01%	0.15%	189.91%	-33.82%	-30.20%	5.47%	15.67%	-8.58%	16.96%	-26.40%
ElapsedTime	-41.53%	0.12%	-0.03%	-0.15%	-0.40%	-95.43%	-3.31%	-0.58%	2.83%	1.99%	-0.79%	1.19%	0.76%

	CERC	CERC3	MILH	VR14
AffectedLength	-17.60%	124.98%	-35.08%	92.23%
ErosionVolume	76.07%	348.49%	-36.84%	282.19%
AccretionVolume	76.08%	348.50%	-36.84%	282.19%
ErosionDistance	-16.27%	156.71%	-47.60%	122.51%
AccretionDistance	-42.01%	0.06%	-74.10%	0.00%
ElapsedTime	-99.20%	-94.10%	-99.48%	-95.29%

change compared to default value
incremental change from smallest to biggest
subjected to errors

Salient results

	ds0 [m]	spread [°]	spread [°]	spread [°]	Aw [-]	Hso [m]	phiw0 [°N]	phiw0 [°N]	phiw0 [°N]	tper [s]	d50 [mm]	tanbeta [1/slope]	d [m]
[from]-[to]	25-50	20-0	20-40	0-40	0-5	0.5-1	45-30	45-60	30-60	6-8	0.1-0.4	0.025-0.0125	4-10
AffectedLength	-0.77%	0.04%	-2.69%	-2.72%	0.00%	70.63%	8.38%	-11.13%	-18.00%	27.47%	-15.67%	-28.44%	-
ErosionVolume	-25.30%	9.59%	-18.77%	-25.88%	-0.24%	424.99%	-22.39%	-25.65%	-4.19%	154.74%	-53.19%	-105.87%	-
AccretionVolume	-25.30%	9.59%	-18.77%	-25.88%	-0.27%	424.99%	-22.39%	-25.65%	-4.19%	154.74%	-53.19%	-105.87%	-
ErosionDistance	-11.90%	2.19%	-13.78%	-15.63%	-3.32%	263.87%	-10.63%	-29.28%	-20.87%	68.38%	-31.83%	-29.04%	-
AccretionDistance	-27.40%	-20.54%	-19.92%	0.78%	-21.14%	448.38%	-41.89%	-36.72%	8.90%	137.85%	-11.62%	-7.59%	-
ElapsedTime	-38.49%	0.62%	-0.16%	-0.78%	-1.54%	-0.29%	0.61%	0.02%	-0.59%	0.29%	-2.47%	0.10%	-

	CERC	CERC3	MILH	VR14
AffectedLength	30.63%	136.68%	-29.26%	101.31%
ErosionVolume	154.84%	877.67%	-22.41%	648.62%
AccretionVolume	154.84%	878.15%	-22.41%	648.65%
ErosionDistance	57.20%	279.83%	-50.39%	254.42%
AccretionDistance	-30.42%	46.86%	-76.57%	31.04%
ElapsedTime	-99.30%	-94.16%	-99.55%	-94.57%

change compared to default value
incremental change from smallest to biggest
subject to errors
different from tombolo

A.2. Post-processing of detailed scenario tombolo sensitivity analysis (wave angle=0°)

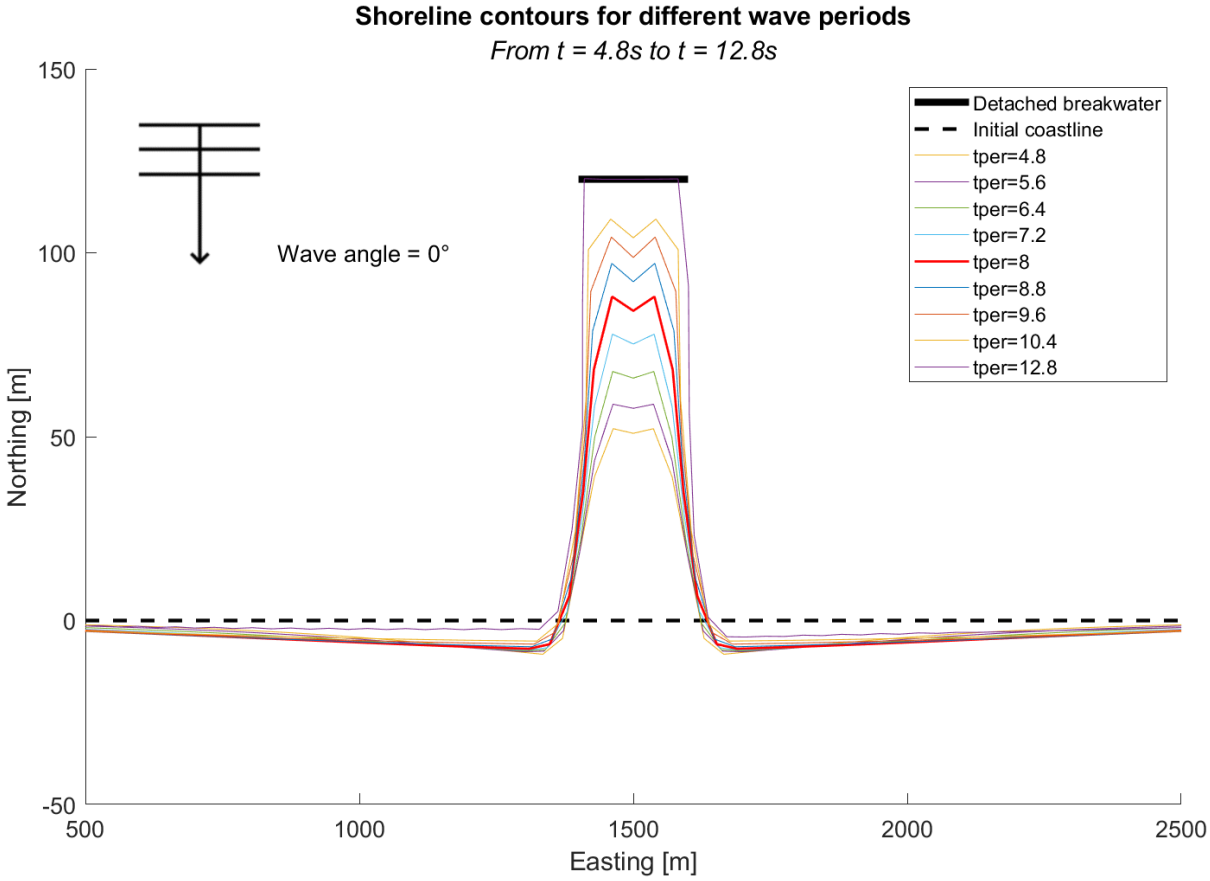

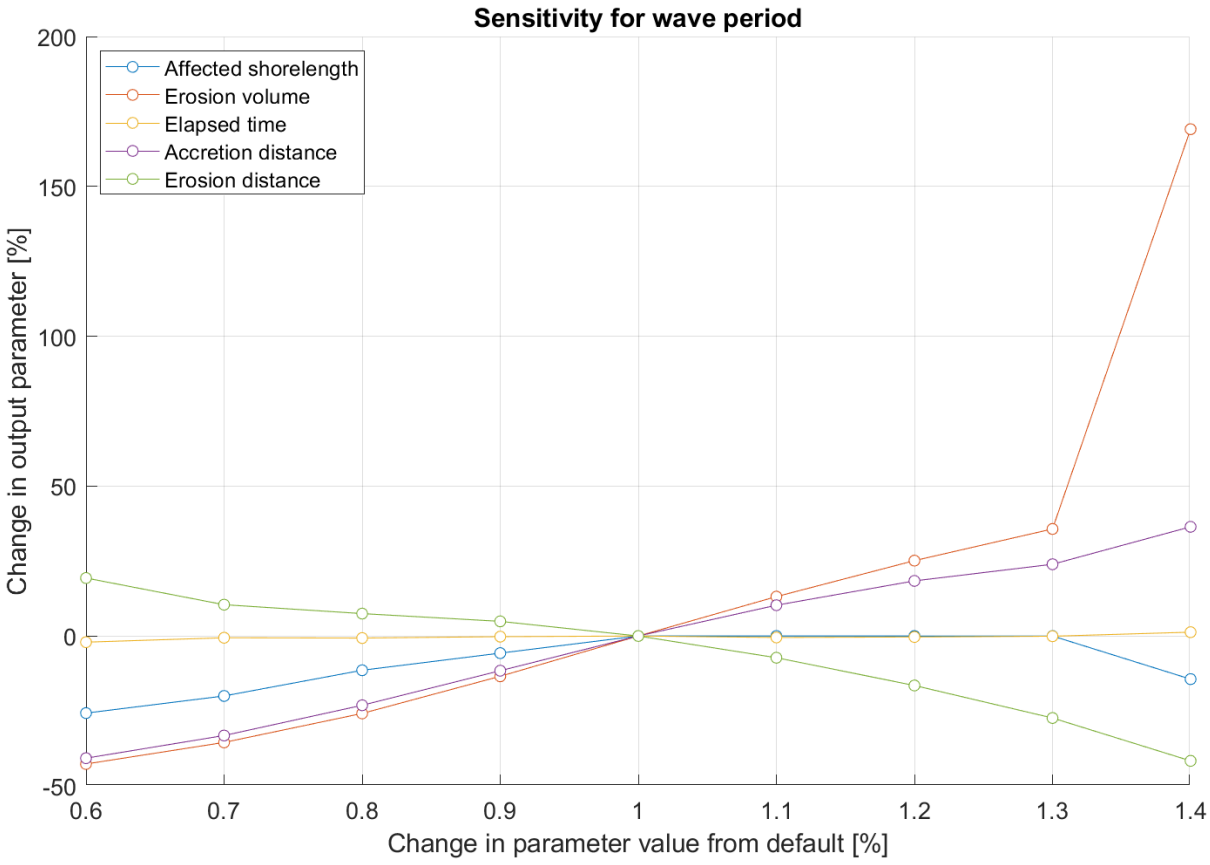

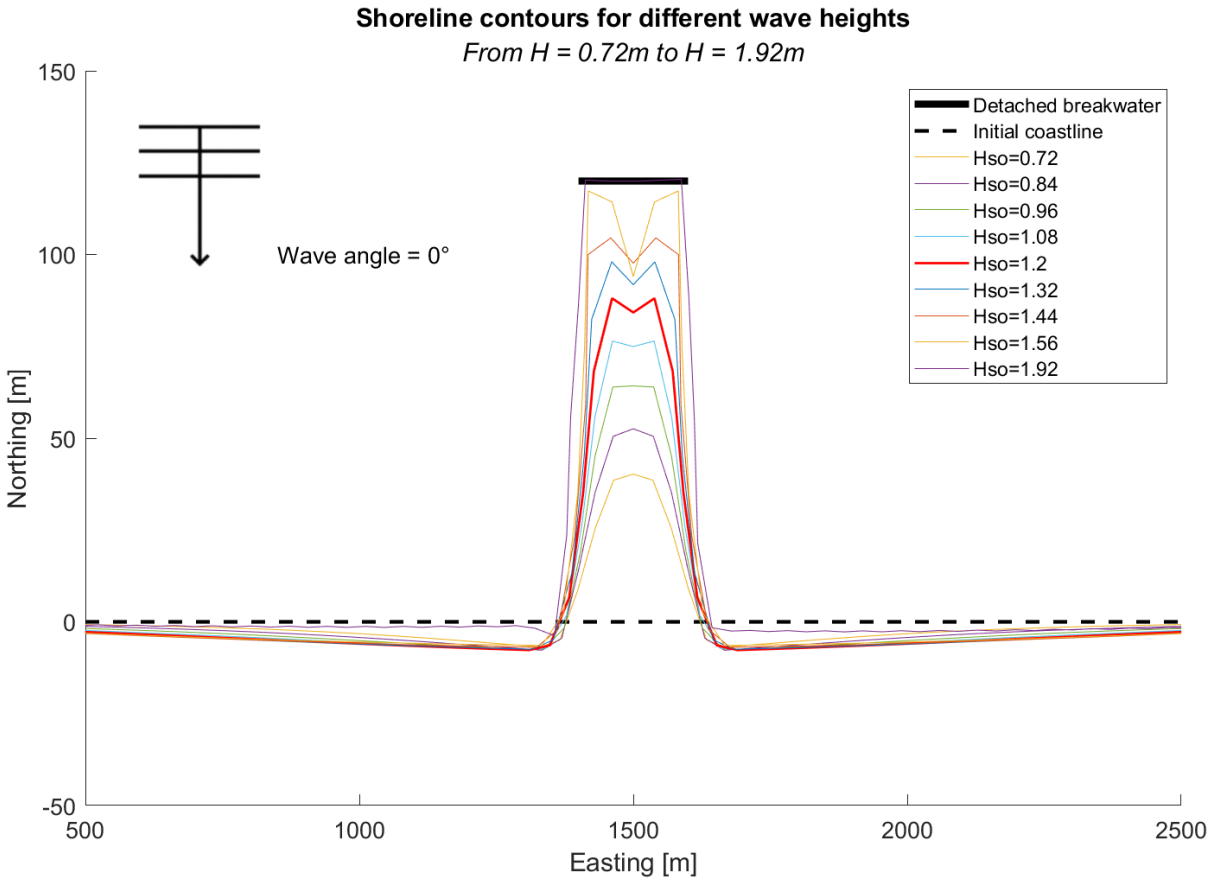
Shoreline contours for different wave heights
From H = 0.72m to H = 1.92m
Wave angle = 0°
Detached breakwater
Initial coastline
Hso=0.72
Hso=0.84
Hso=0.96
Hso=1.08
Hso=1.2
Hso=1.32
Hso=1.44
Hso=1.56
Hso=1.92
Northing [m]
Easting [m]
150
100
50
0
-50
500
1000
1500
2000
2500

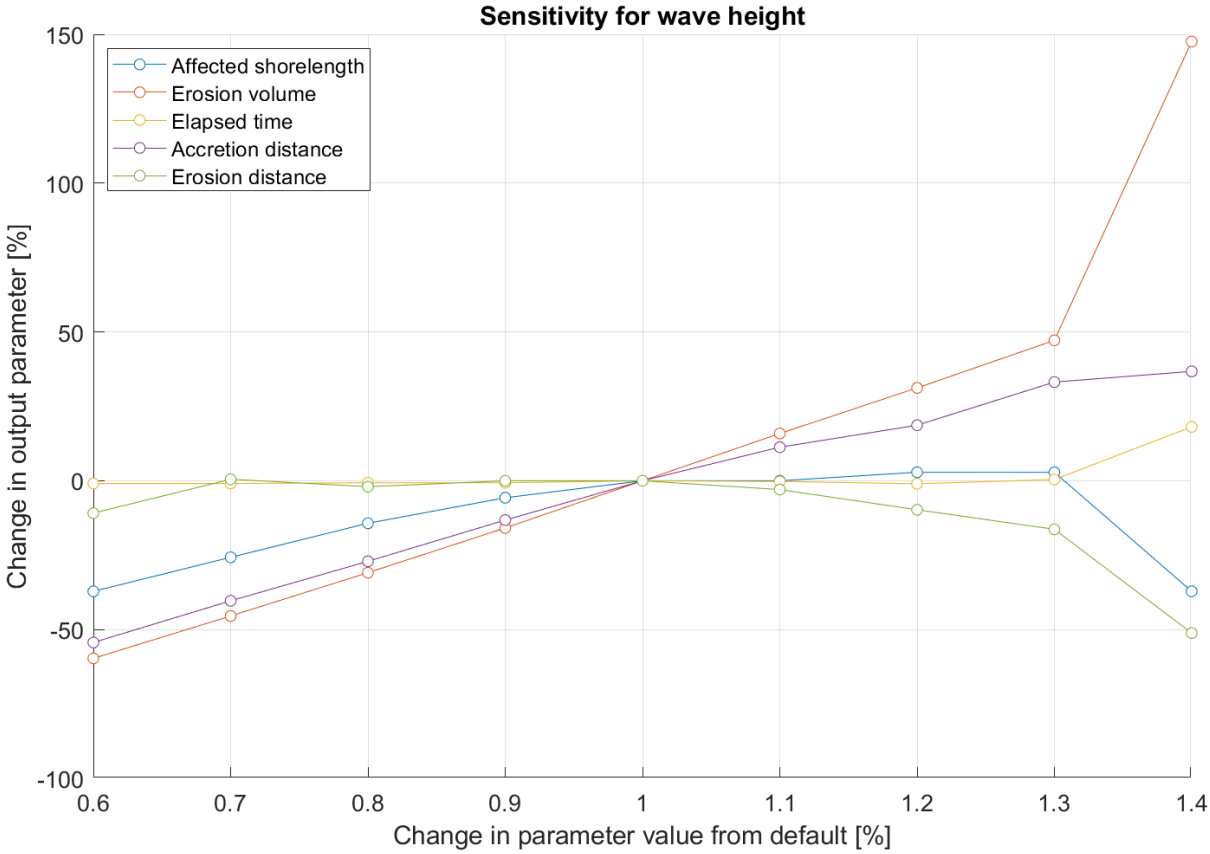
Sensitivity for wave height
Affected shorelength
Erosion volume
Elapsed time
Accretion distance
Erosion distance
Change in output parameter [%]
Change in parameter value from default [%]
150
100
50
0
-50
-100
0.6
0.7
0.8
0.9
1
1.1
1.2
1.3
1.4

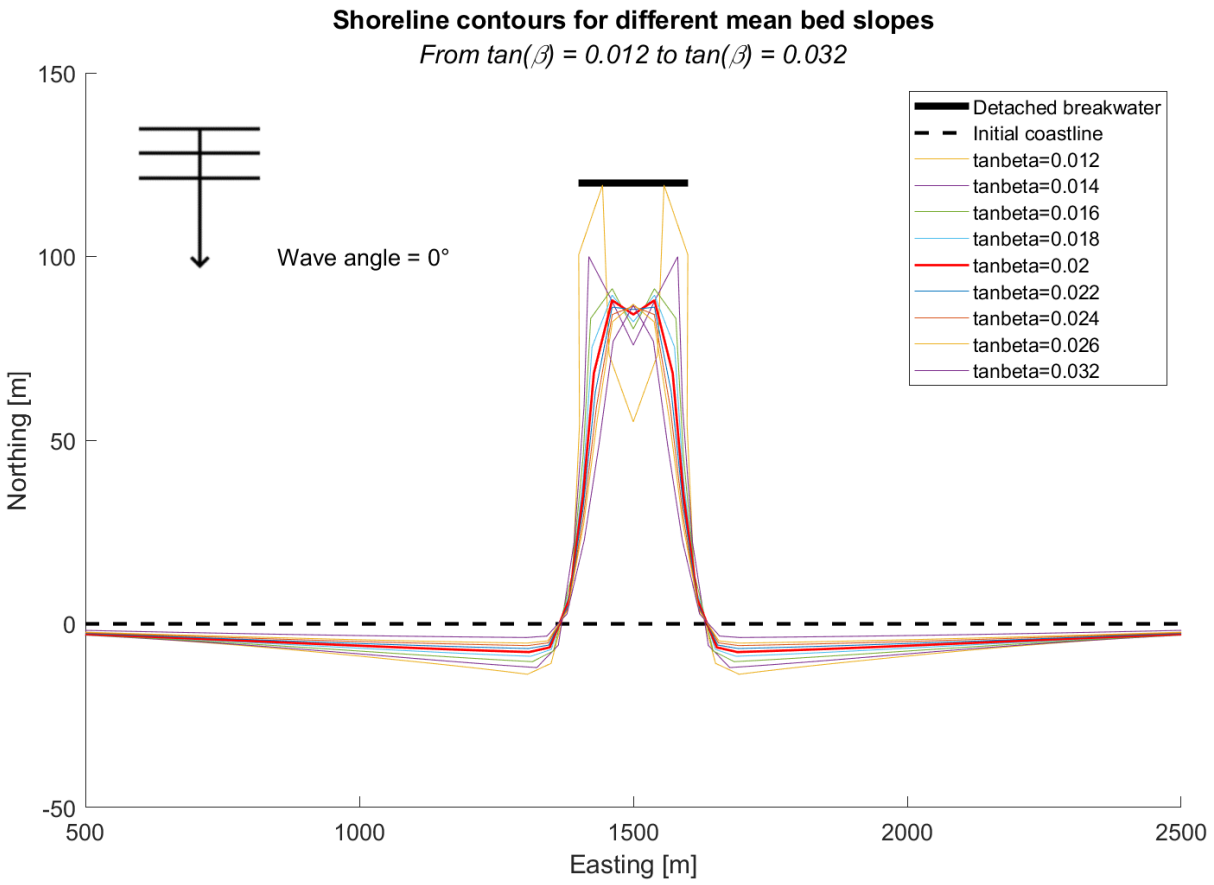
Shoreline contours for different mean bed slopes
From tan(β) = 0.012 to tan(β) = 0.032
Wave angle = 0°
Detached breakwater
Initial coastline
tanbeta=0.012
tanbeta=0.014
tanbeta=0.016
tanbeta=0.018
tanbeta=0.02
tanbeta=0.022
tanbeta=0.024
tanbeta=0.026
tanbeta=0.032
Northing [m]
Easting [m]
150
100
50
0
-50
500
1000
1500
2000
2500

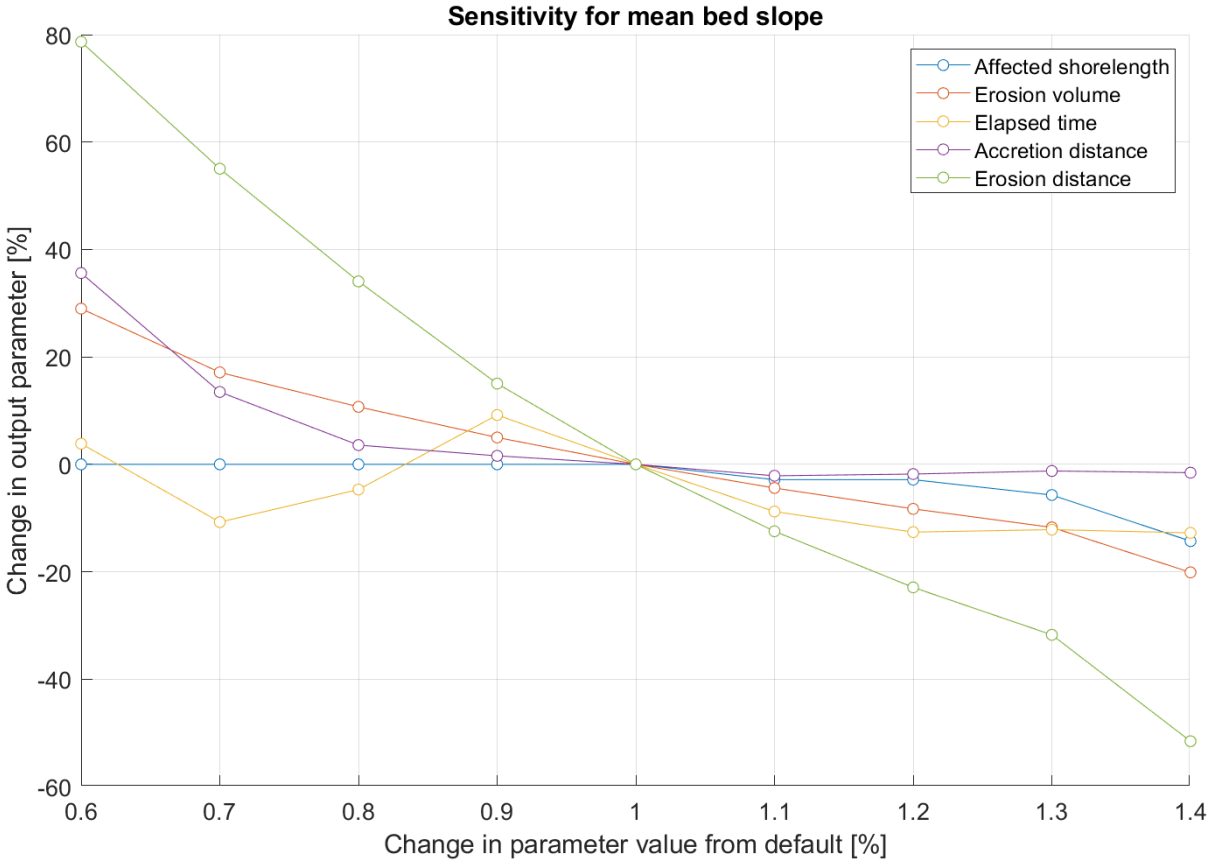
Sensitivity for mean bed slope
Affected shorelength
Erosion volume
Elapsed time
Accretion distance
Erosion distance
Change in output parameter [%]
Change in parameter value from default [%]
80
60
40
20
0
-20
-40
-60
0.6
0.7
0.8
0.9
1
1.1
1.2
1.3
1.4

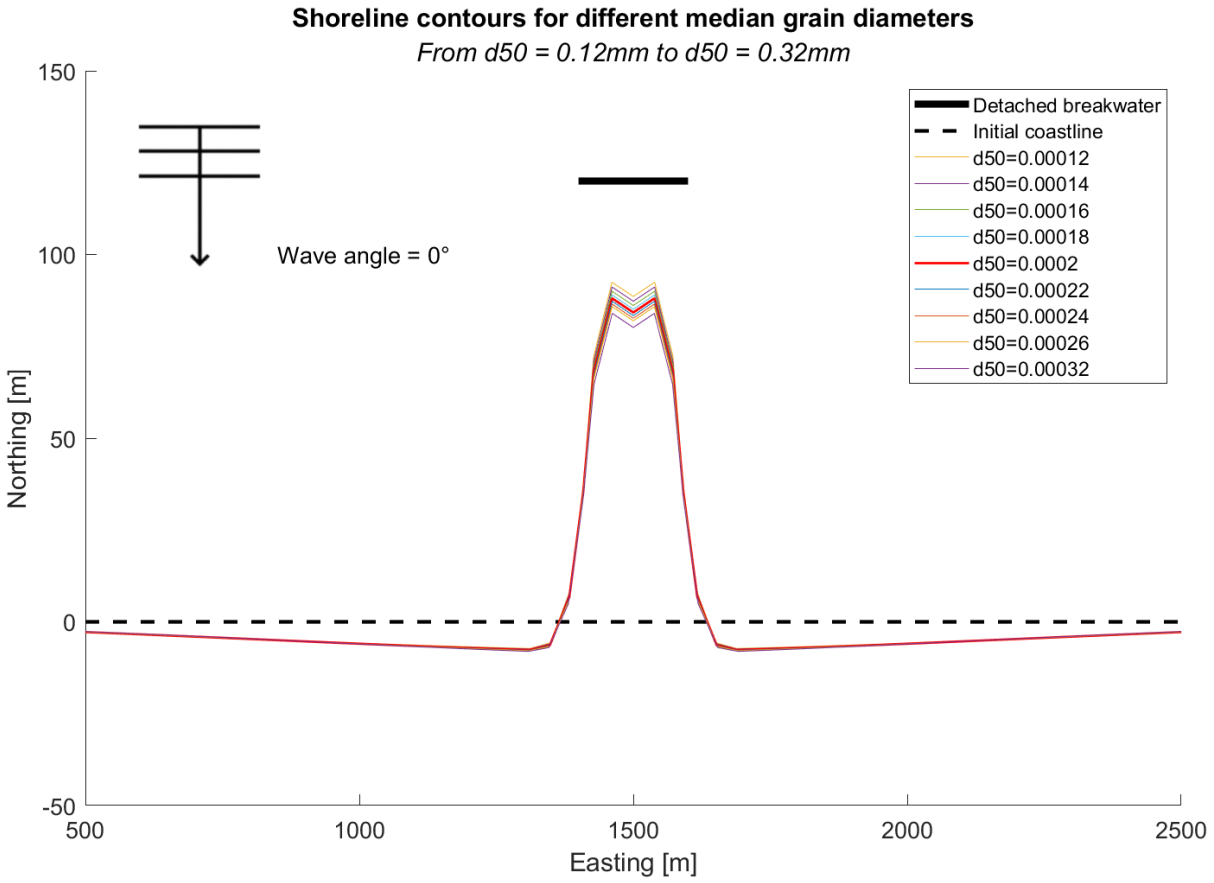
Shoreline contours for different median grain diameters
From d50 = 0.12mm to d50 = 0.32mm
Wave angle = 0°
Detached breakwater
Initial coastline
d50=0.00012
d50=0.00014
d50=0.00016
d50=0.00018
d50=0.0002
d50=0.00022
d50=0.00024
d50=0.00026
d50=0.00032
Northing [m]
Easting [m]
150
100
50
0
-50
500
1000
1500
2000
2500

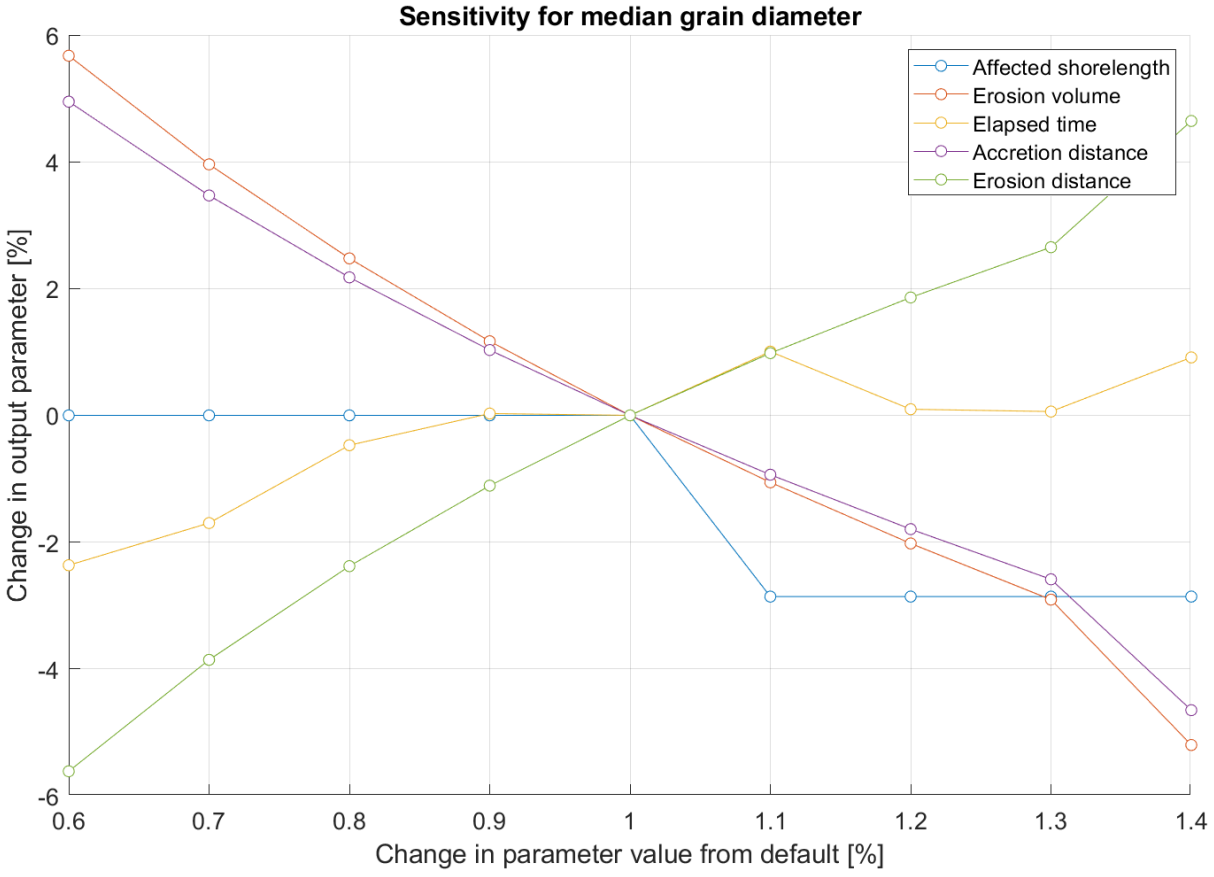
Sensitivity for median grain diameter
Affected shorelength
Erosion volume
Elapsed time
Accretion distance
Erosion distance
Change in output parameter [%]
Change in parameter value from default [%]
6
4
2
0
-2
-4
-6
0.6
0.7
0.8
0.9
1
1.1
1.2
1.3
1.4

A.3. Post-processing of detailed scenario tombolo sensitivity analysis (wave angle=20°)

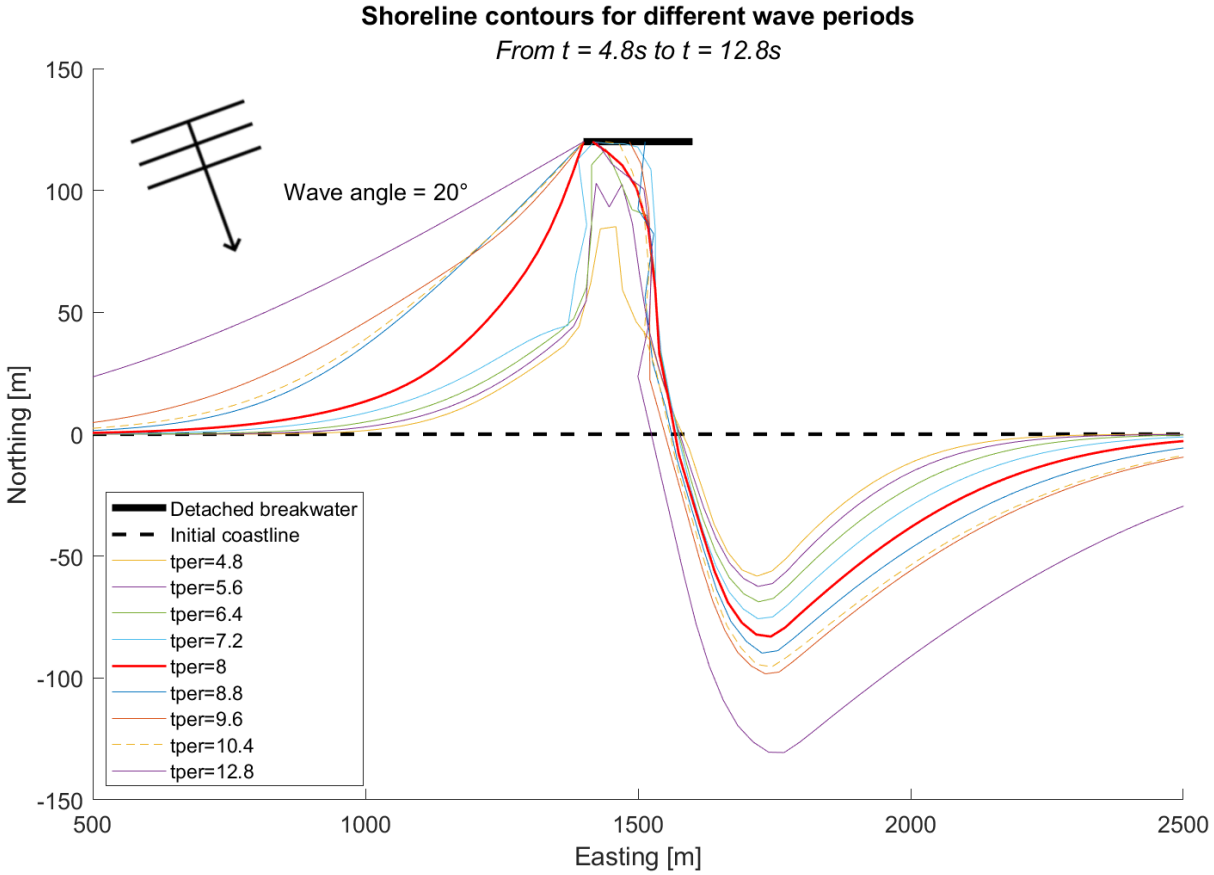

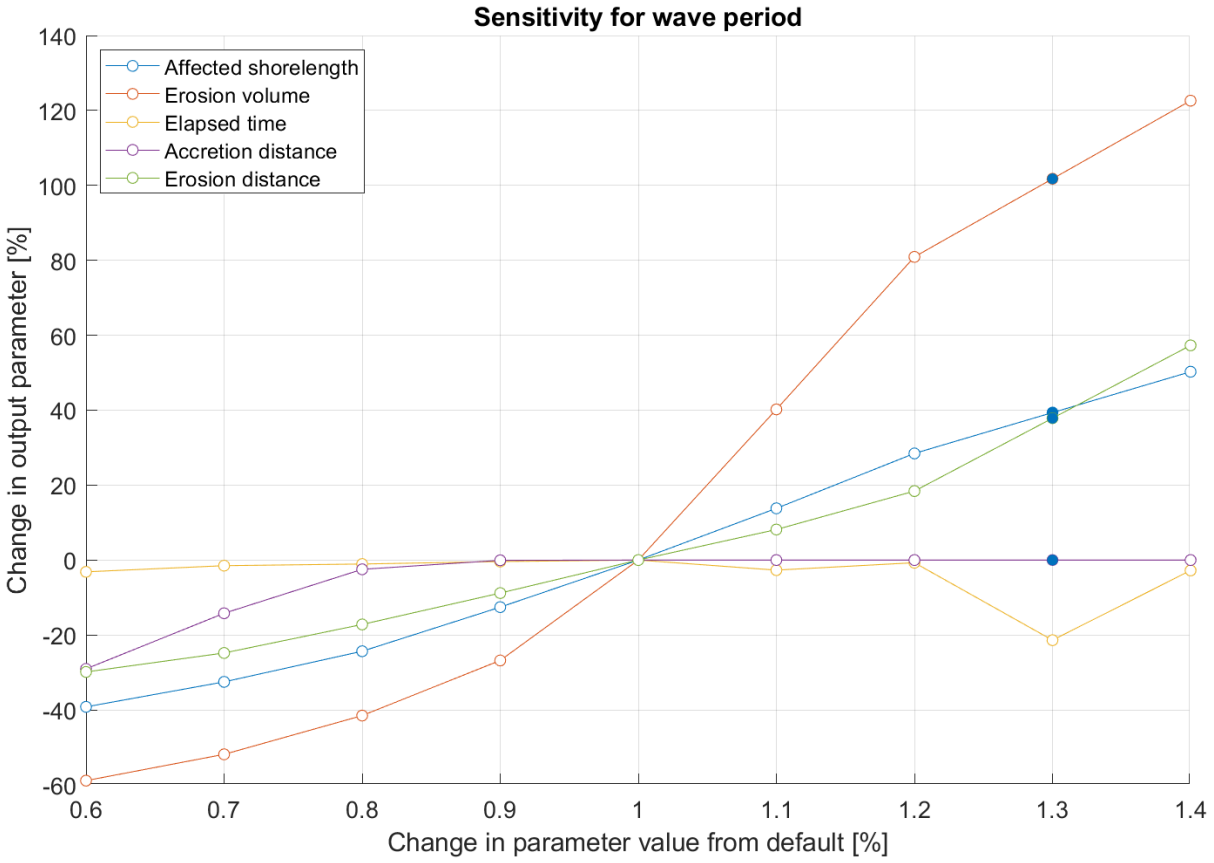

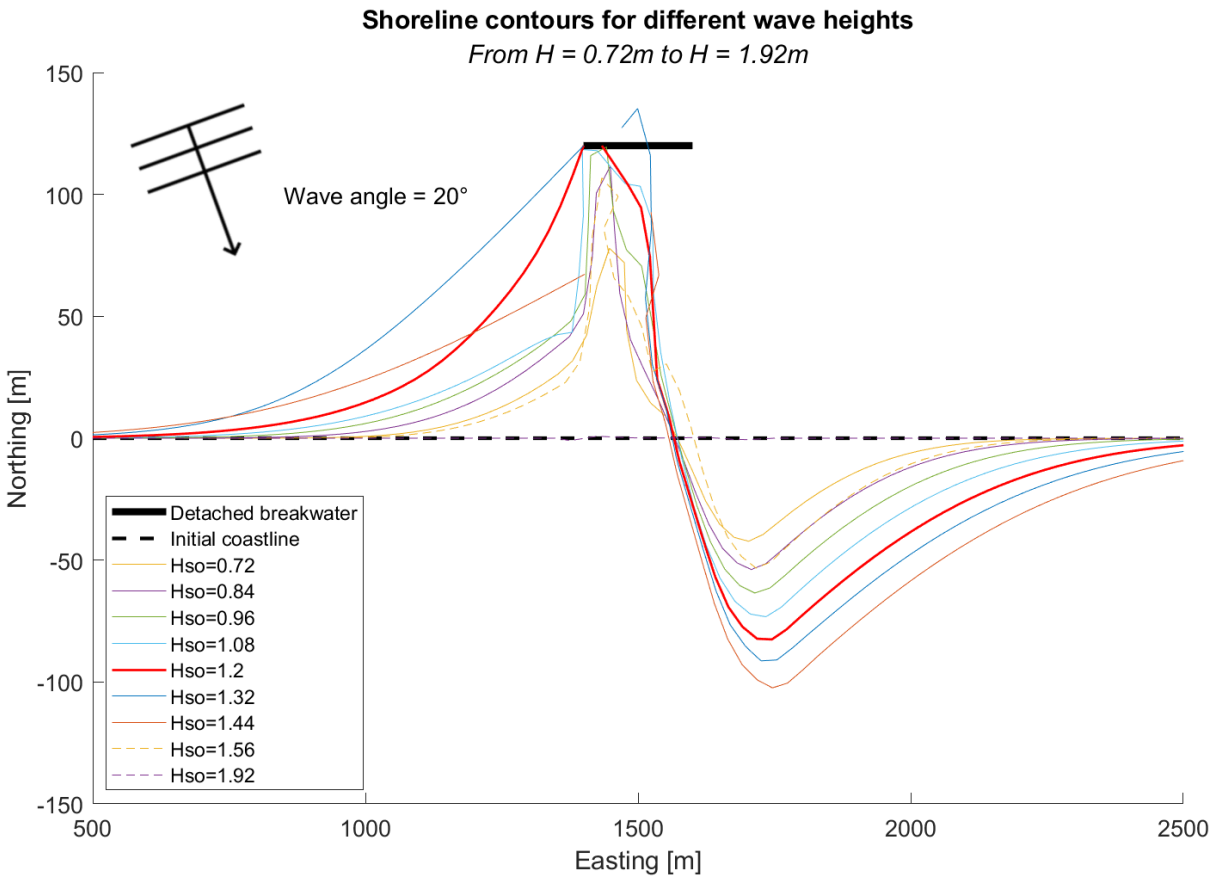
Shoreline contours for different wave heights
From H = 0.72m to H = 1.92m
Wave angle = 20°
Northing [m]
Easting [m]
Detached breakwater
Initial coastline
Hso=0.72
Hso=0.84
Hso=0.96
Hso=1.08
Hso=1.2
Hso=1.32
Hso=1.44
Hso=1.56
Hso=1.92

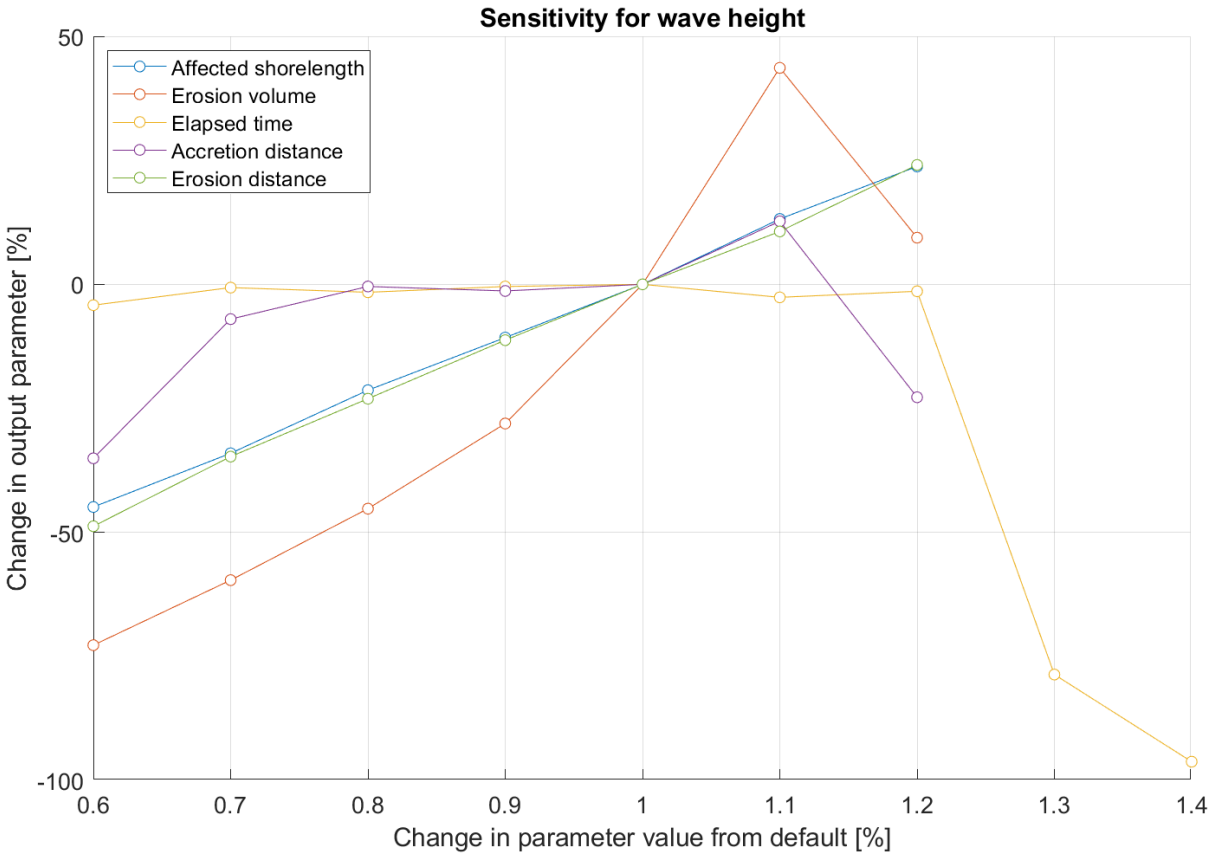
Sensitivity for wave height
Affected shorelength
Erosion volume
Elapsed time
Accretion distance
Erosion distance
Change in output parameter [%]
Change in parameter value from default [%]

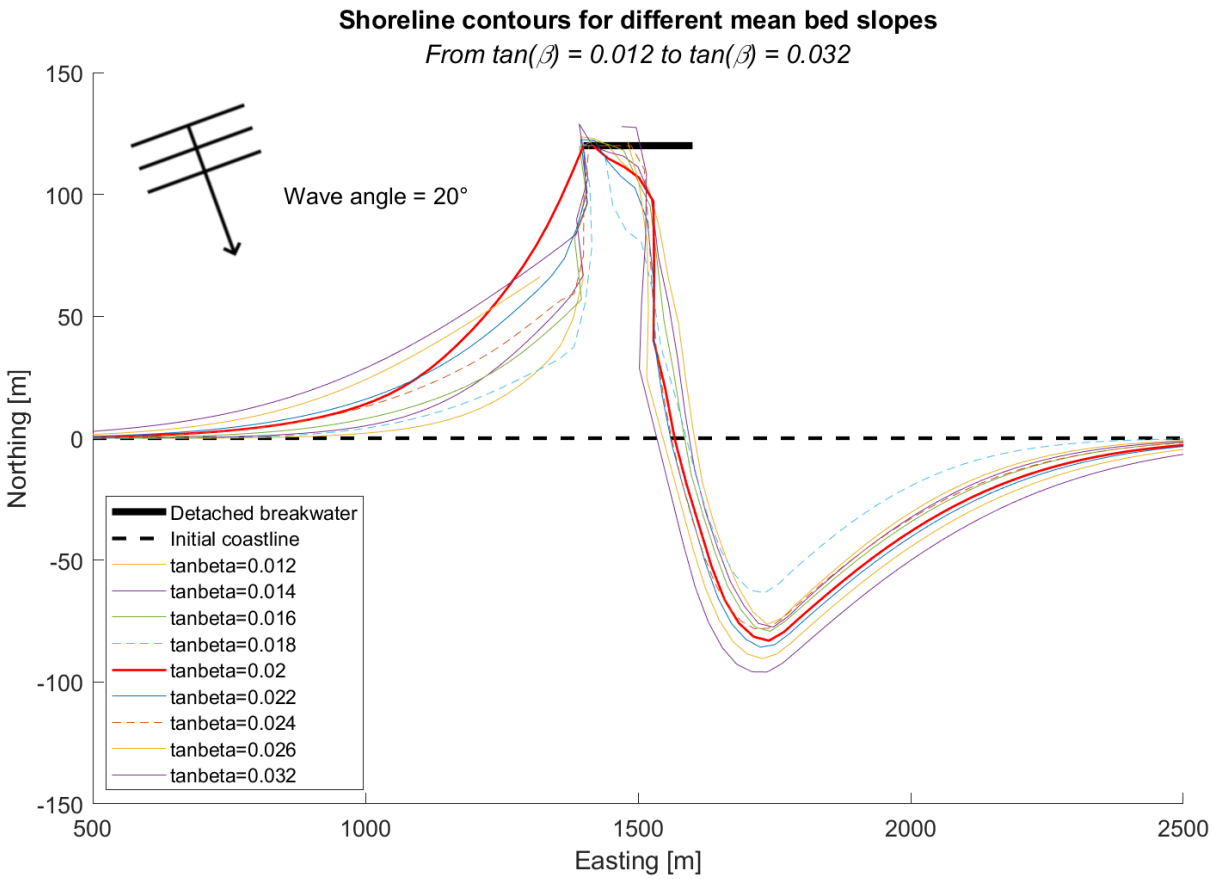
Shoreline contours for different mean bed slopes
From tan(β) = 0.012 to tan(β) = 0.032
Wave angle = 20°
Northing [m]
Easting [m]
Detached breakwater
Initial coastline
tanbeta=0.012
tanbeta=0.014
tanbeta=0.016
tanbeta=0.018
tanbeta=0.02
tanbeta=0.022
tanbeta=0.024
tanbeta=0.026
tanbeta=0.032

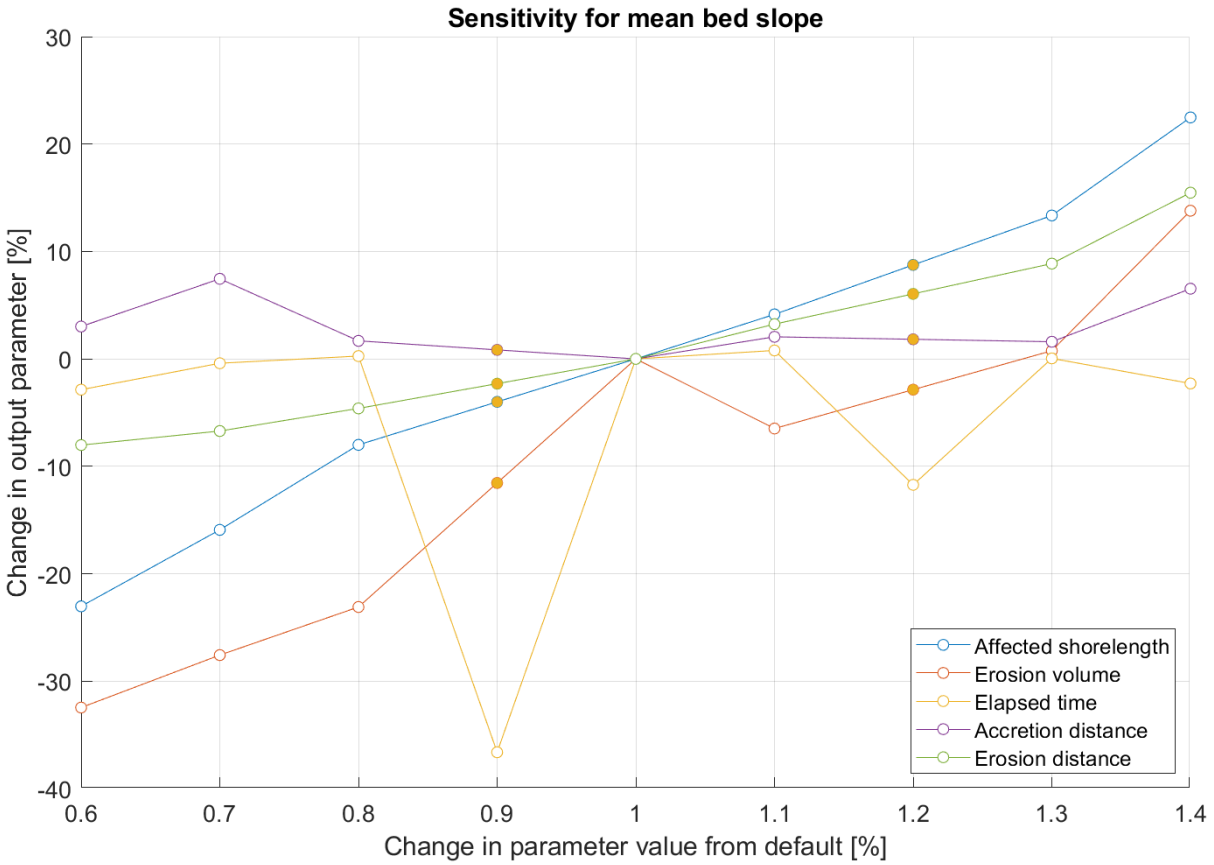
Sensitivity for mean bed slope
Change in output parameter [%]
Change in parameter value from default [%]
Affected shorelength
Erosion volume
Elapsed time
Accretion distance
Erosion distance

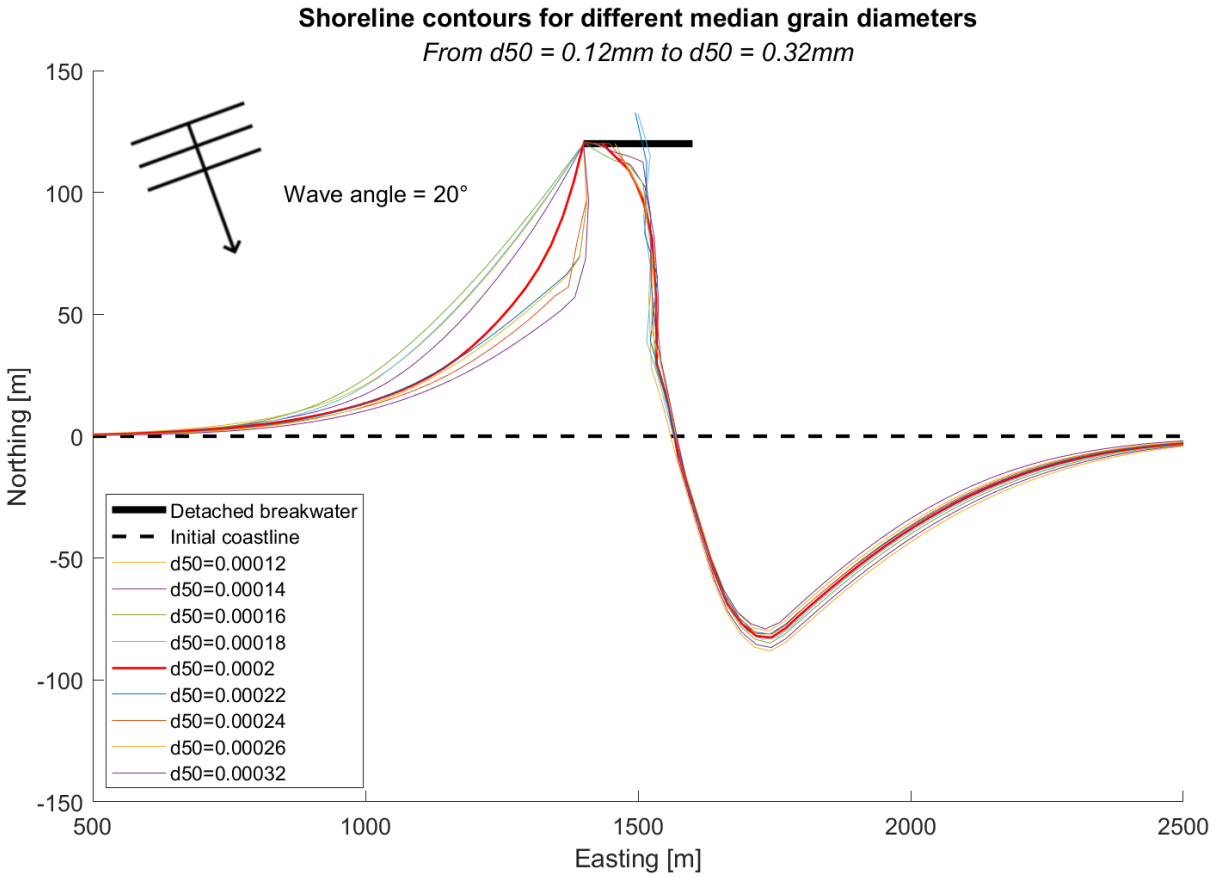
Shoreline contours for different median grain diameters
From d50 = 0.12mm to d50 = 0.32mm
Wave angle = 20°
Northing [m]
Easting [m]
Detached breakwater
Initial coastline
d50=0.00012
d50=0.00014
d50=0.00016
d50=0.00018
d50=0.0002
d50=0.00022
d50=0.00024
d50=0.00026
d50=0.00032

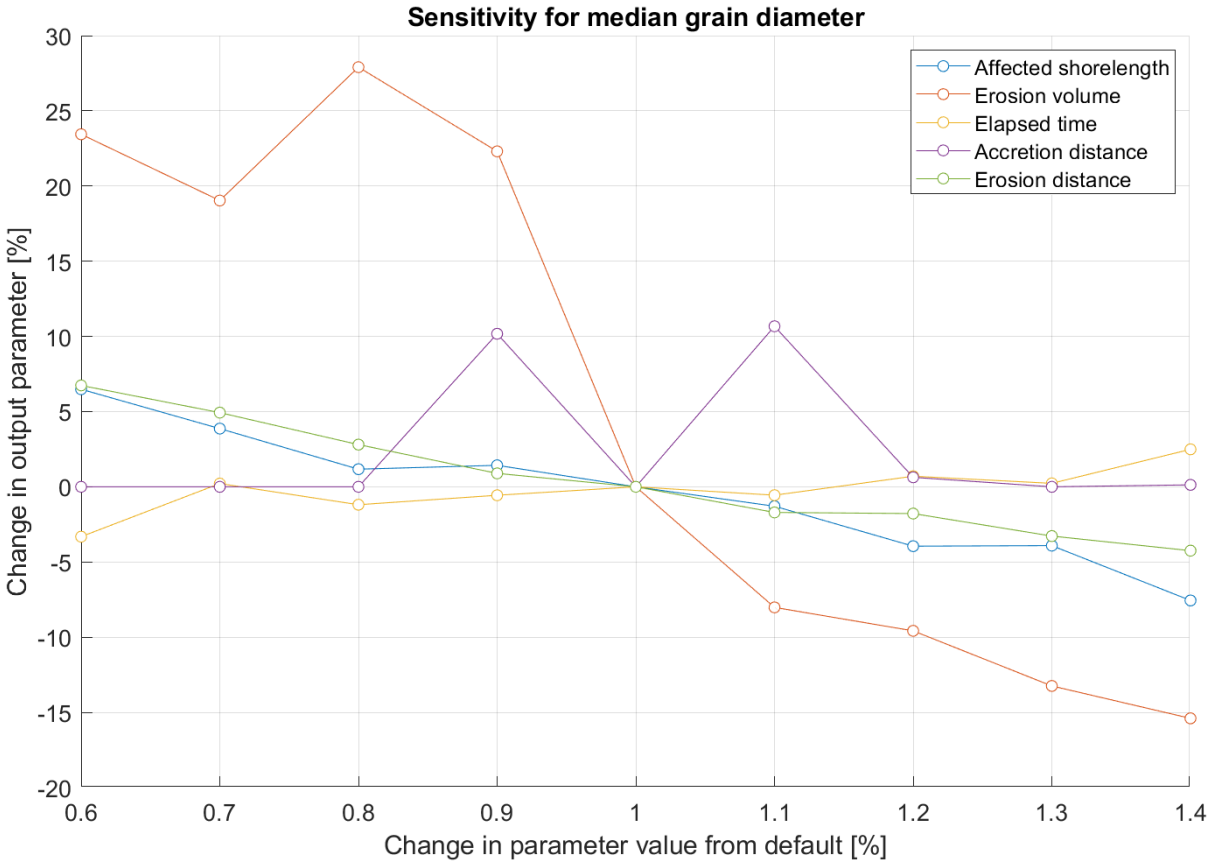
Sensitivity for median grain diameter
Affected shorelength
Erosion volume
Elapsed time
Accretion distance
Erosion distance
Change in output parameter [%]
Change in parameter value from default [%]

A.4. Post-processing of detailed scenario tombolo sensitivity analysis (wave angle=45°)

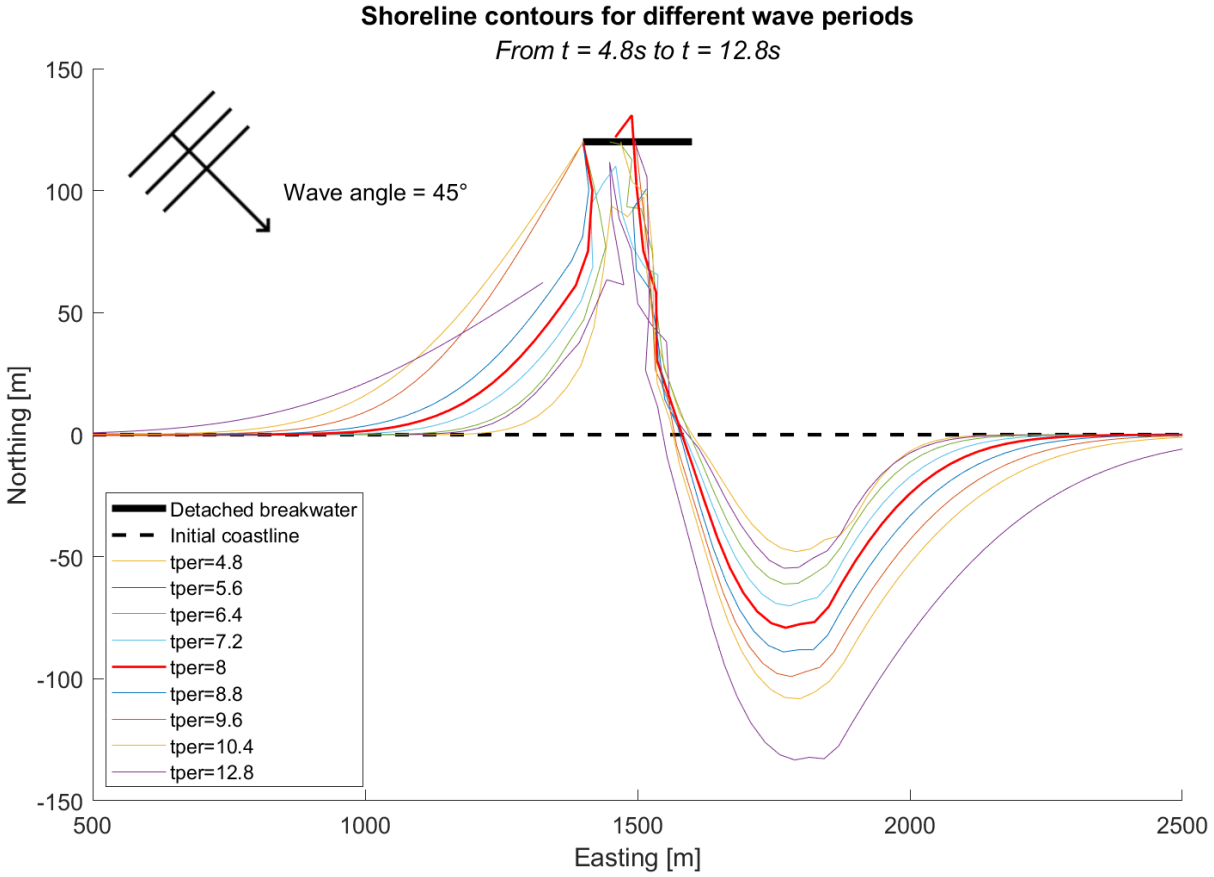

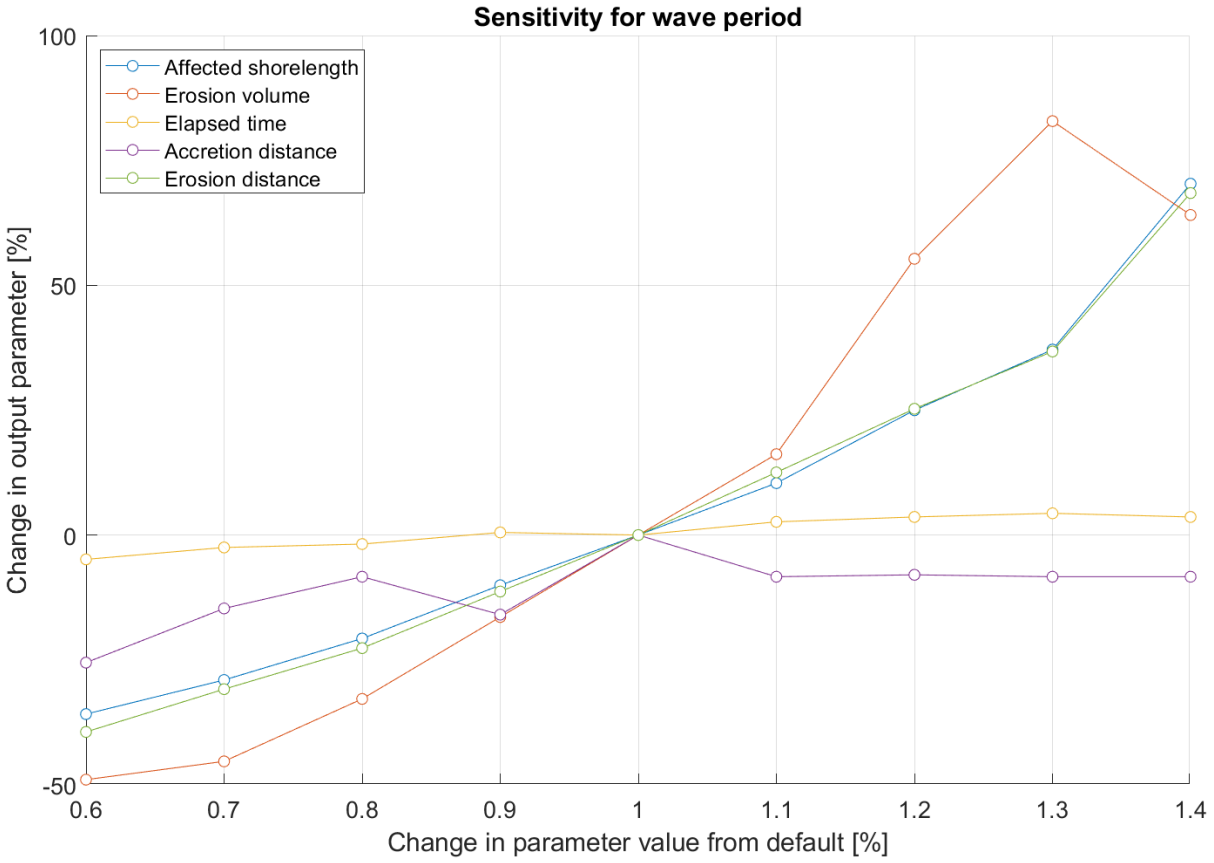

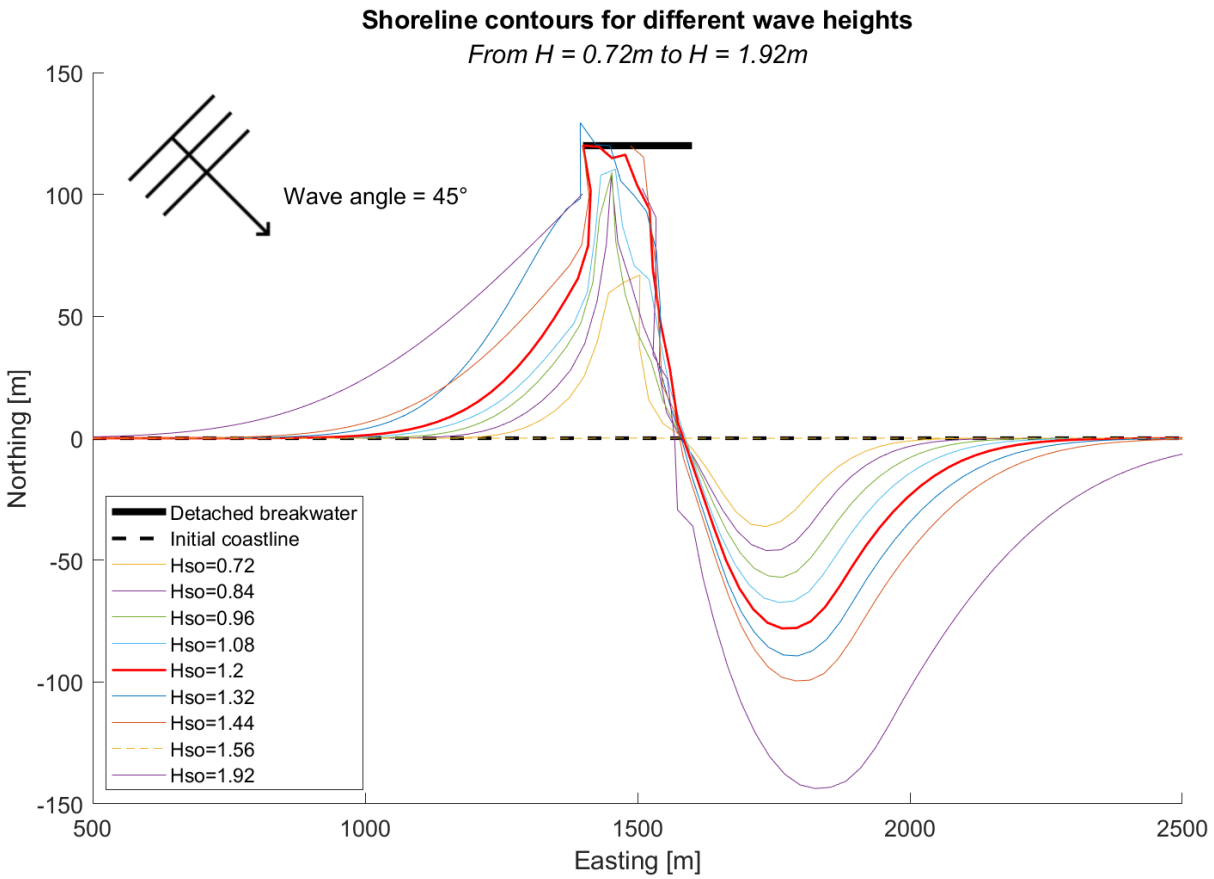
Shoreline contours for different wave heights
From H = 0.72m to H = 1.92m
Wave angle = 45°
Northing [m]
Easting [m]
Detached breakwater
Initial coastline
Hso=0.72
Hso=0.84
Hso=0.96
Hso=1.08
Hso=1.2
Hso=1.32
Hso=1.44
Hso=1.56
Hso=1.92

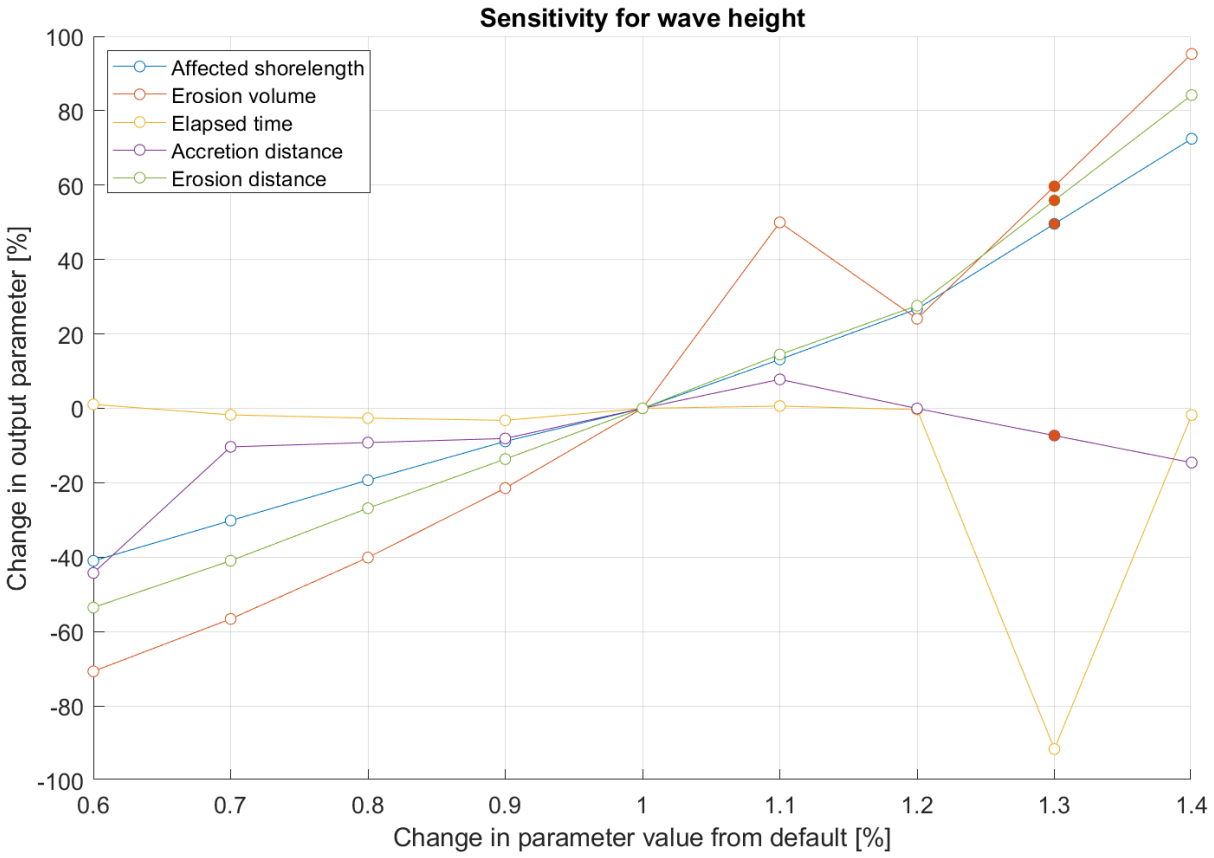
Sensitivity for wave height
Affected shorelength
Erosion volume
Elapsed time
Accretion distance
Erosion distance
Change in output parameter [%]
Change in parameter value from default [%]

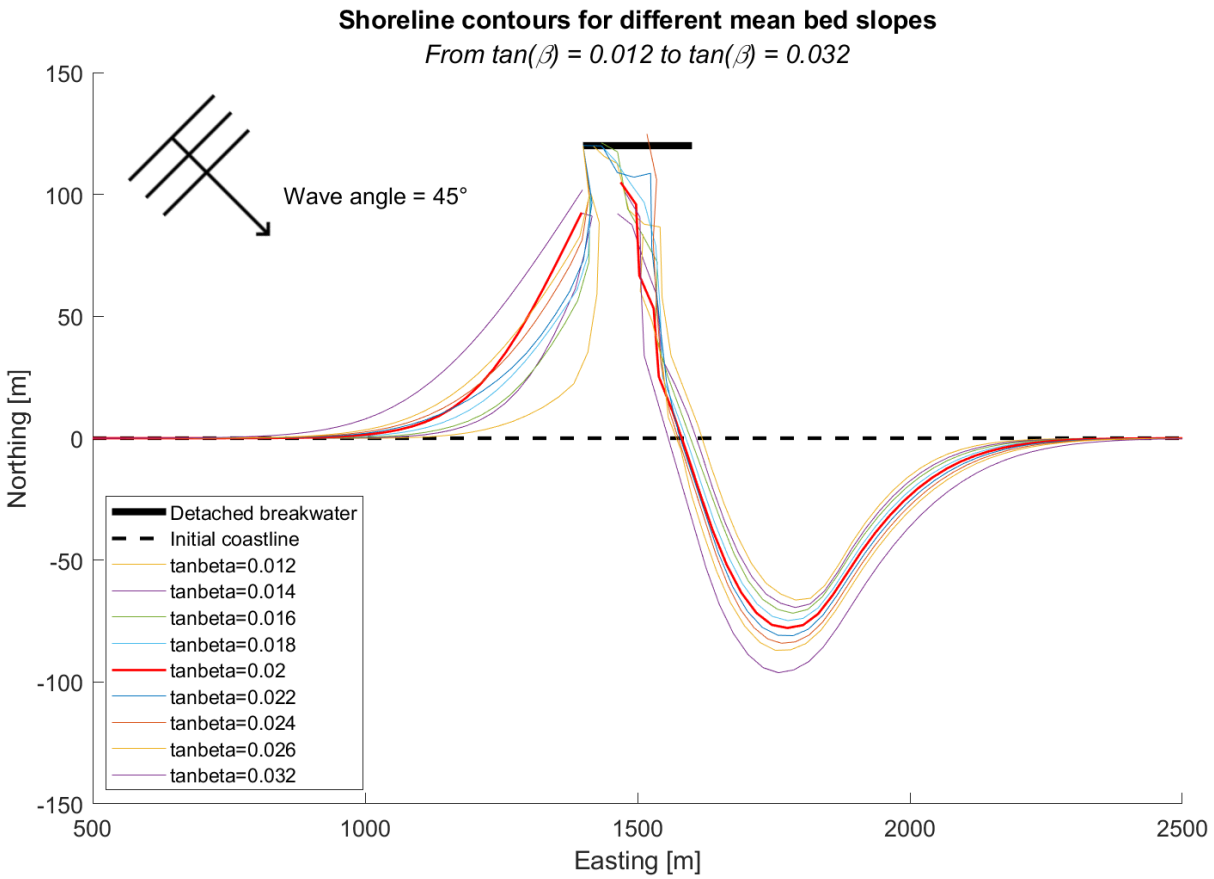
Shoreline contours for different mean bed slopes
From tan(β) = 0.012 to tan(β) = 0.032
Wave angle = 45°
Northing [m]
Easting [m]
Detached breakwater
Initial coastline
tanbeta=0.012
tanbeta=0.014
tanbeta=0.016
tanbeta=0.018
tanbeta=0.02
tanbeta=0.022
tanbeta=0.024
tanbeta=0.026
tanbeta=0.032

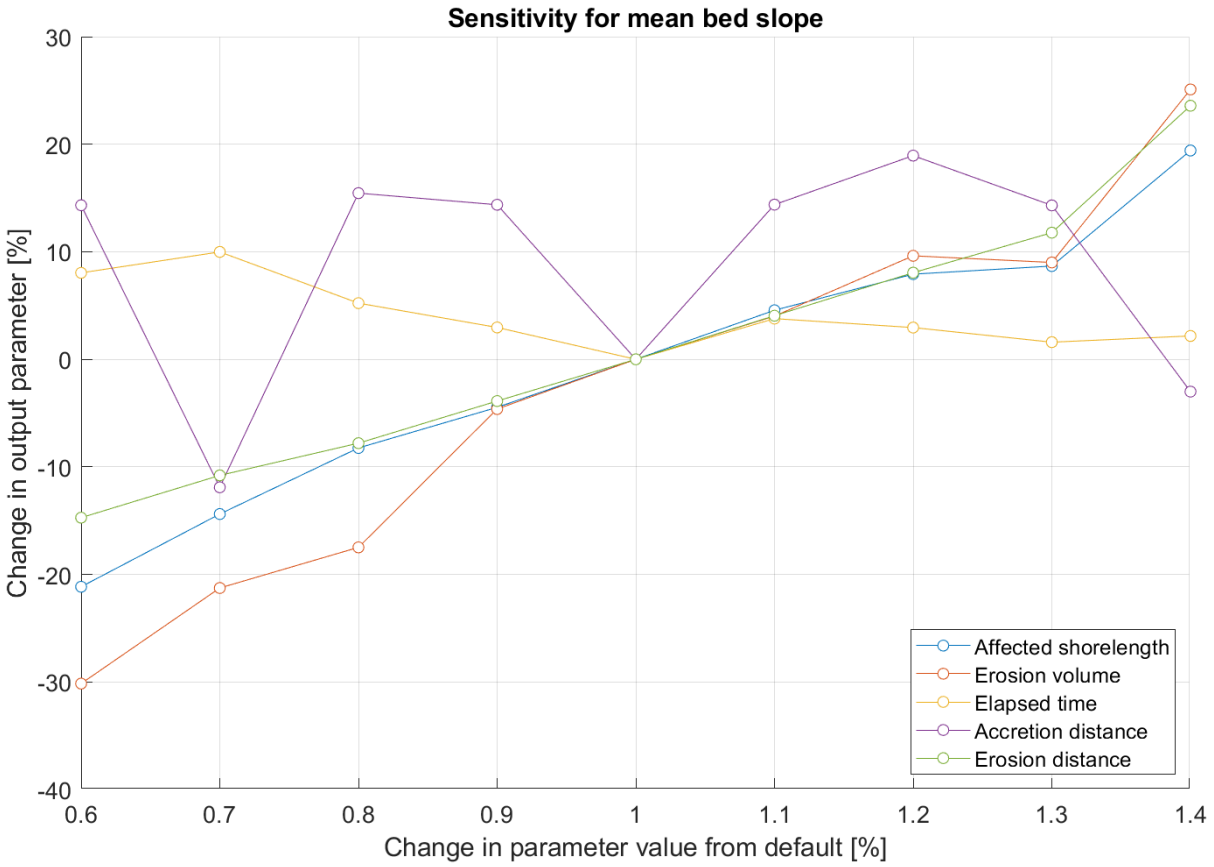
Sensitivity for mean bed slope
Change in output parameter [%]
Change in parameter value from default [%]
Affected shorelength
Erosion volume
Elapsed time
Accretion distance
Erosion distance

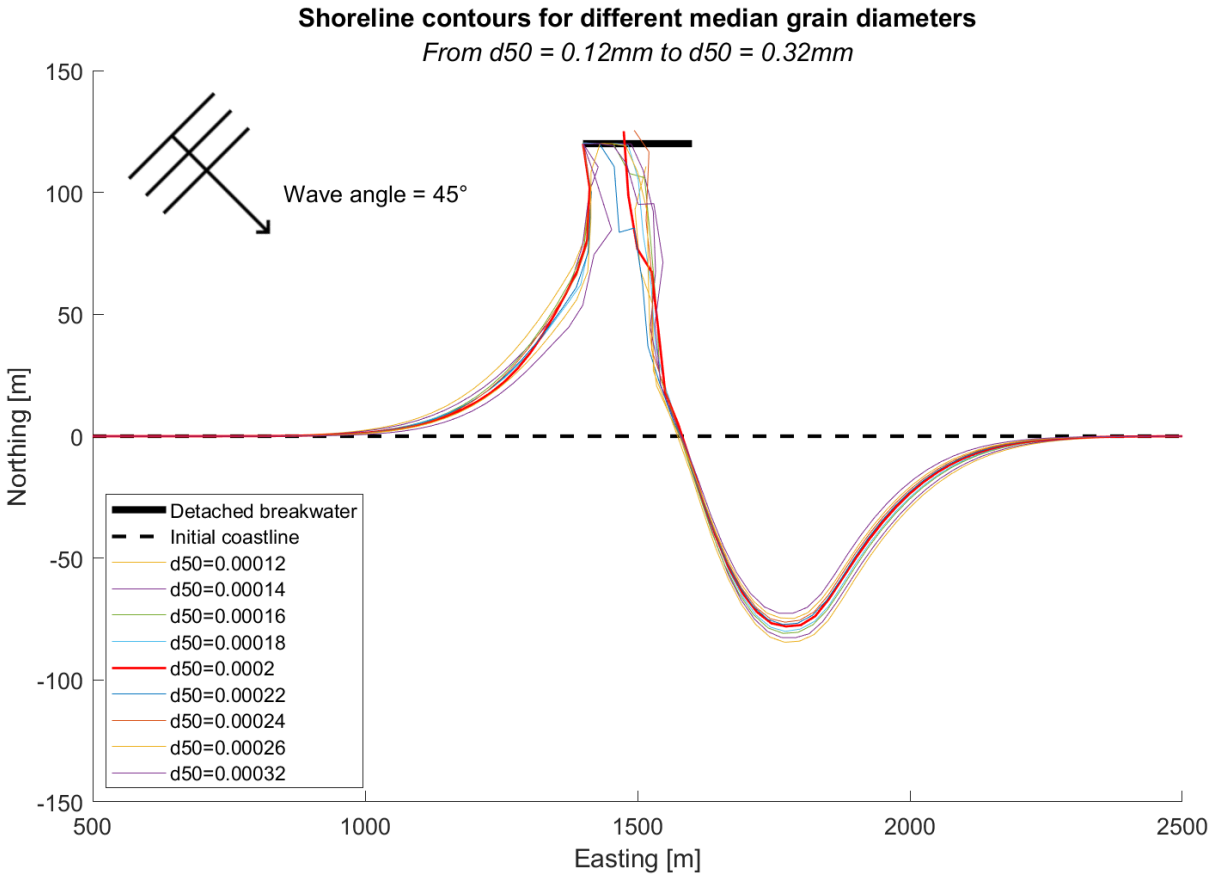
Shoreline contours for different median grain diameters
From d50 = 0.12mm to d50 = 0.32mm
Wave angle = 45°
Detached breakwater
Initial coastline
d50=0.00012
d50=0.00014
d50=0.00016
d50=0.00018
d50=0.0002
d50=0.00022
d50=0.00024
d50=0.00026
d50=0.00032
Northing [m]
Easting [m]
150
100
50
0
-50
-100
-150
500
1000
1500
2000
2500

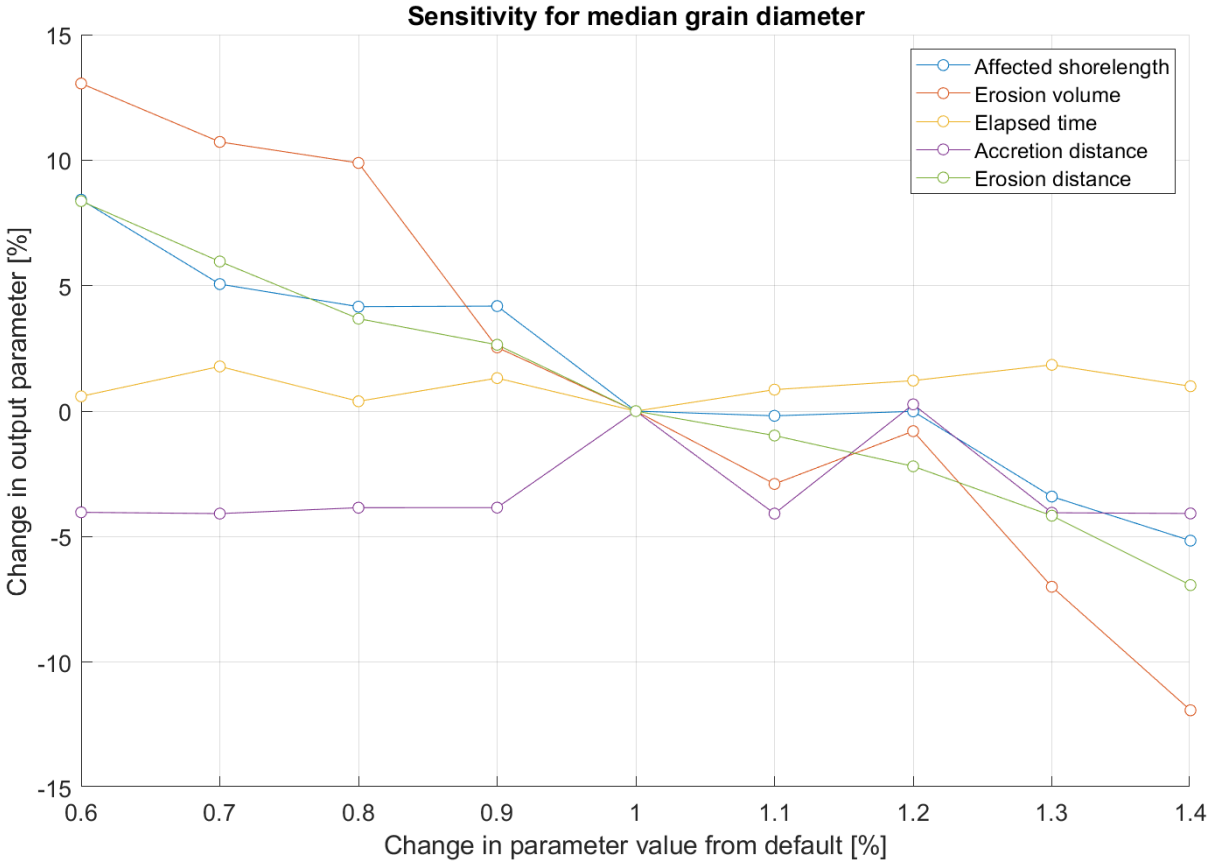
Sensitivity for median grain diameter
Affected shorelength
Erosion volume
Elapsed time
Accretion distance
Erosion distance
Change in output parameter [%]
Change in parameter value from default [%]
15
10
5
0
-5
-10
-15
0.6
0.7
0.8
0.9
1
1.1
1.2
1.3
1.4

A.5. Post-processing of detailed salient sensitivity analysis (wave angle=0°)

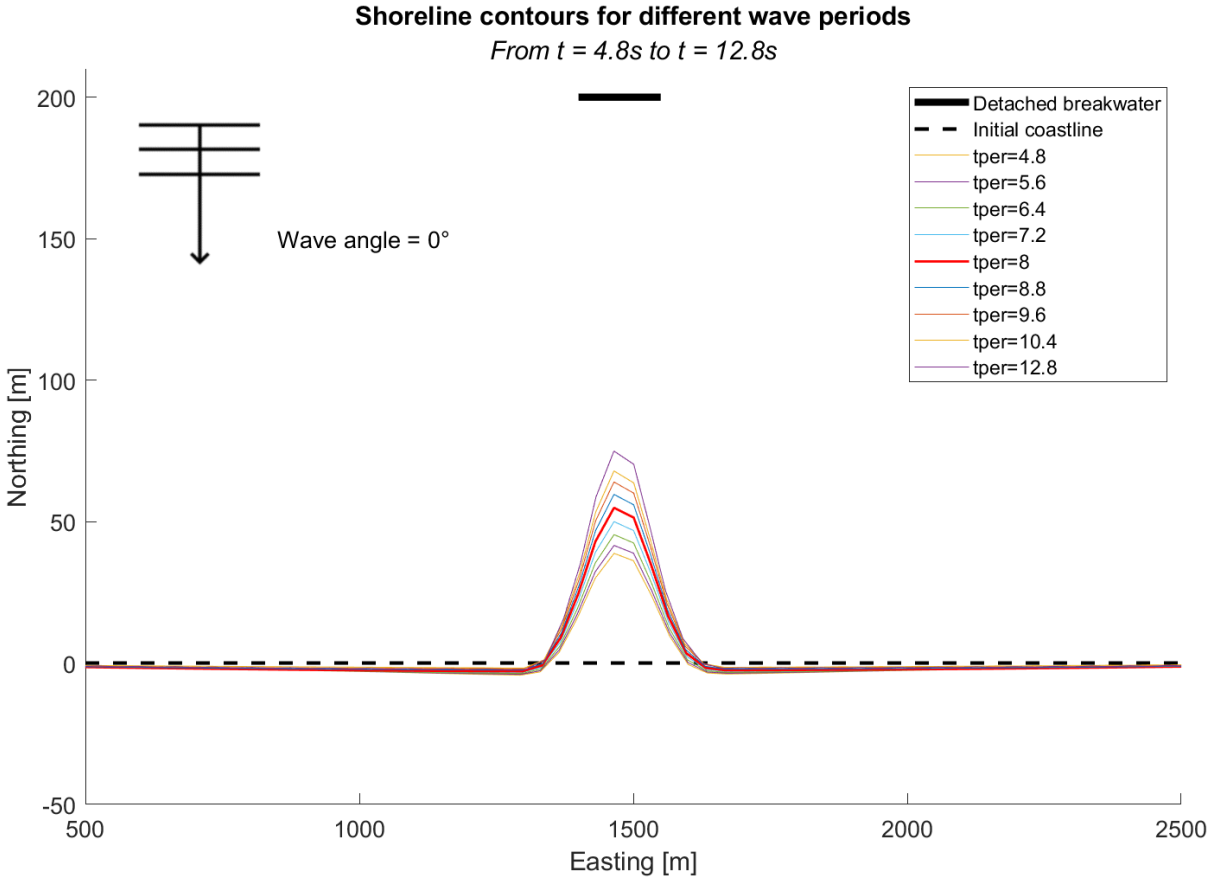

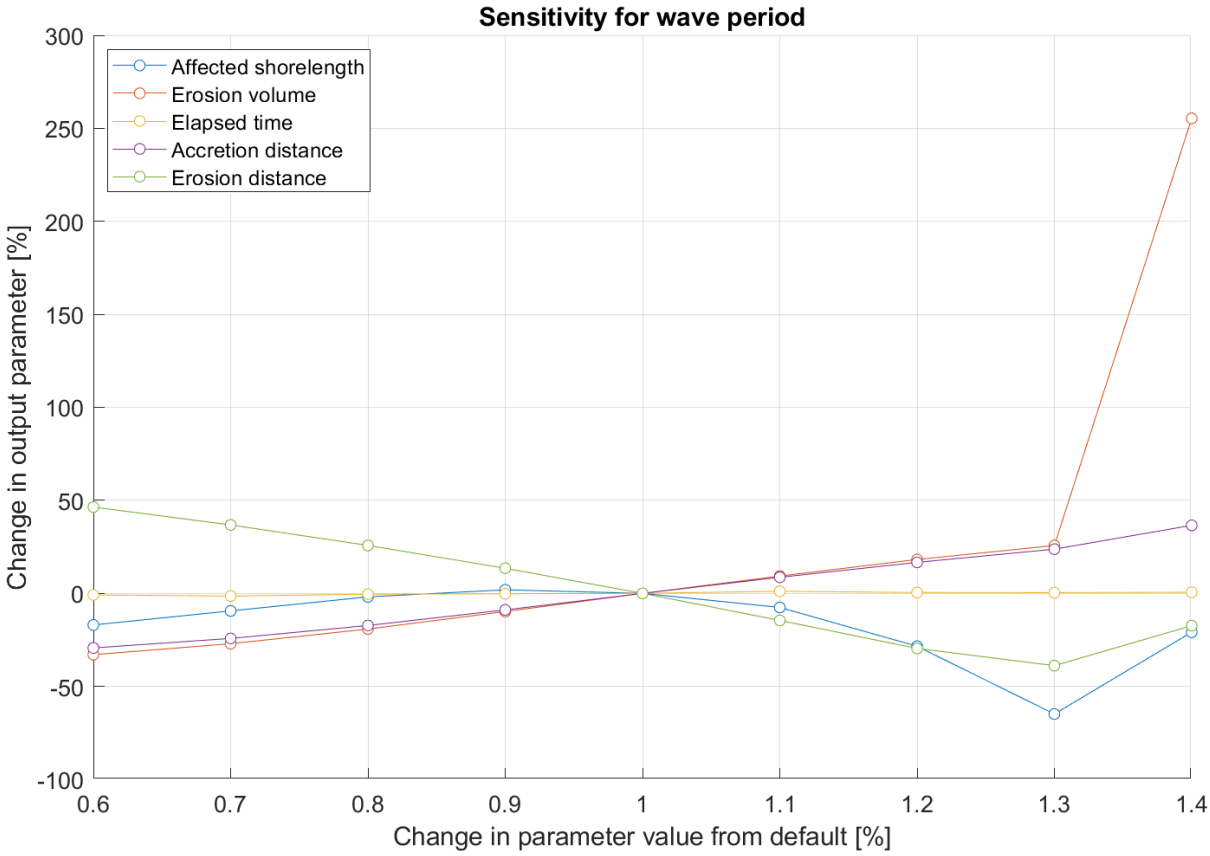

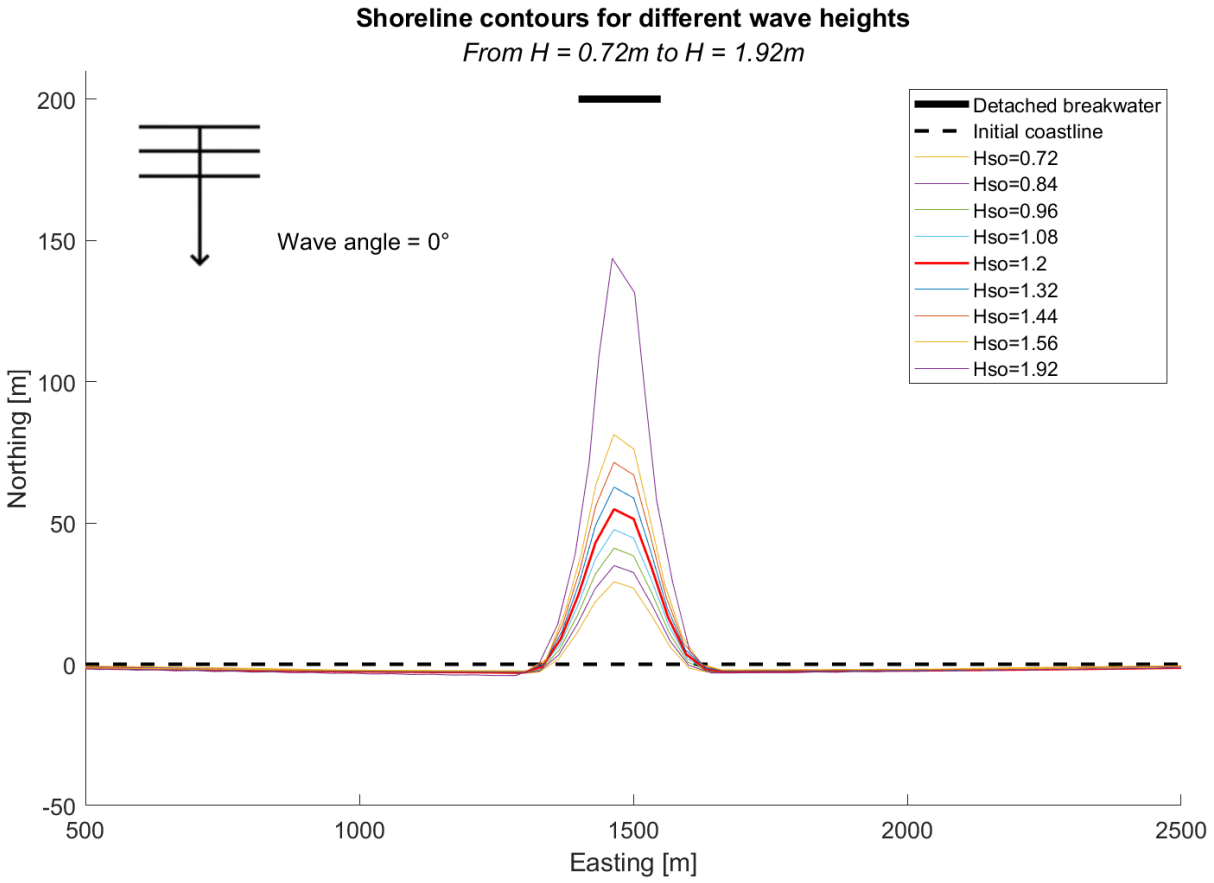
Shoreline contours for different wave heights
From H = 0.72m to H = 1.92m
Wave angle = 0°
Detached breakwater
Initial coastline
Hso=0.72
Hso=0.84
Hso=0.96
Hso=1.08
Hso=1.2
Hso=1.32
Hso=1.44
Hso=1.56
Hso=1.92
Northing [m]
Easting [m]
200
150
100
50
0
-50
500
1000
1500
2000
2500

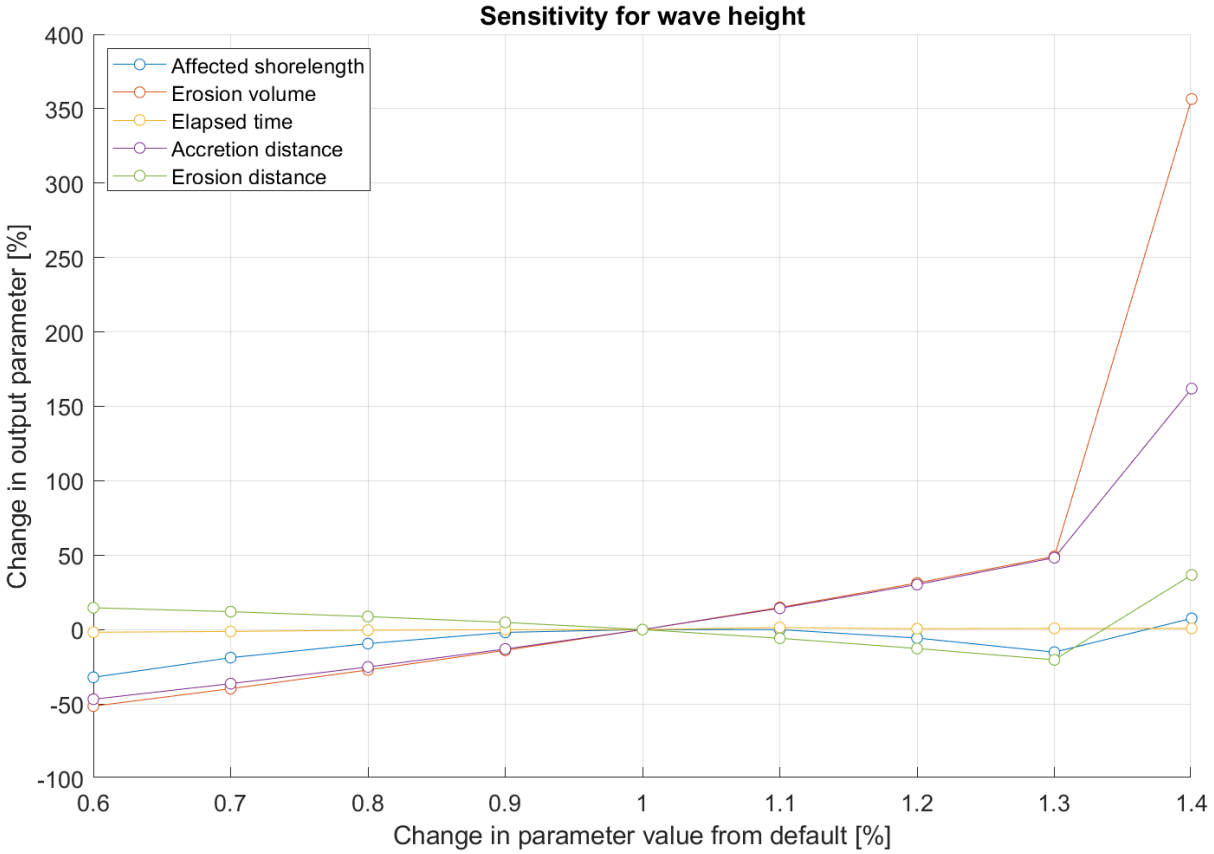
Sensitivity for wave height
Affected shorelength
Erosion volume
Elapsed time
Accretion distance
Erosion distance
Change in output parameter [%]
Change in parameter value from default [%]
400
350
300
250
200
150
100
50
0
-50
-100
0.6
0.7
0.8
0.9
1
1.1
1.2
1.3
1.4

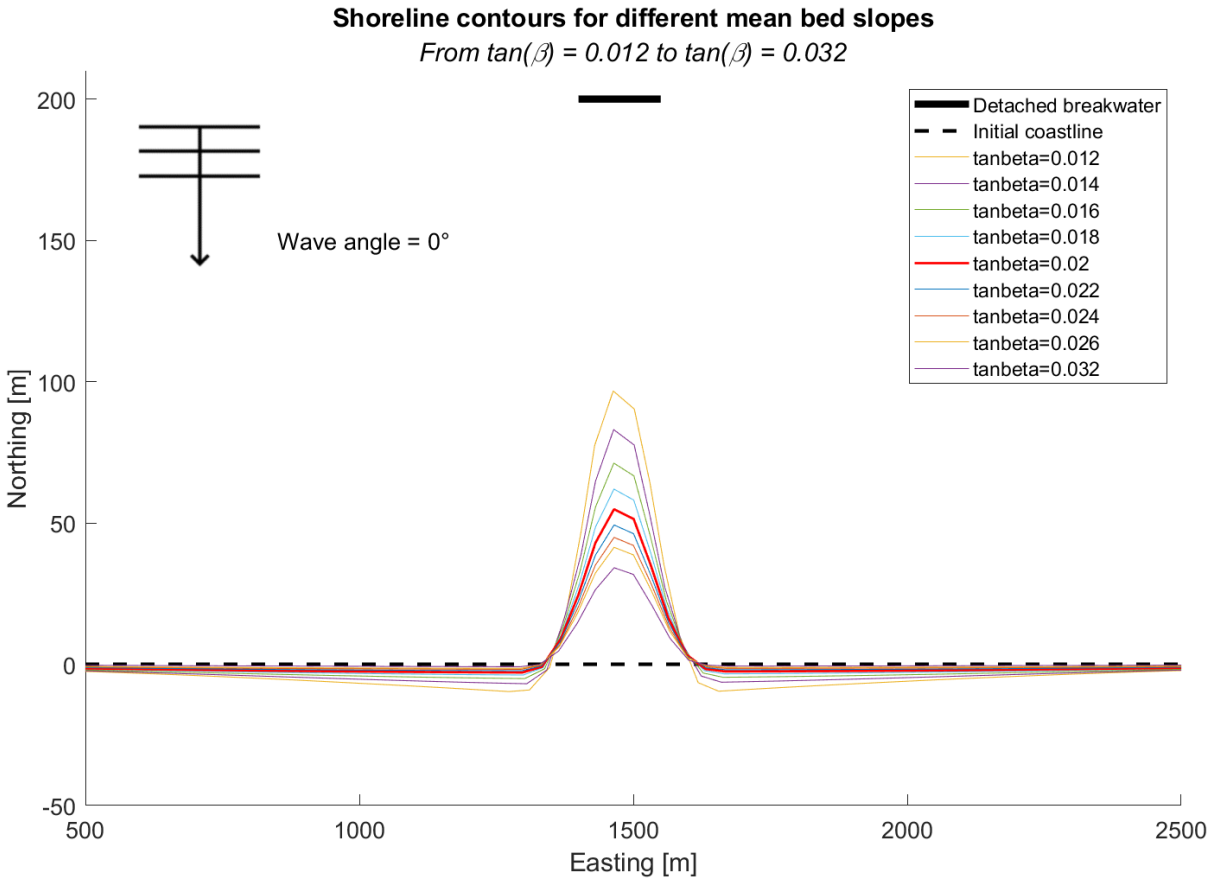
Shoreline contours for different mean bed slopes
From tan(β) = 0.012 to tan(β) = 0.032
Wave angle = 0°
Detached breakwater
Initial coastline
tanbeta=0.012
tanbeta=0.014
tanbeta=0.016
tanbeta=0.018
tanbeta=0.02
tanbeta=0.022
tanbeta=0.024
tanbeta=0.026
tanbeta=0.032
Northing [m]
Easting [m]
200
150
100
50
0
-50
500
1000
1500
2000
2500

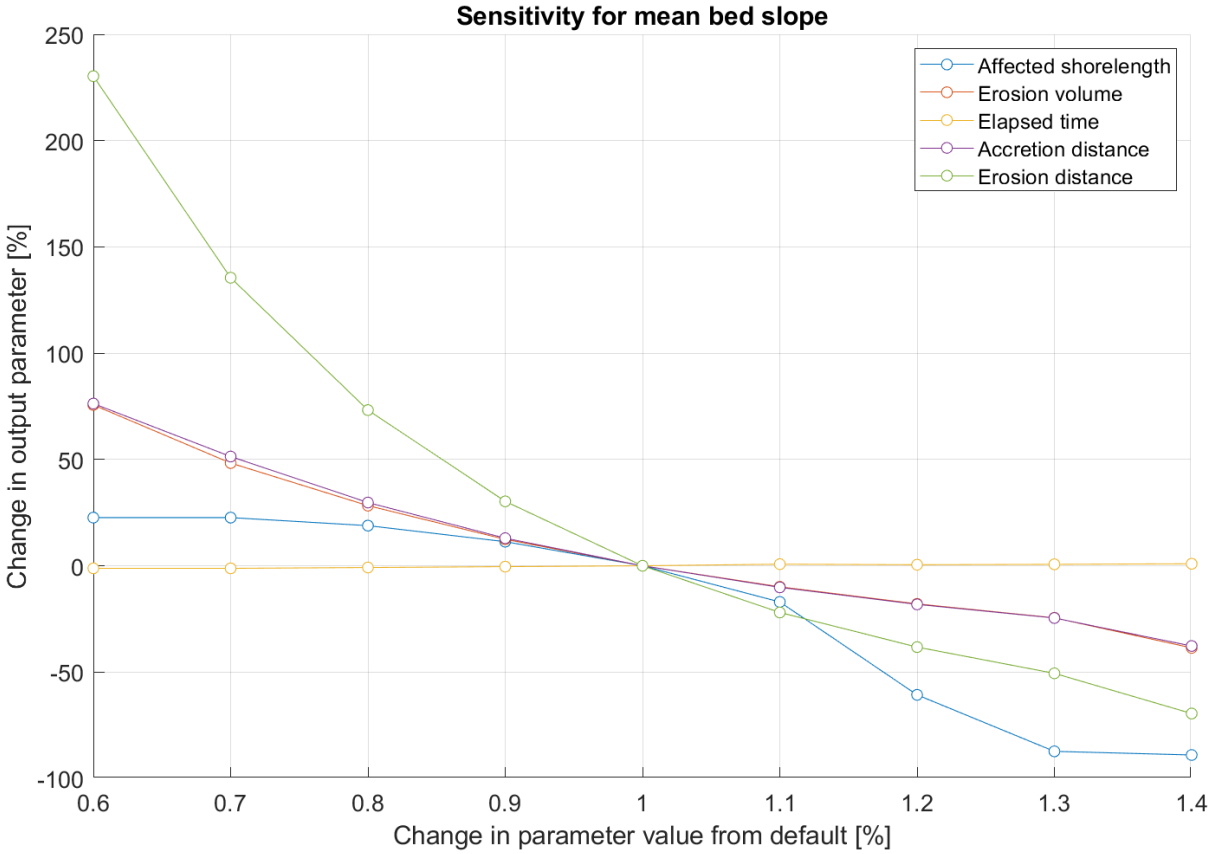
Sensitivity for mean bed slope
Affected shorelength
Erosion volume
Elapsed time
Accretion distance
Erosion distance
Change in output parameter [%]
Change in parameter value from default [%]
250
200
150
100
50
0
-50
-100
0.6
0.7
0.8
0.9
1
1.1
1.2
1.3
1.4

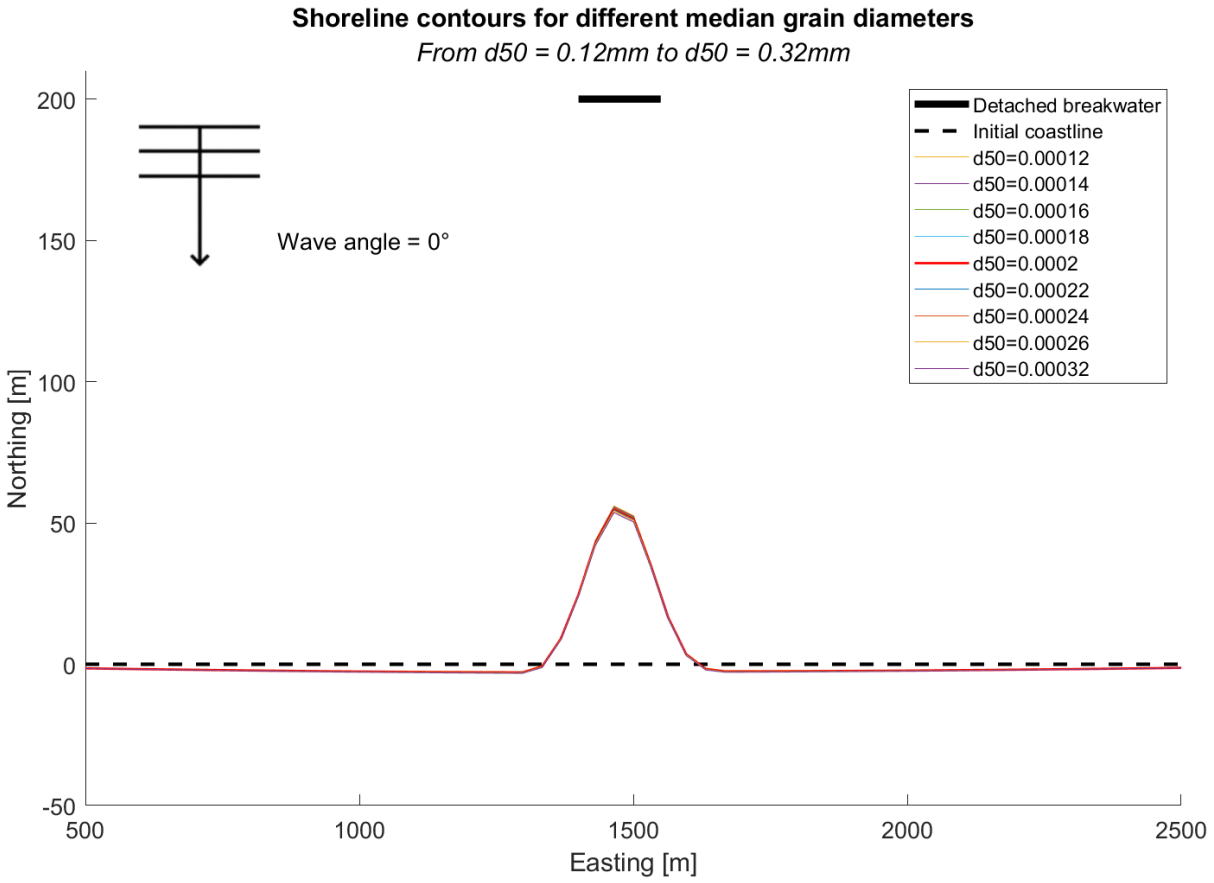
Shoreline contours for different median grain diameters
From d50 = 0.12mm to d50 = 0.32mm
Wave angle = 0°
Detached breakwater
Initial coastline
d50=0.00012
d50=0.00014
d50=0.00016
d50=0.00018
d50=0.0002
d50=0.00022
d50=0.00024
d50=0.00026
d50=0.00032
Northing [m]
Easting [m]
200
150
100
50
0
-50
500
1000
1500
2000
2500

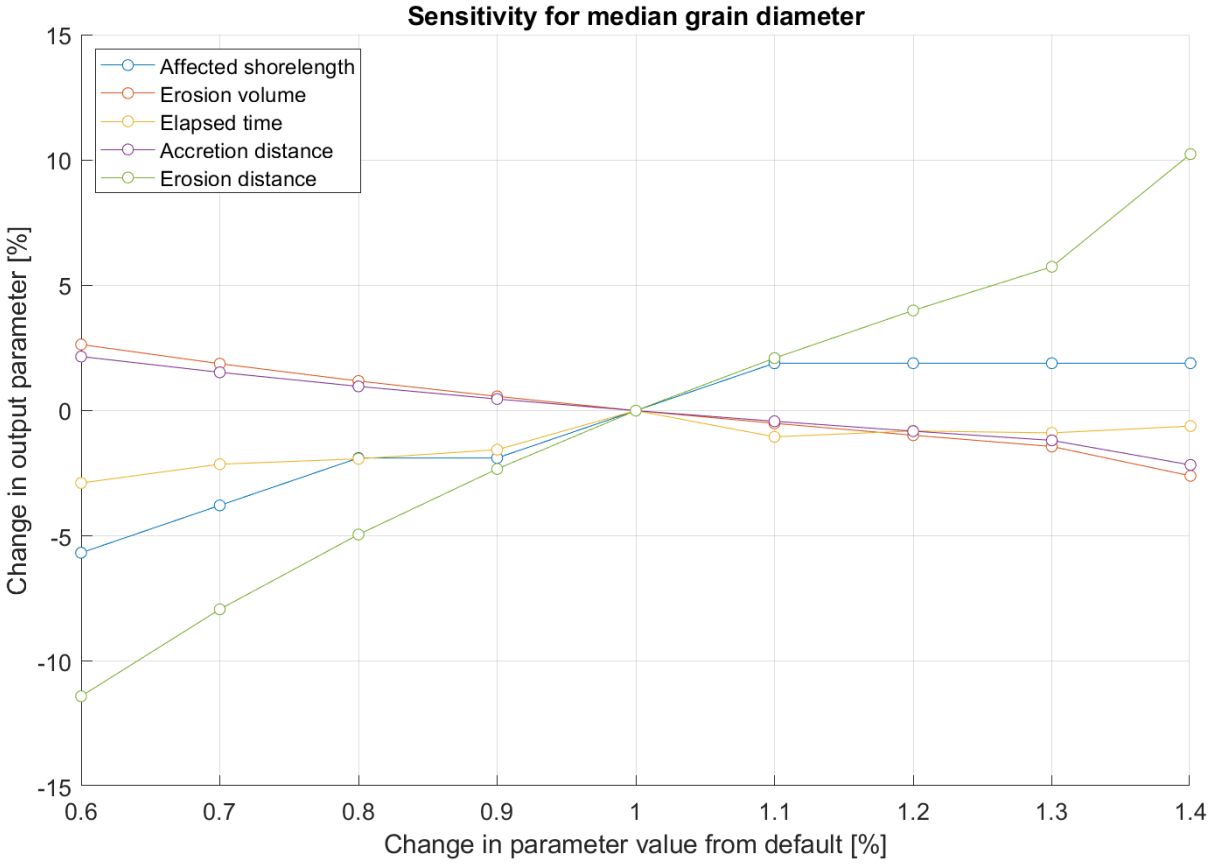
Sensitivity for median grain diameter
Affected shorelength
Erosion volume
Elapsed time
Accretion distance
Erosion distance
Change in output parameter [%]
Change in parameter value from default [%]
15
10
5
0
-5
-10
-15
0.6
0.7
0.8
0.9
1
1.1
1.2
1.3
1.4

A.6. Post-processing of detailed salient sensitivity analysis (wave angle=20°)

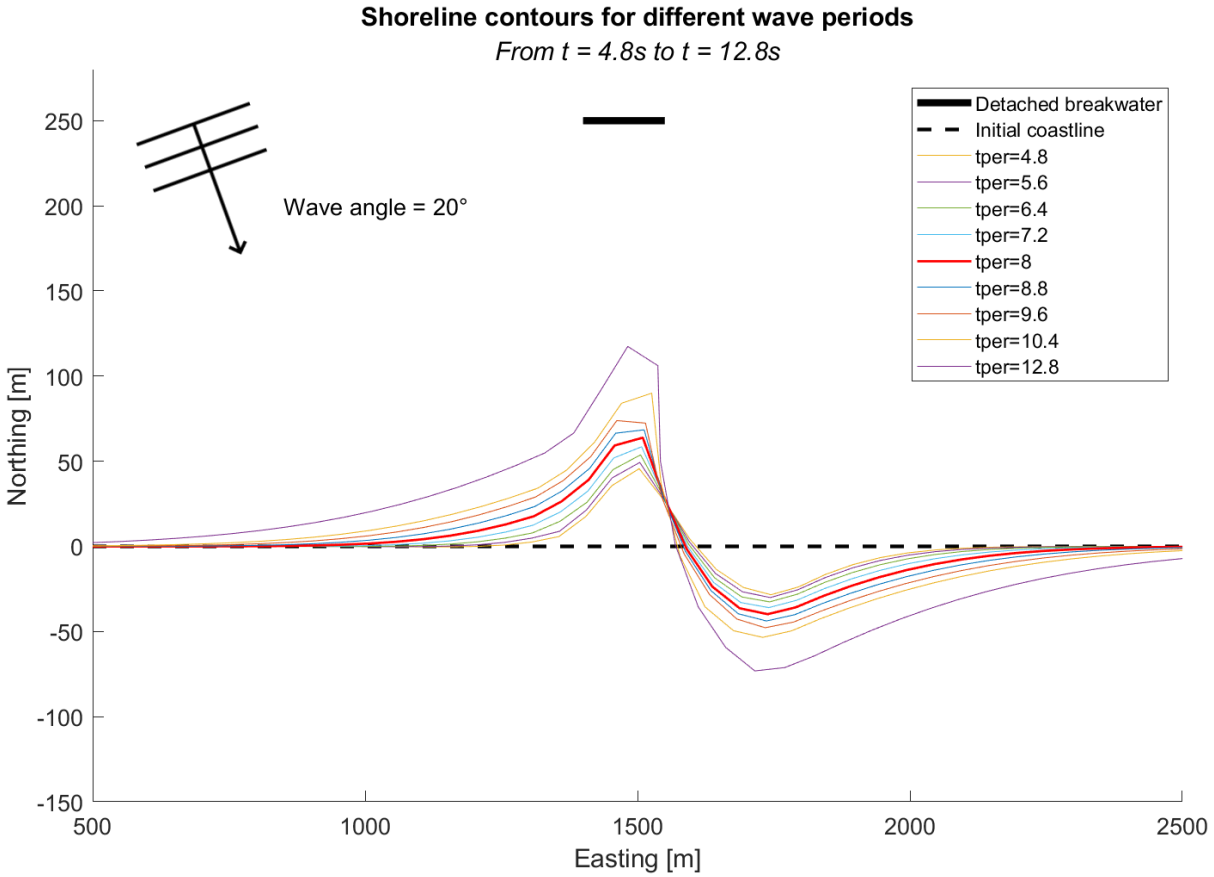

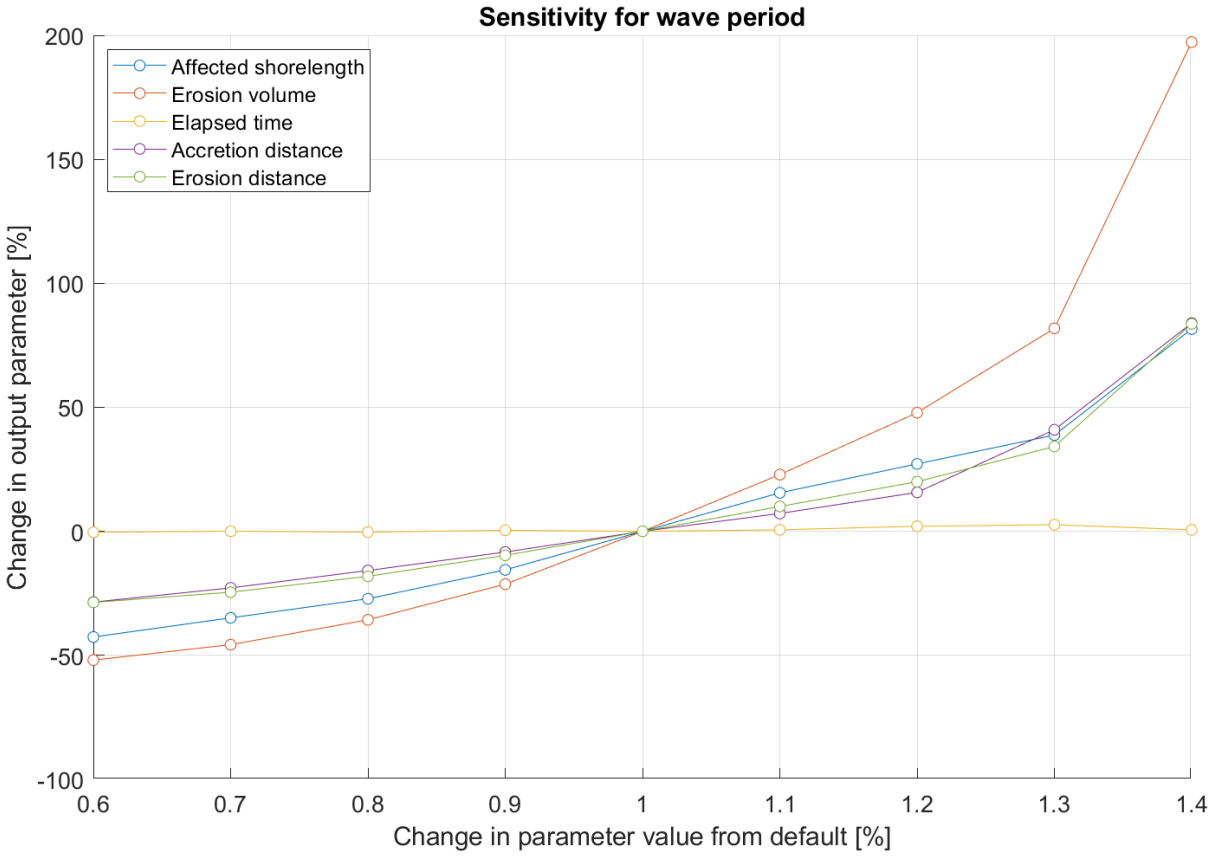

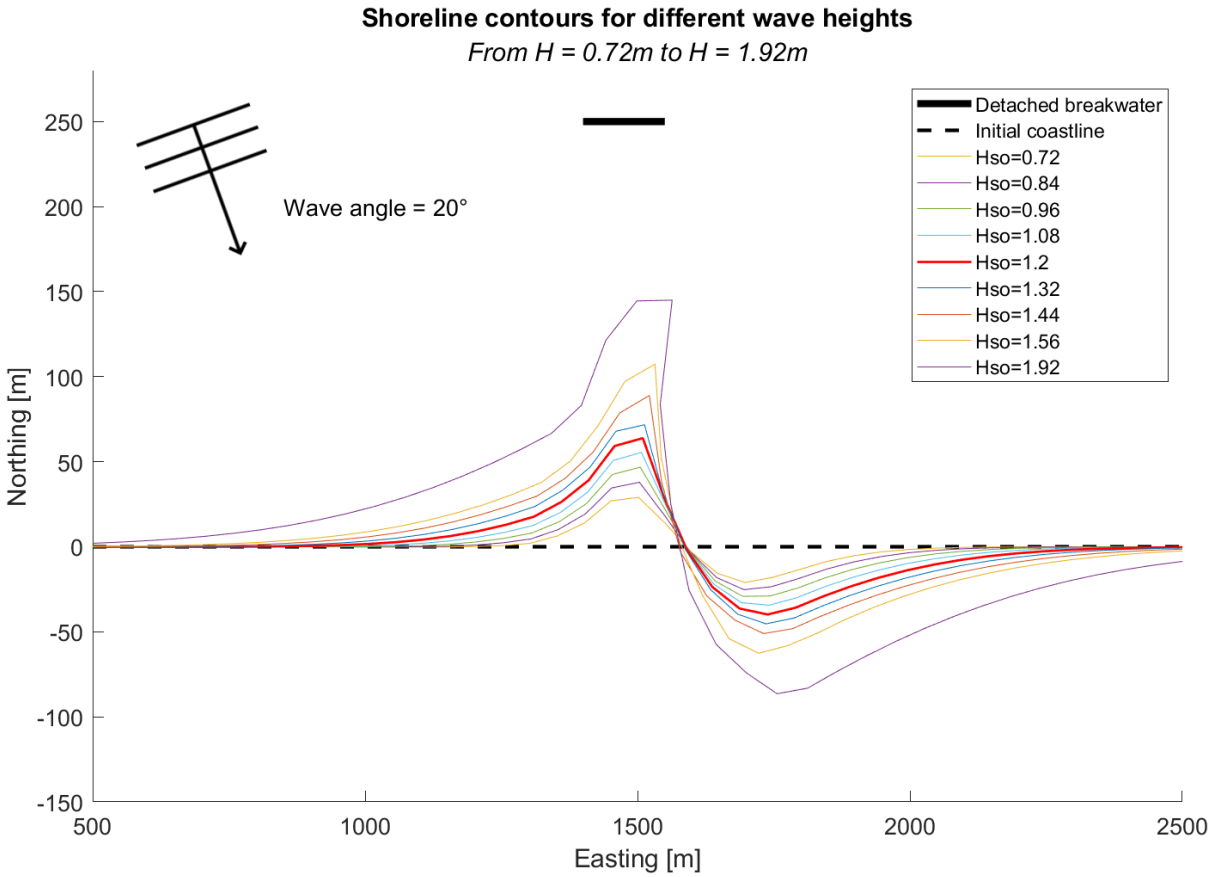
Shoreline contours for different wave heights
From H = 0.72m to H = 1.92m
Wave angle = 20°
Detached breakwater
Initial coastline
Hso=0.72
Hso=0.84
Hso=0.96
Hso=1.08
Hso=1.2
Hso=1.32
Hso=1.44
Hso=1.56
Hso=1.92
Northing [m]
Easting [m]
250
200
150
100
50
0
-50
-100
-150
500
1000
1500
2000
2500

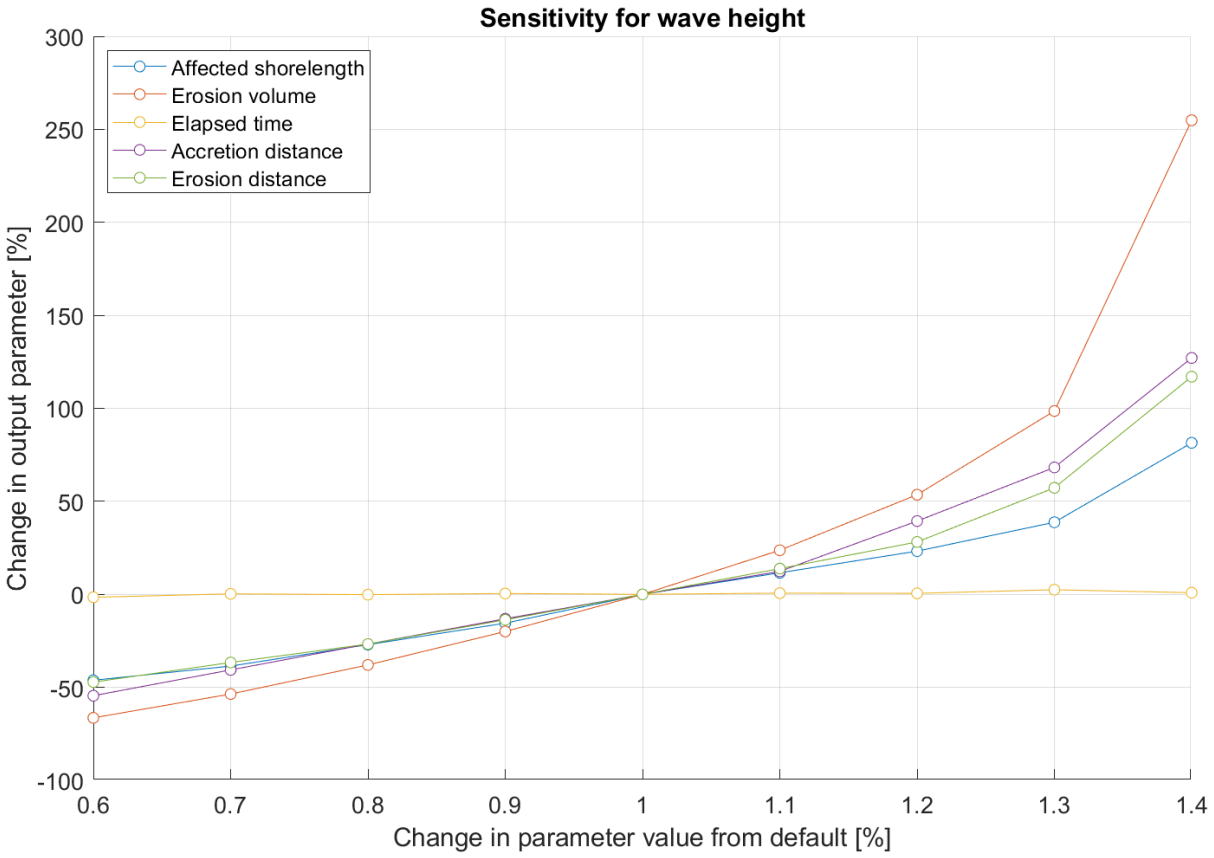
Sensitivity for wave height
Affected shorelength
Erosion volume
Elapsed time
Accretion distance
Erosion distance
Change in output parameter [%]
Change in parameter value from default [%]
300
250
200
150
100
50
0
-50
-100
0.6
0.7
0.8
0.9
1
1.1
1.2
1.3
1.4

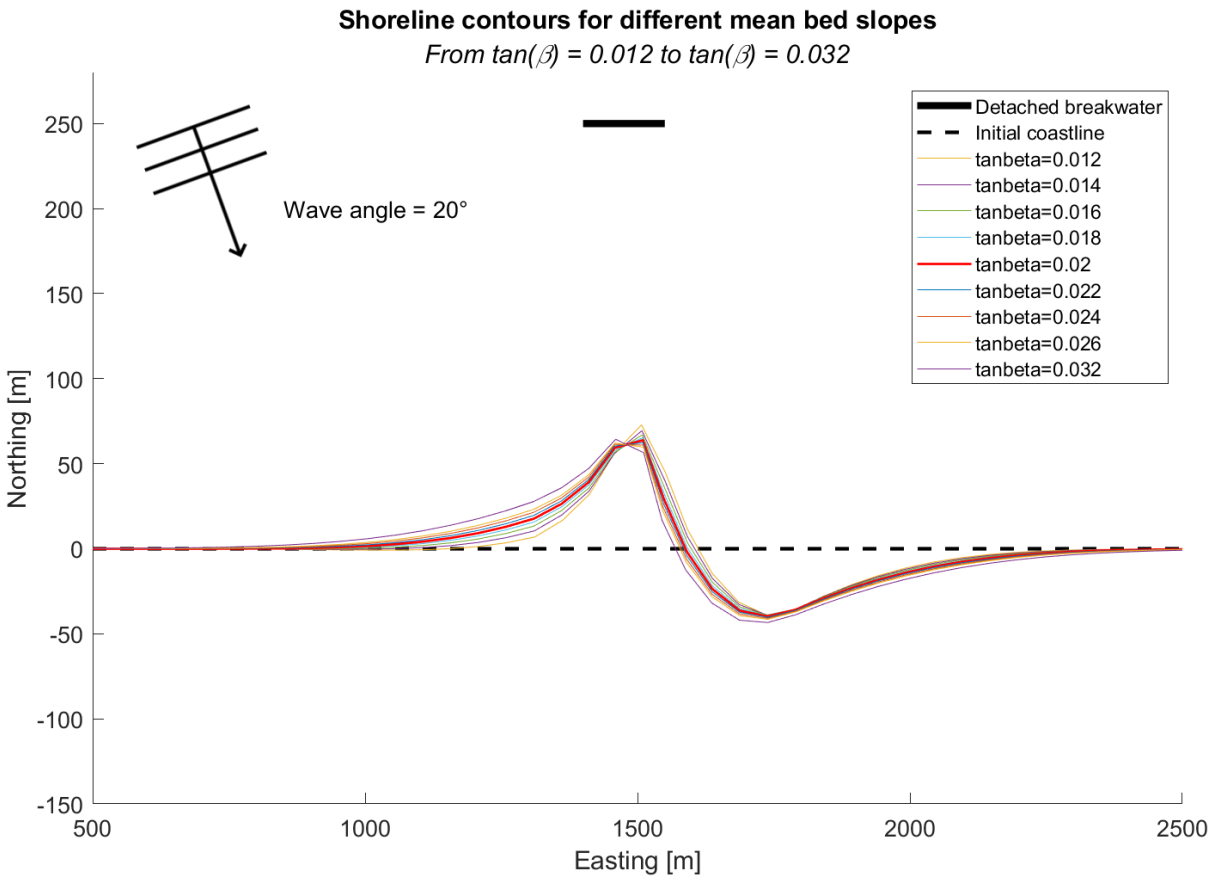
Shoreline contours for different mean bed slopes
From tan(β) = 0.012 to tan(β) = 0.032
Wave angle = 20°
Detached breakwater
Initial coastline
tanbeta=0.012
tanbeta=0.014
tanbeta=0.016
tanbeta=0.018
tanbeta=0.02
tanbeta=0.022
tanbeta=0.024
tanbeta=0.026
tanbeta=0.032
Northing [m]
Easting [m]
250
200
150
100
50
0
-50
-100
-150
500
1000
1500
2000
2500

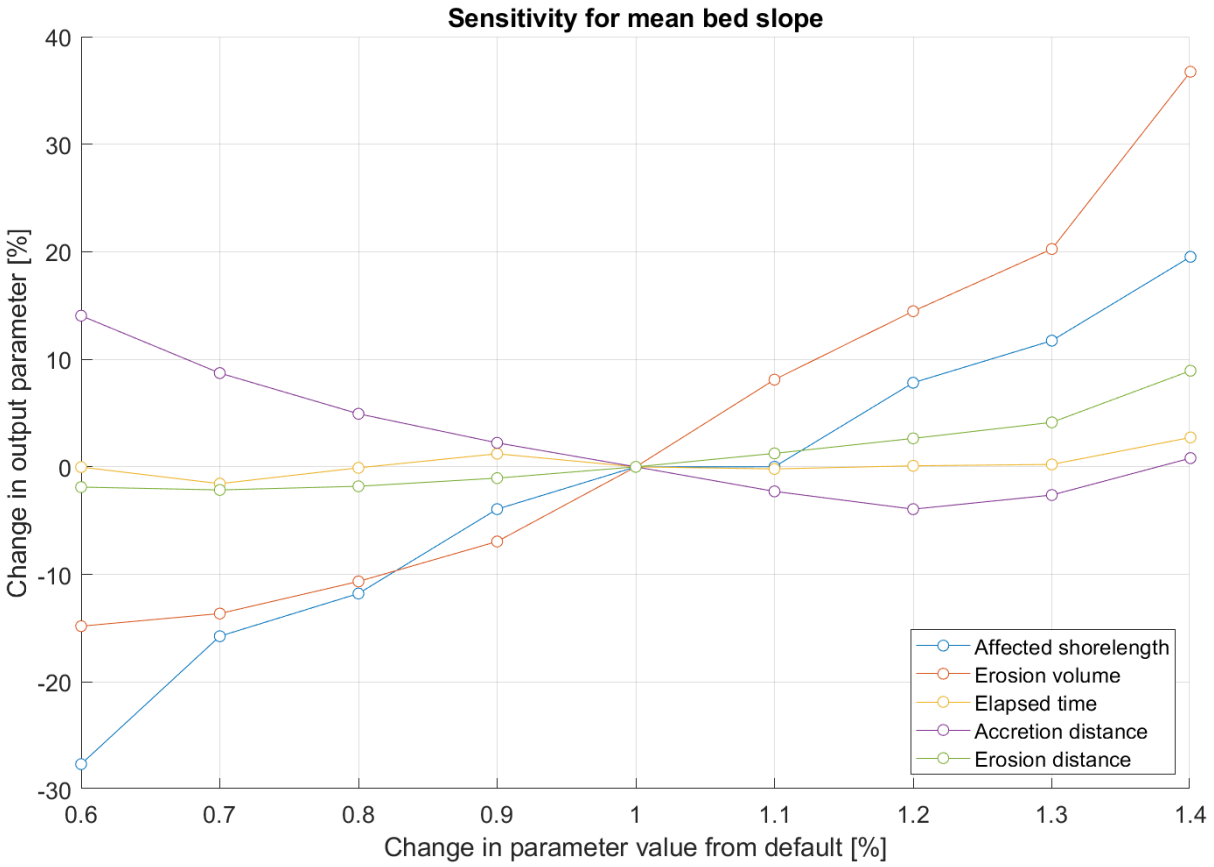
Sensitivity for mean bed slope
Change in output parameter [%]
Change in parameter value from default [%]
Affected shorelength
Erosion volume
Elapsed time
Accretion distance
Erosion distance
40
30
20
10
0
-10
-20
-30
0.6
0.7
0.8
0.9
1
1.1
1.2
1.3
1.4

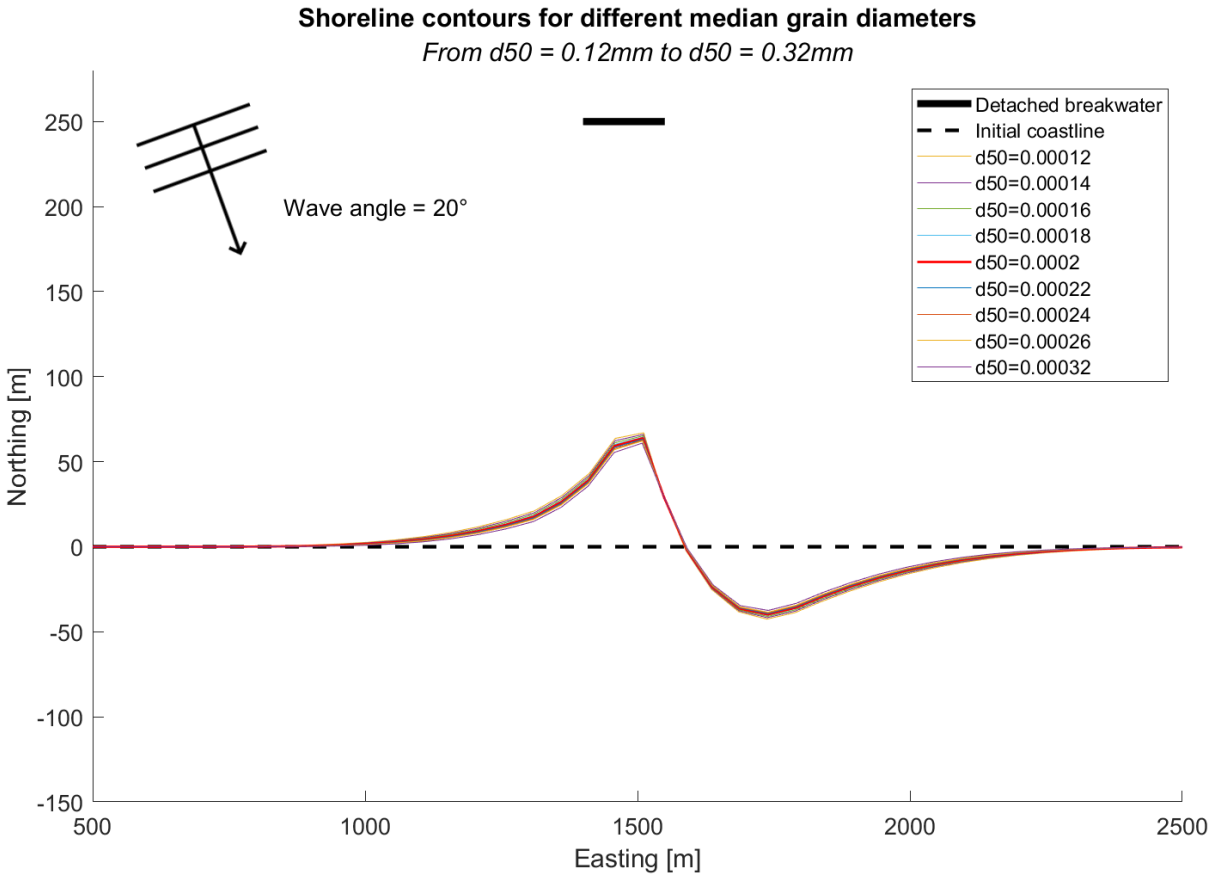
Shoreline contours for different median grain diameters
From d50 = 0.12mm to d50 = 0.32mm
Wave angle = 20°
Detached breakwater
Initial coastline
d50=0.00012
d50=0.00014
d50=0.00016
d50=0.00018
d50=0.0002
d50=0.00022
d50=0.00024
d50=0.00026
d50=0.00032
Northing [m]
Easting [m]
250
200
150
100
50
0
-50
-100
-150
500
1000
1500
2000
2500

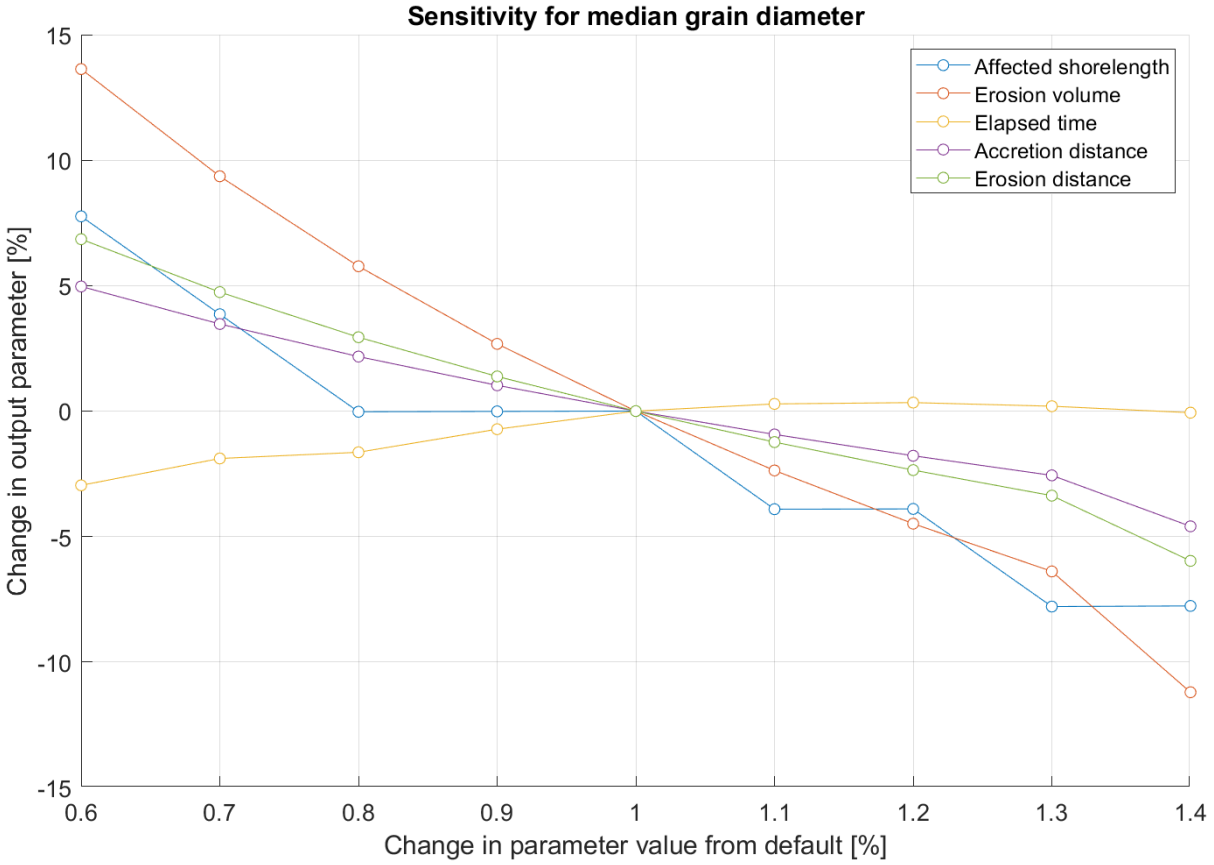
Sensitivity for median grain diameter
Affected shorelength
Erosion volume
Elapsed time
Accretion distance
Erosion distance
Change in output parameter [%]
Change in parameter value from default [%]
15
10
5
0
-5
-10
-15
0.6
0.7
0.8
0.9
1
1.1
1.2
1.3
1.4

A.7. Sensitivity difference between output parameters

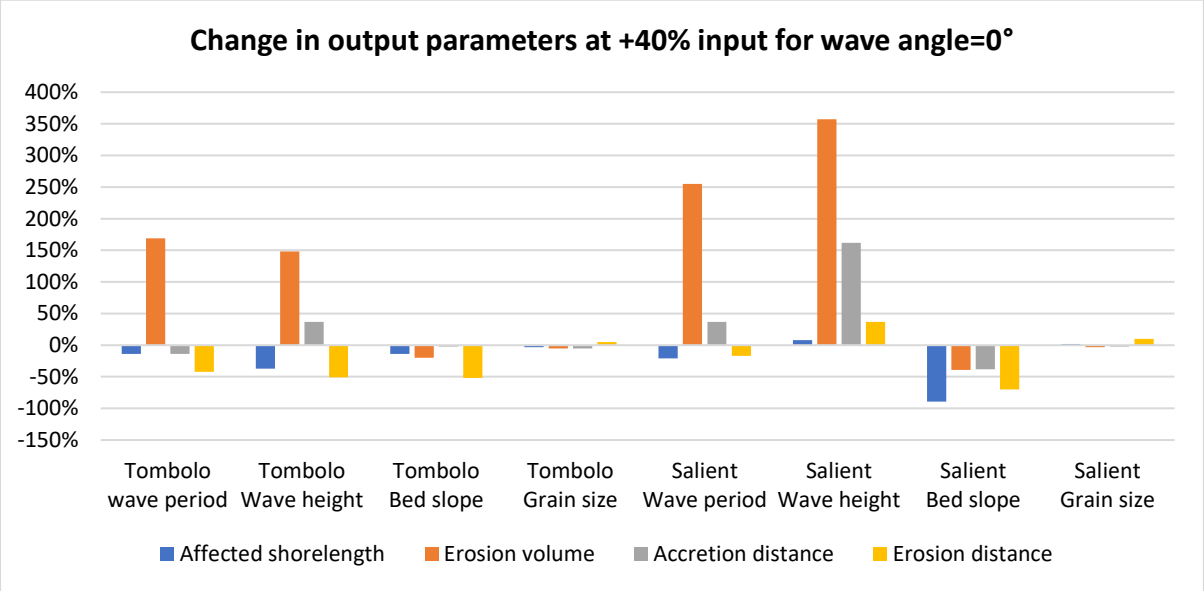

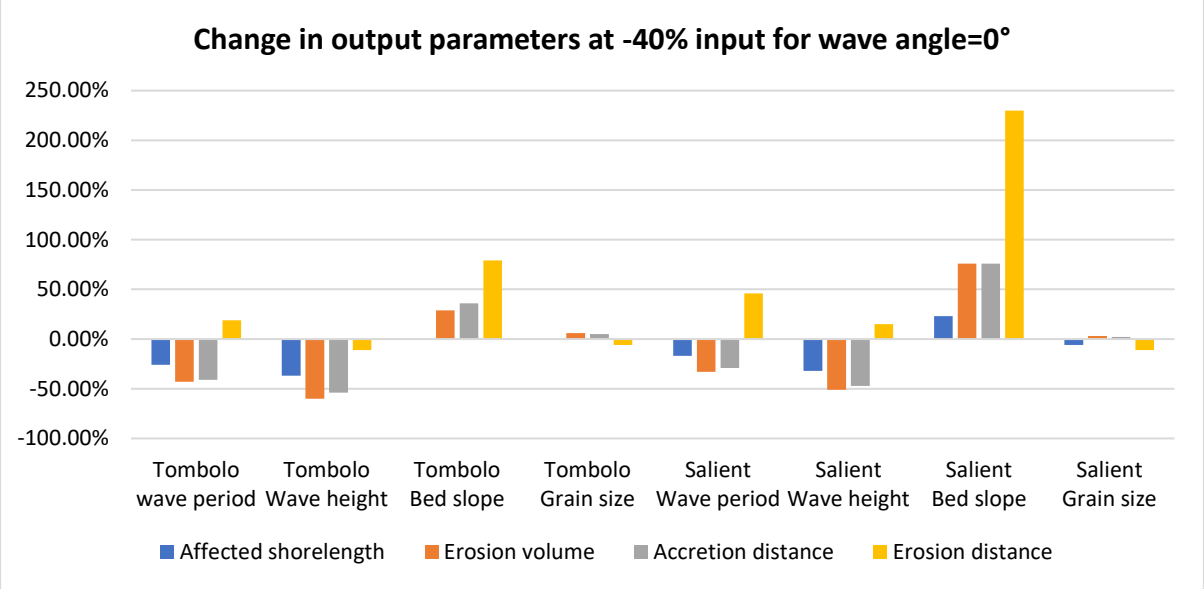

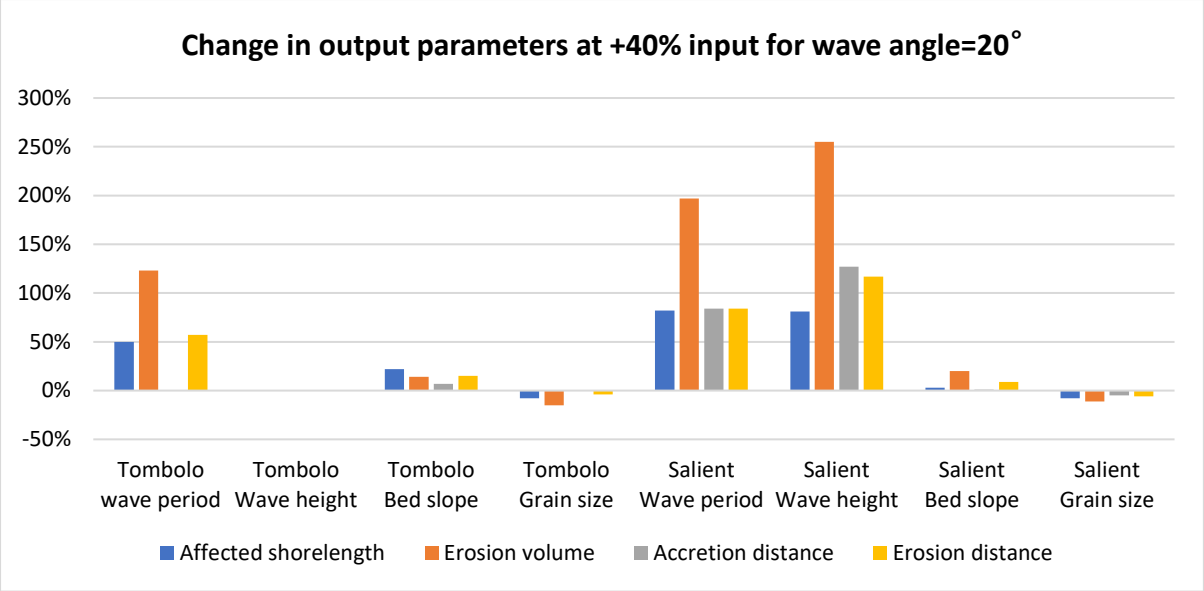
Change in output parameters at +40% input for wave angle=20°
300%
250%
200%
150%
100%
50%
0%
-50%
Tombolo wave period
Tombolo Wave height
Tombolo Bed slope
Tombolo Grain size
Salient Wave period
Salient Wave height
Salient Bed slope
Salient Grain size
Affected shorelength
Erosion volume
Accretion distance
Erosion distance

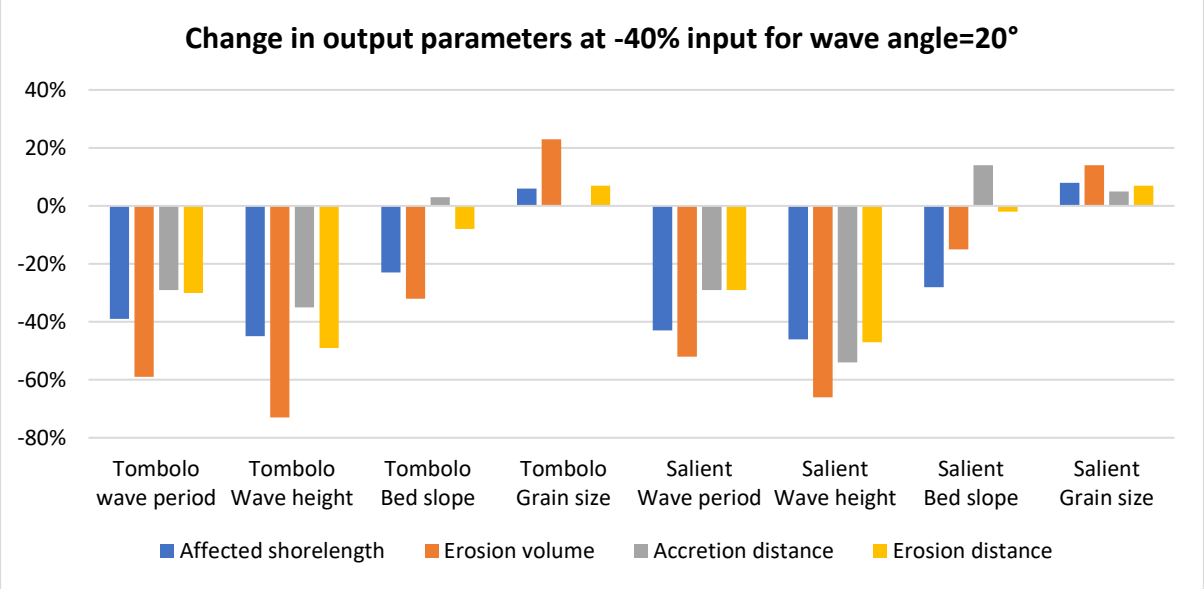
Change in output parameters at -40% input for wave angle=20°
40%
20%
0%
-20%
-40%
-60%
-80%
Tombolo wave period
Tombolo Wave height
Tombolo Bed slope
Tombolo Grain size
Salient Wave period
Salient Wave height
Salient Bed slope
Salient Grain size
Affected shorelength
Erosion volume
Accretion distance
Erosion distance

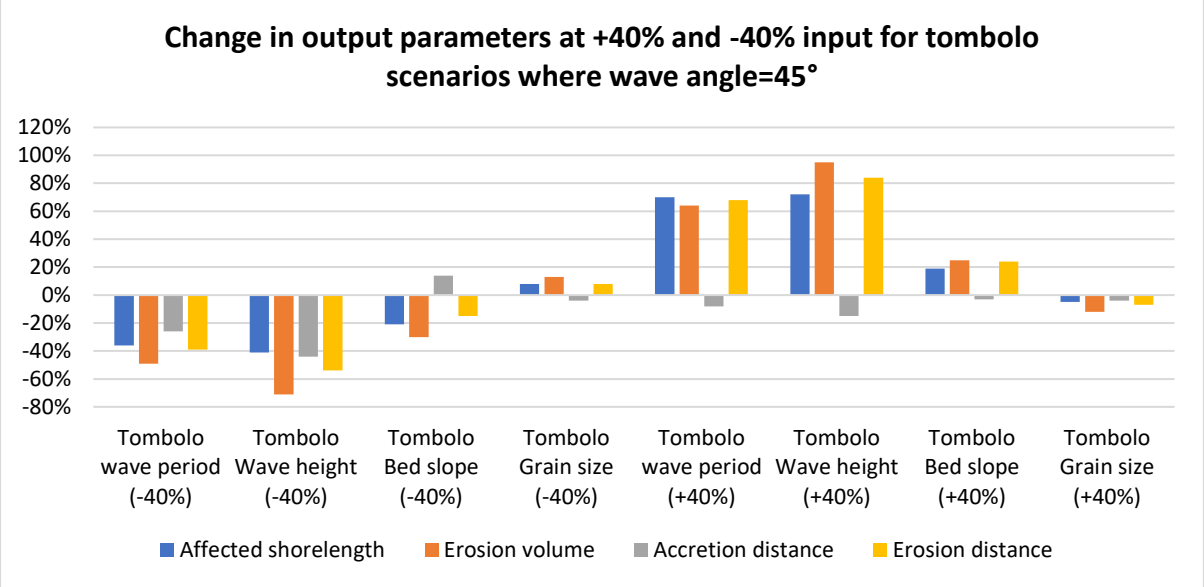
Change in output parameters at +40% and -40% input for tombolo scenarios where wave angle=45°
120%
100%
80%
60%
40%
20%
0%
-20%
-40%
-60%
-80%
Tombolo wave period (-40%)
Tombolo Wave height (-40%)
Tombolo Bed slope (-40%)
Tombolo Grain size (-40%)
Tombolo wave period (+40%)
Tombolo Wave height (+40%)
Tombolo Bed slope (+40%)
Tombolo Grain size (+40%)
Affected shorelength
Erosion volume
Accretion distance
Erosion distance

Appendix B – Model validation and performance tests

B.1. Post-processing model performance static equilibrium time

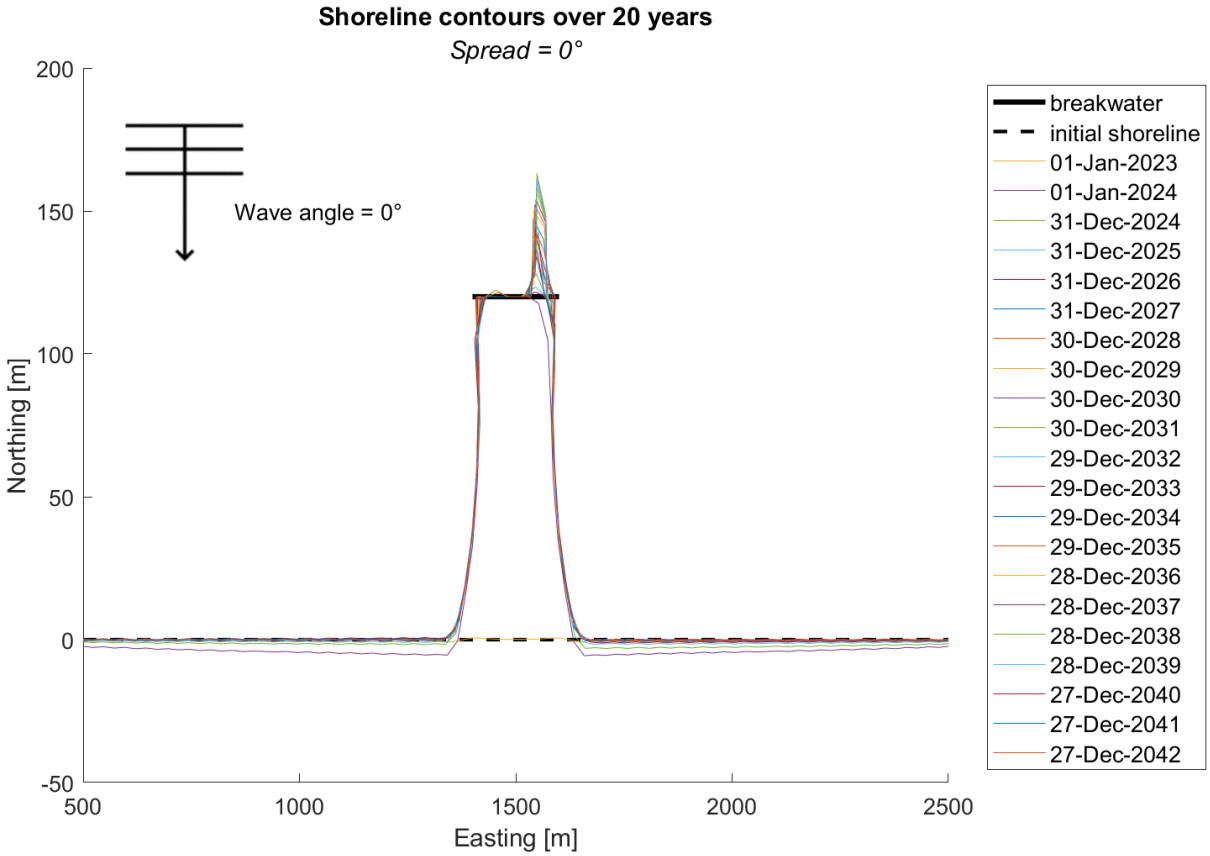

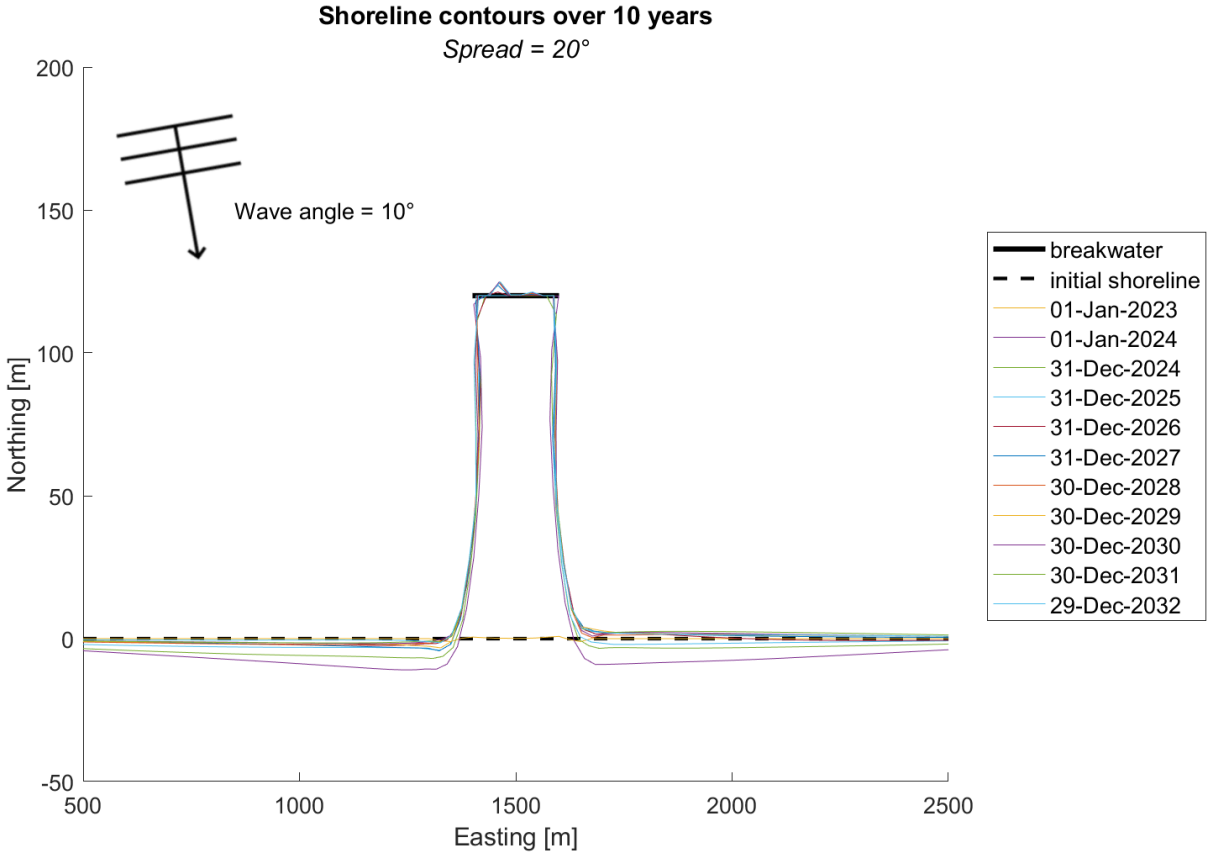

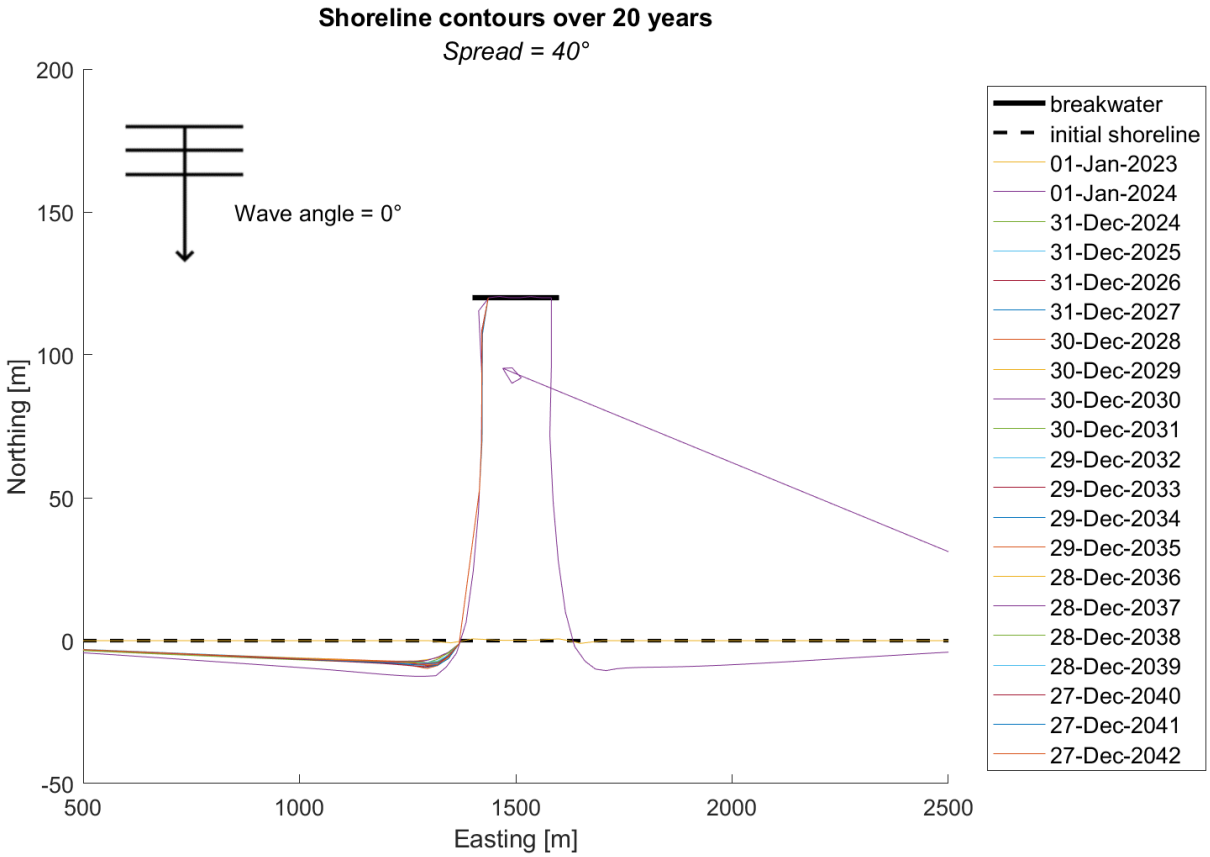
Shoreline contours over 20 years
Spread = 40°
Wave angle = 0°
Northing [m]
Easting [m]
200
150
100
50
0
-50
500
1000
1500
2000
2500
breakwater
initial shoreline
01-Jan-2023
01-Jan-2024
31-Dec-2024
31-Dec-2025
31-Dec-2026
31-Dec-2027
30-Dec-2028
30-Dec-2029
30-Dec-2030
30-Dec-2031
29-Dec-2032
29-Dec-2033
29-Dec-2034
29-Dec-2035
28-Dec-2036
28-Dec-2037
28-Dec-2038
28-Dec-2039
27-Dec-2040
27-Dec-2041
27-Dec-2042

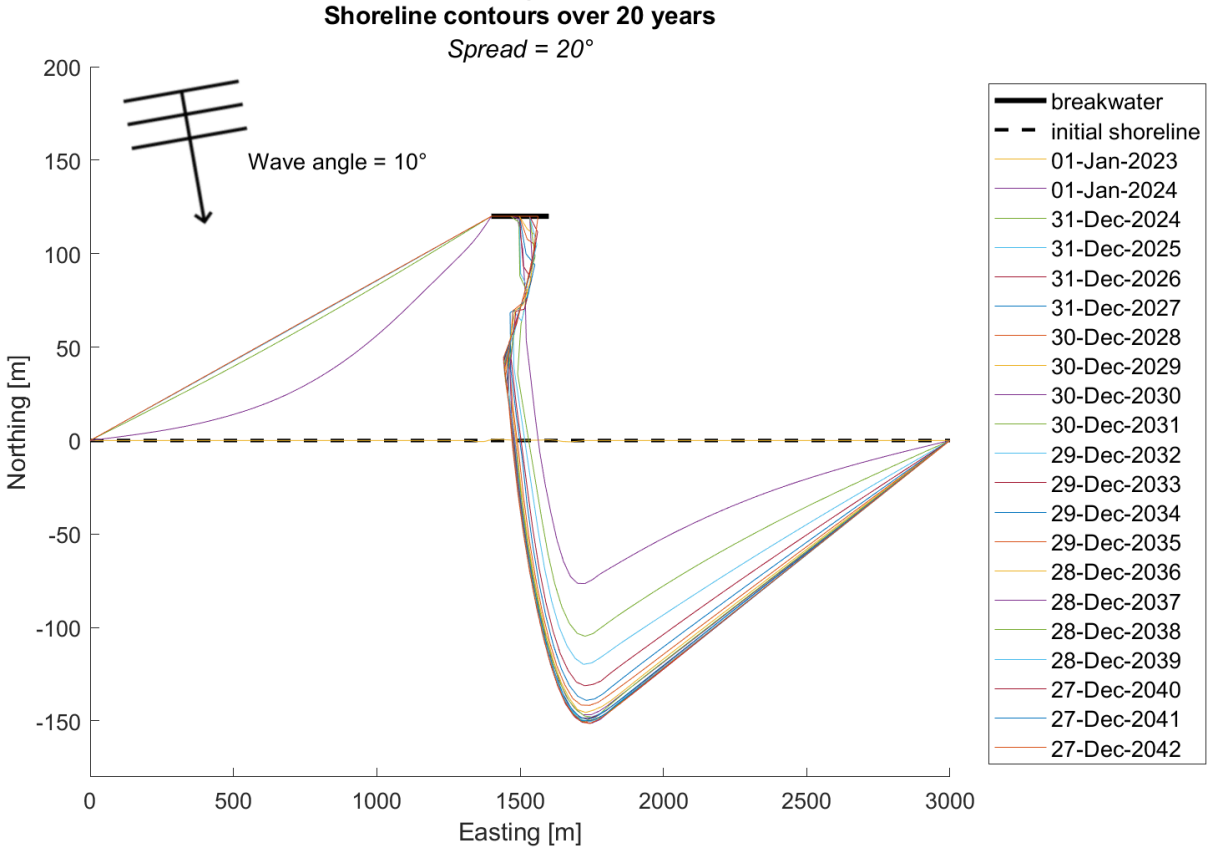
Shoreline contours over 20 years
Spread = 20°
Wave angle = 10°
Northing [m]
Easting [m]
200
150
100
50
0
-50
-100
-150
0
500
1000
1500
2000
2500
3000
breakwater
initial shoreline
01-Jan-2023
01-Jan-2024
31-Dec-2024
31-Dec-2025
31-Dec-2026
31-Dec-2027
30-Dec-2028
30-Dec-2029
30-Dec-2030
30-Dec-2031
29-Dec-2032
29-Dec-2033
29-Dec-2034
29-Dec-2035
28-Dec-2036
28-Dec-2037
28-Dec-2038
28-Dec-2039
27-Dec-2040
27-Dec-2041
27-Dec-2042

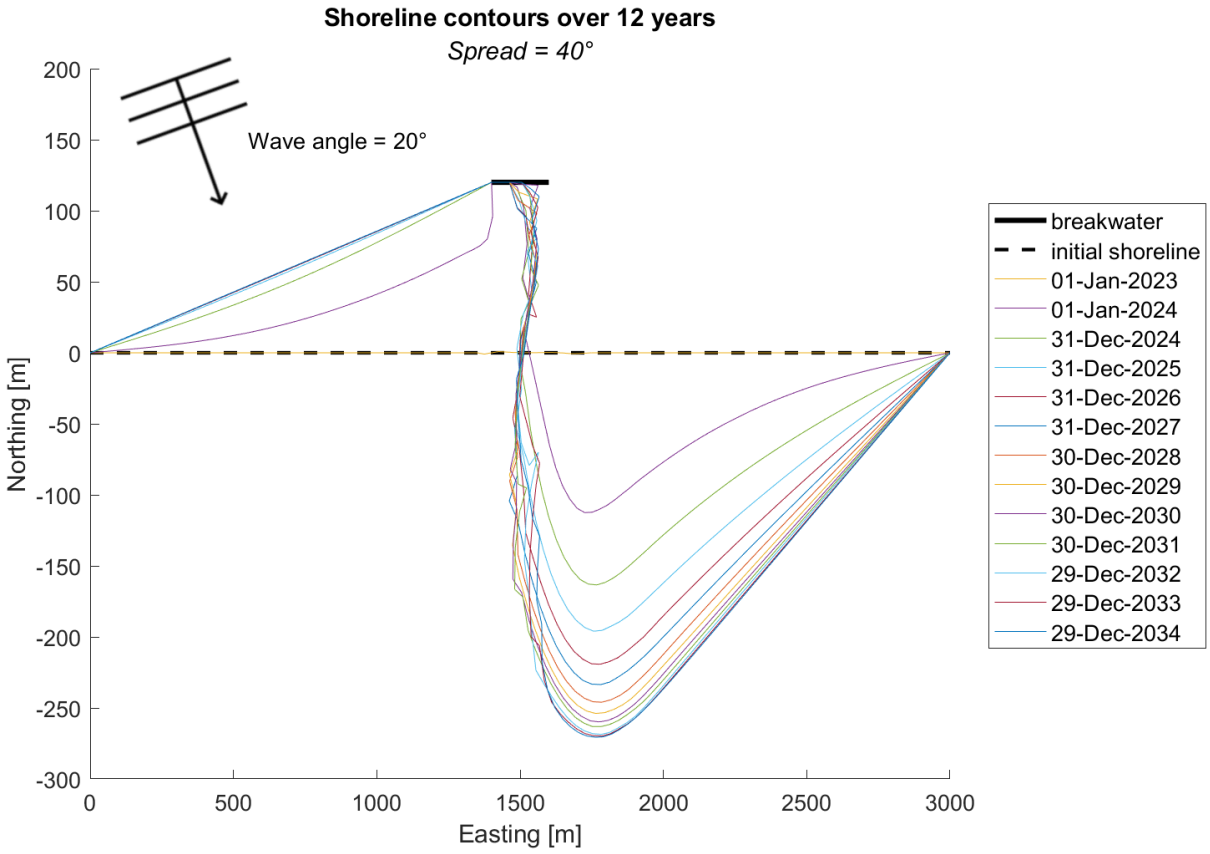
Shoreline contours over 12 years
Spread = 40°
Wave angle = 20°
Northing [m]
Easting [m]
200
150
100
50
0
-50
-100
-150
-200
-250
-300
0
500
1000
1500
2000
2500
3000
breakwater
initial shoreline
01-Jan-2023
01-Jan-2024
31-Dec-2024
31-Dec-2025
31-Dec-2026
31-Dec-2027
30-Dec-2028
30-Dec-2029
30-Dec-2030
30-Dec-2031
29-Dec-2032
29-Dec-2033
29-Dec-2034

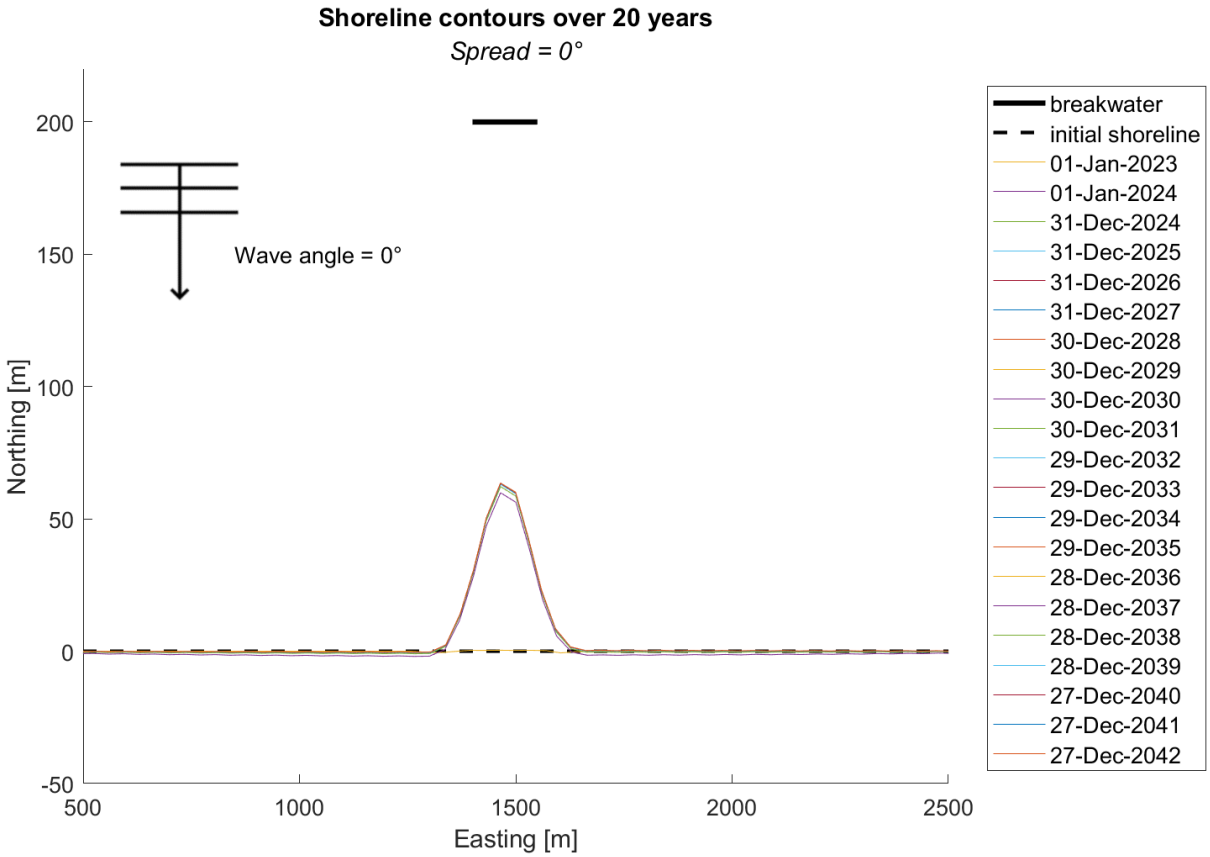
Shoreline contours over 20 years
Spread = 0°
Wave angle = 0°
Northing [m]
Easting [m]
200
150
100
50
0
-50
500
1000
1500
2000
2500
breakwater
initial shoreline
01-Jan-2023
01-Jan-2024
31-Dec-2024
31-Dec-2025
31-Dec-2026
31-Dec-2027
30-Dec-2028
30-Dec-2029
30-Dec-2030
30-Dec-2031
29-Dec-2032
29-Dec-2033
29-Dec-2034
29-Dec-2035
28-Dec-2036
28-Dec-2037
28-Dec-2038
28-Dec-2039
27-Dec-2040
27-Dec-2041
27-Dec-2042

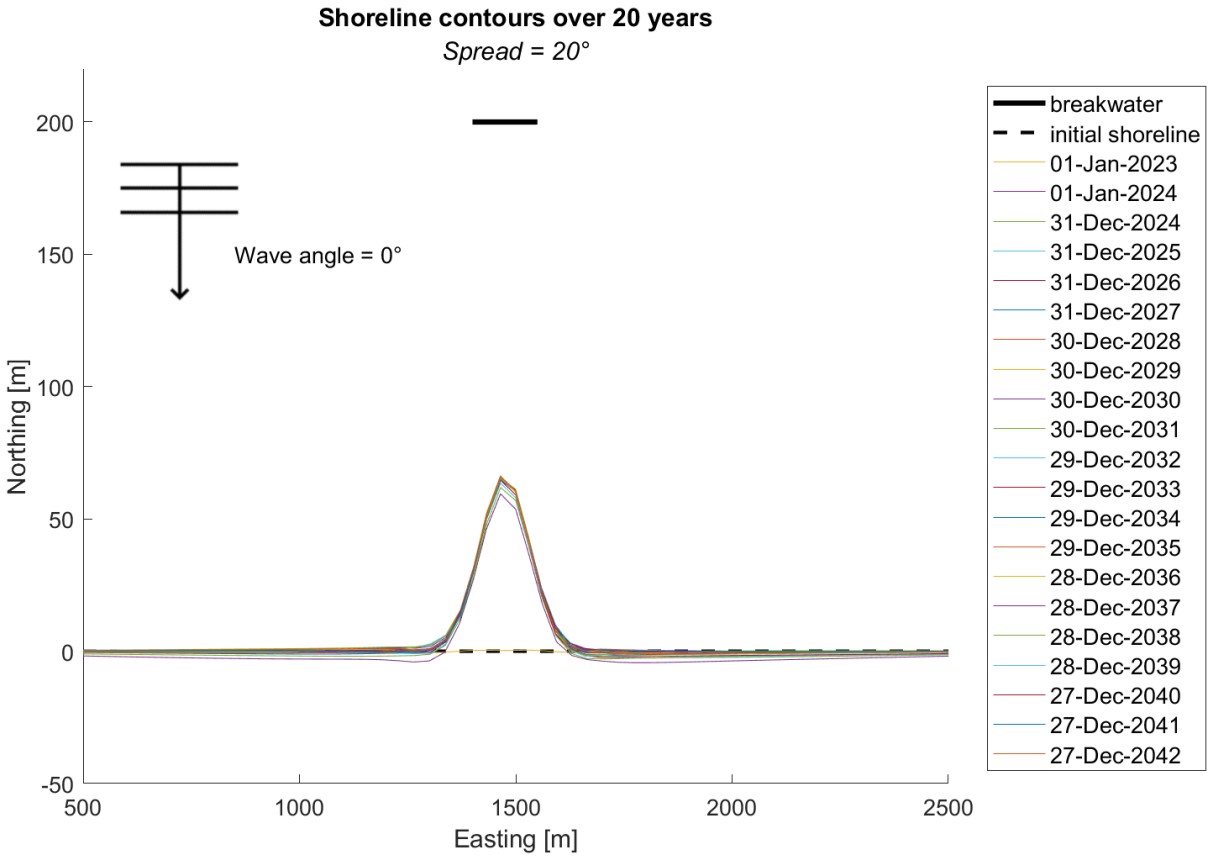
Shoreline contours over 20 years
Spread = 20°
Wave angle = 0°
Northing [m]
Easting [m]
200
150
100
50
0
-50
500
1000
1500
2000
2500
breakwater
initial shoreline
01-Jan-2023
01-Jan-2024
31-Dec-2024
31-Dec-2025
31-Dec-2026
31-Dec-2027
30-Dec-2028
30-Dec-2029
30-Dec-2030
30-Dec-2031
29-Dec-2032
29-Dec-2033
29-Dec-2034
29-Dec-2035
28-Dec-2036
28-Dec-2037
28-Dec-2038
28-Dec-2039
27-Dec-2040
27-Dec-2041
27-Dec-2042

B.2. Post-processing model performance salient parameters

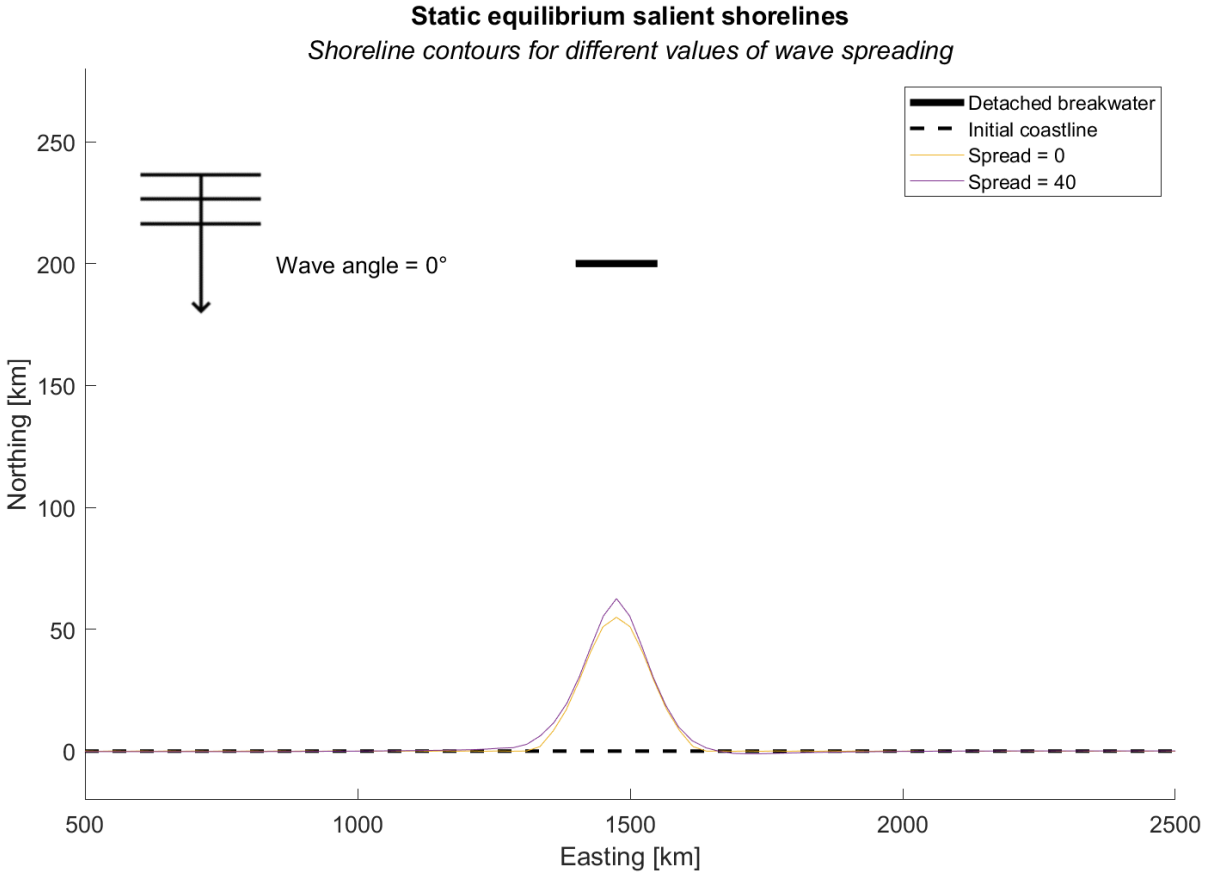

B.3. Post-processing model performance tombolo parameters

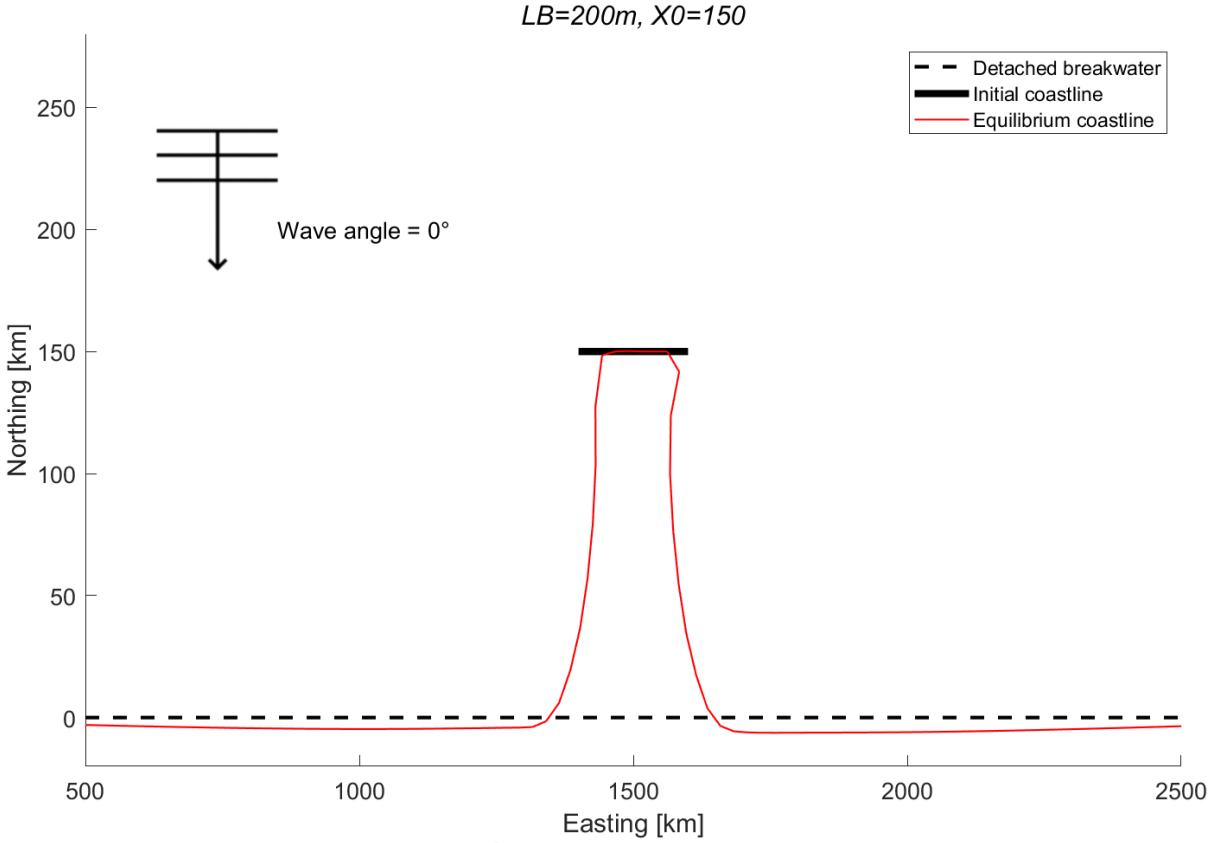

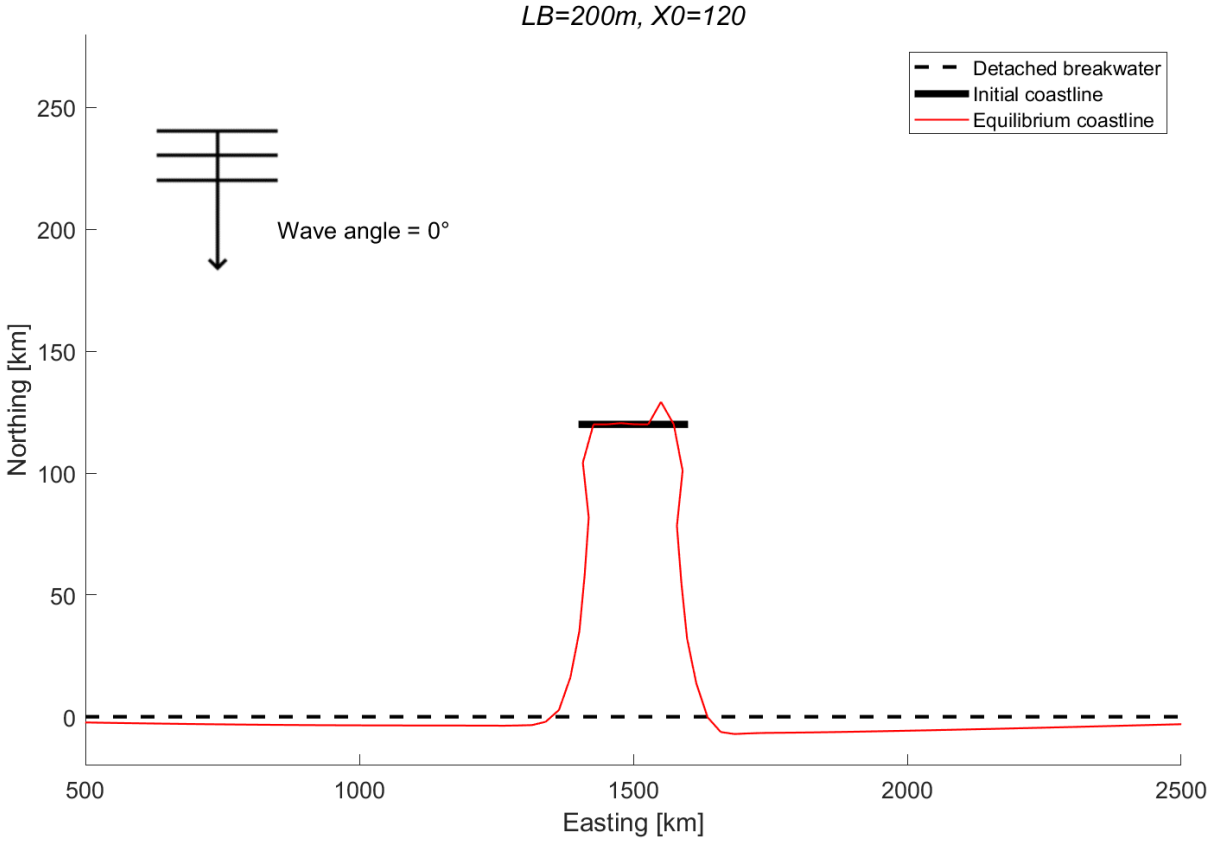

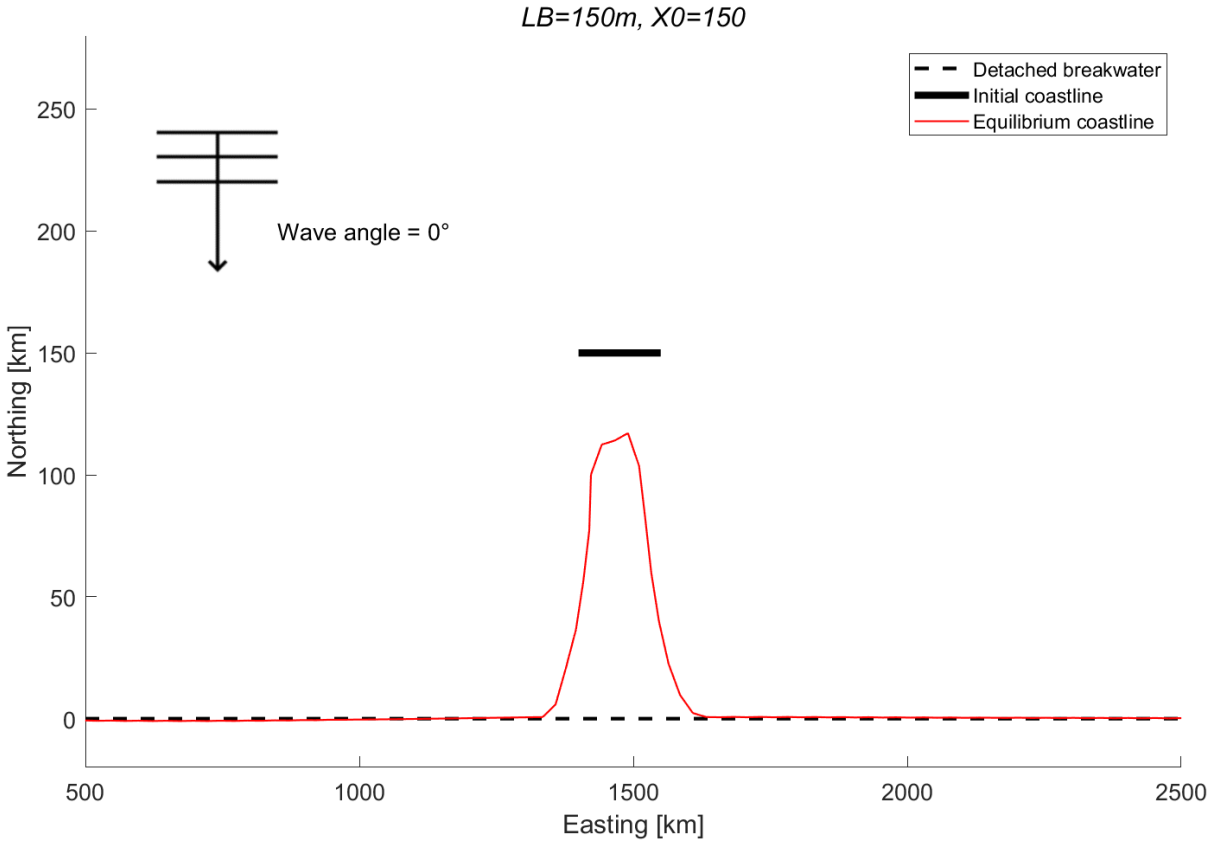
LB=150m, X0=150
Detached breakwater
Initial coastline
Equilibrium coastline
Wave angle = 0°
Northing [km]
Easting [km]
0
50
100
150
200
250
500
1000
1500
2000
2500

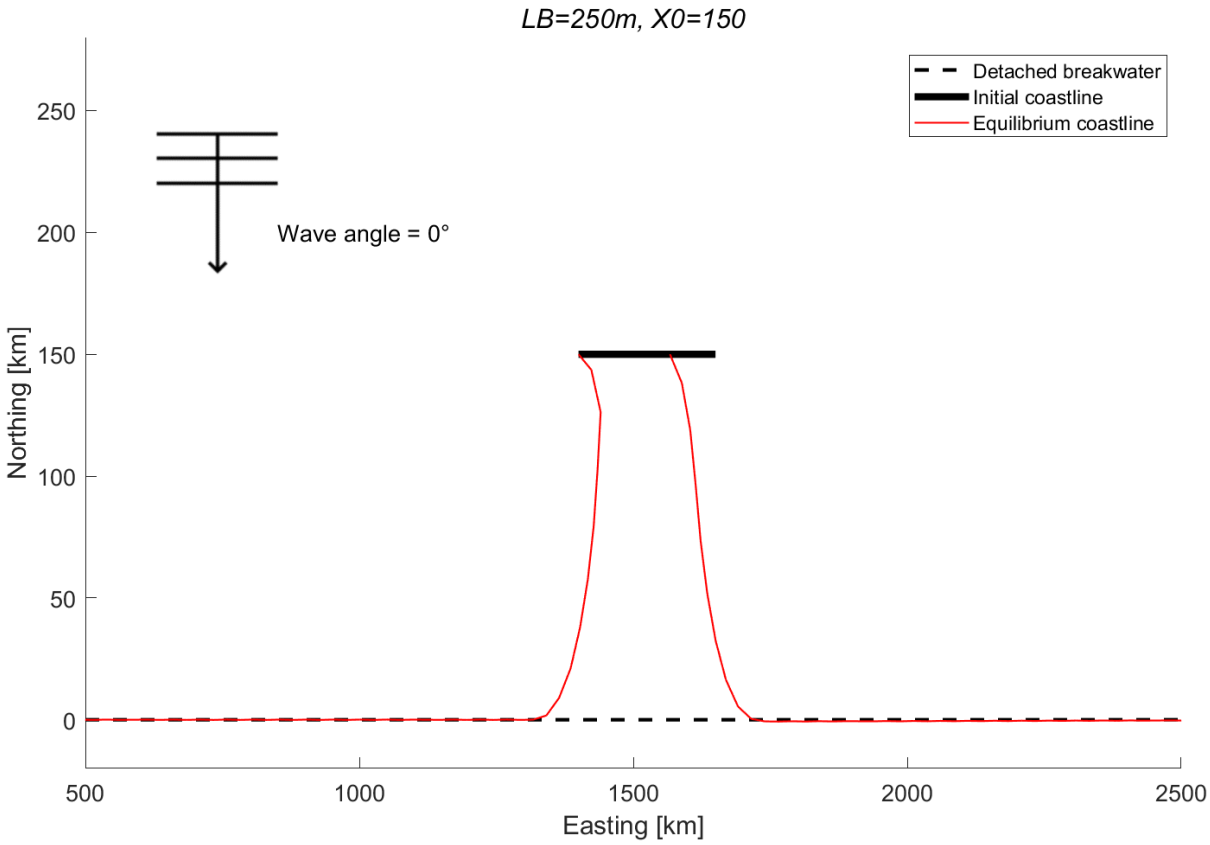
LB=250m, X0=150
Detached breakwater
Initial coastline
Equilibrium coastline
Wave angle = 0°
Northing [km]
Easting [km]
0
50
100
150
200
250
500
1000
1500
2000
2500

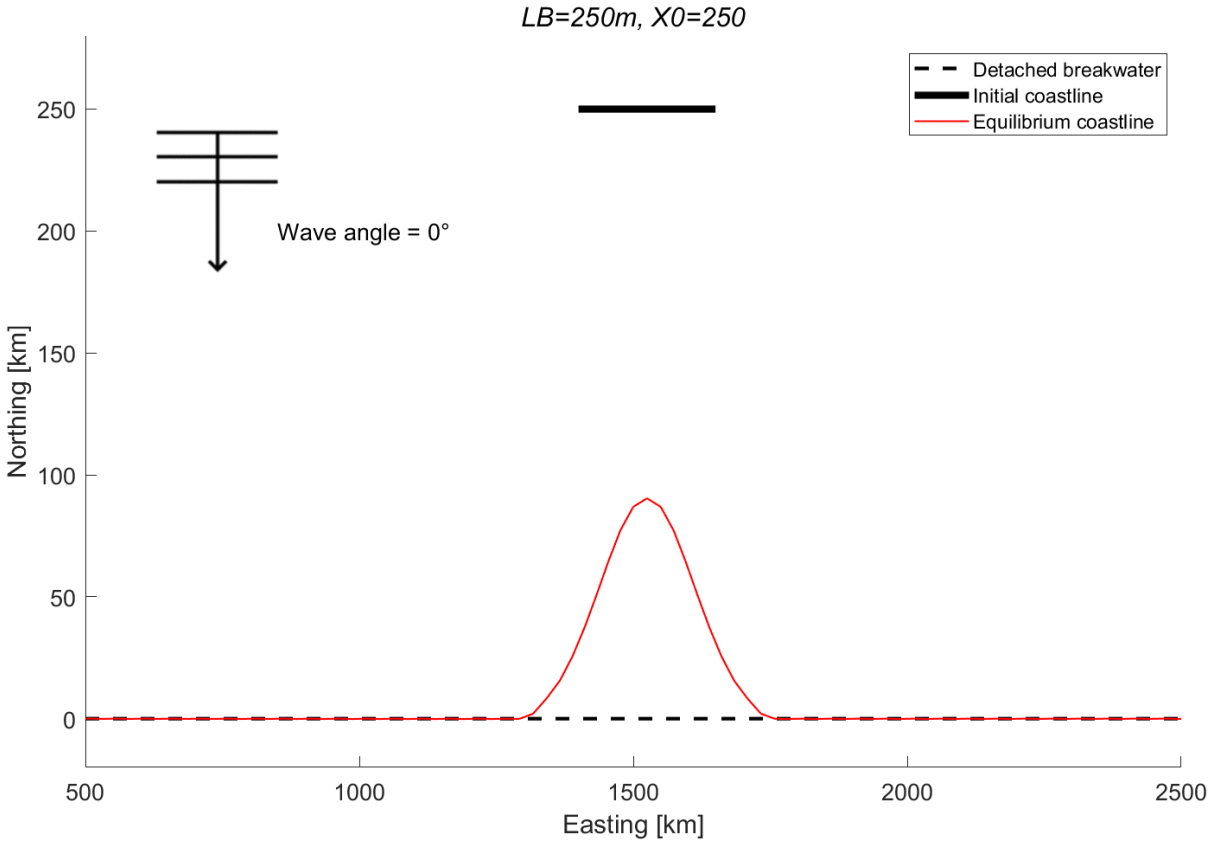
LB=250m, X0=250
Detached breakwater
Initial coastline
Equilibrium coastline
Wave angle = 0°
Northing [km]
Easting [km]
0
50
100
150
200
250
500
1000
1500
2000
2500

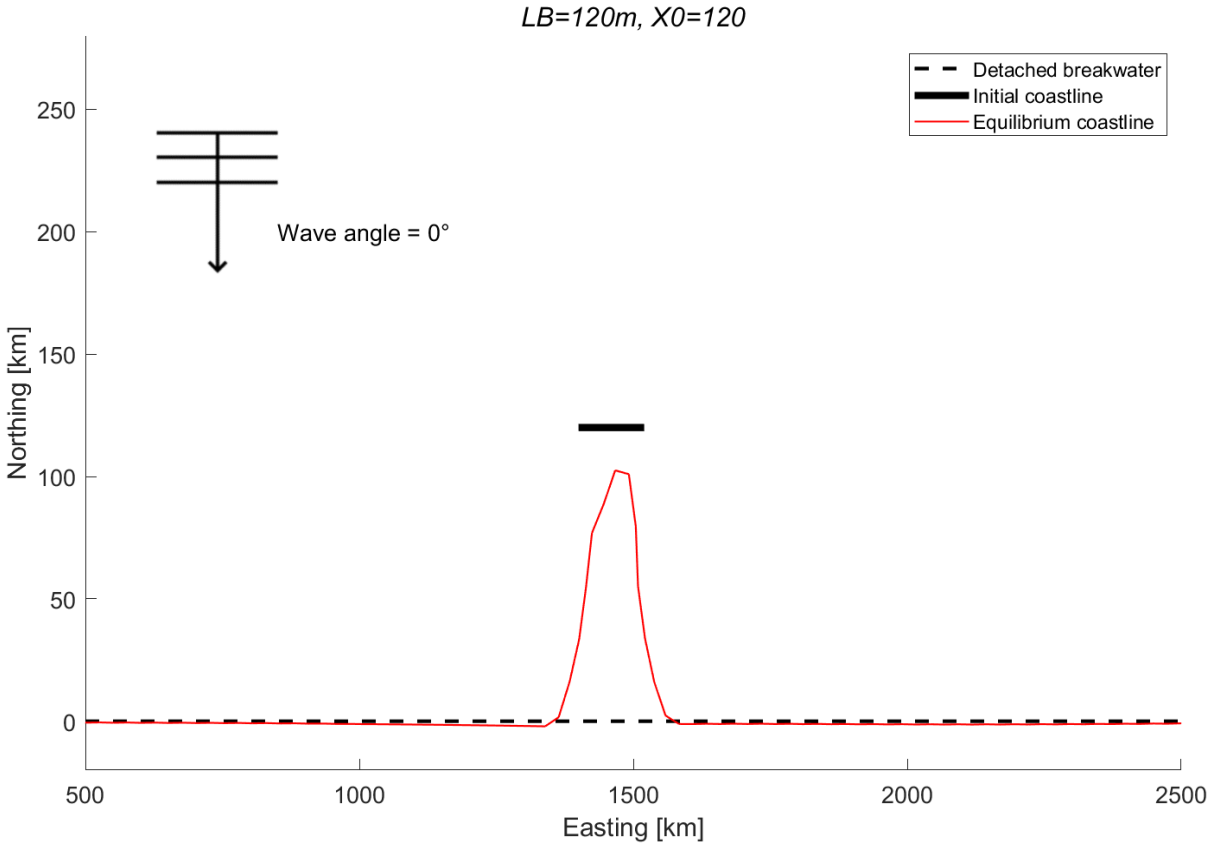
LB=120m, X0=120
Detached breakwater
Initial coastline
Equilibrium coastline
Wave angle = 0°
Northing [km]
Easting [km]
0
50
100
150
200
250
500
1000
1500
2000
2500

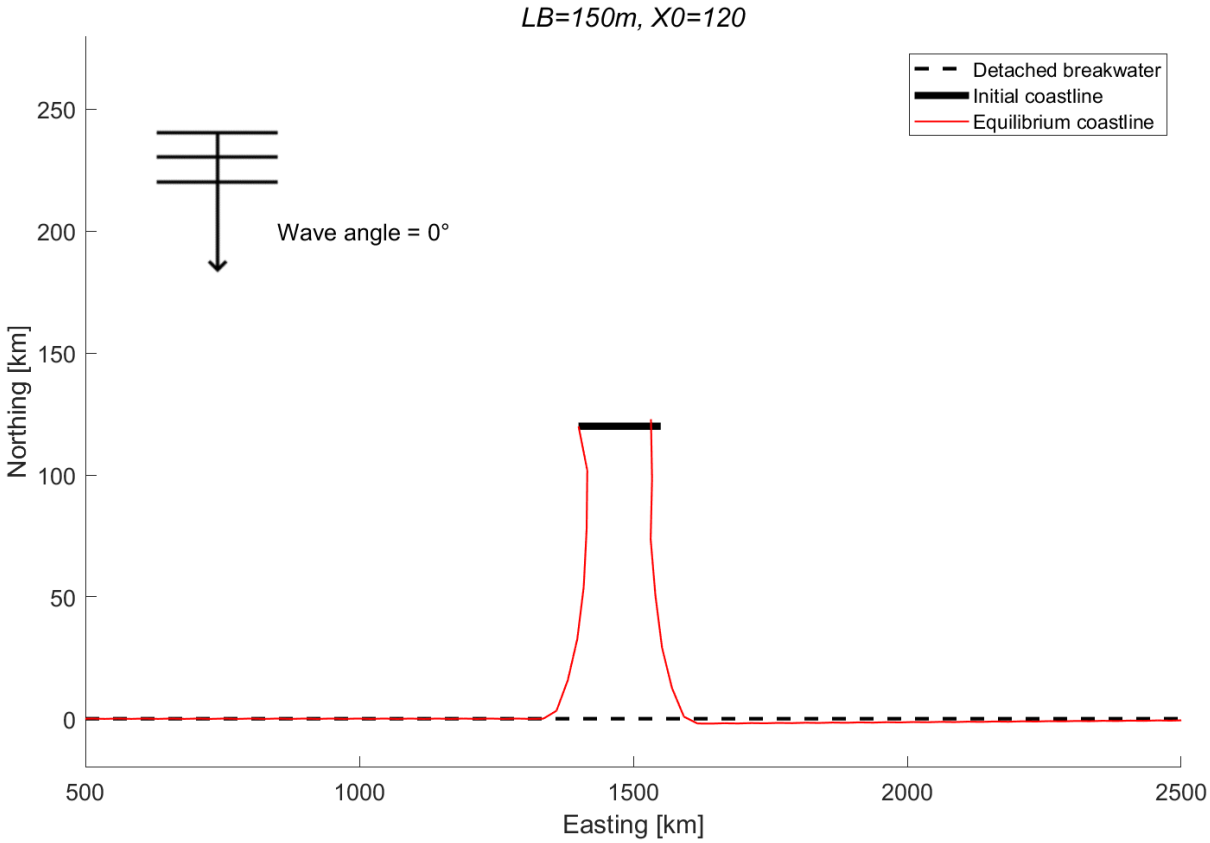
LB=150m, X0=120
Detached breakwater
Initial coastline
Equilibrium coastline
Wave angle = 0°
Northing [km]
Easting [km]
0
50
100
150
200
250
500
1000
1500
2000
2500

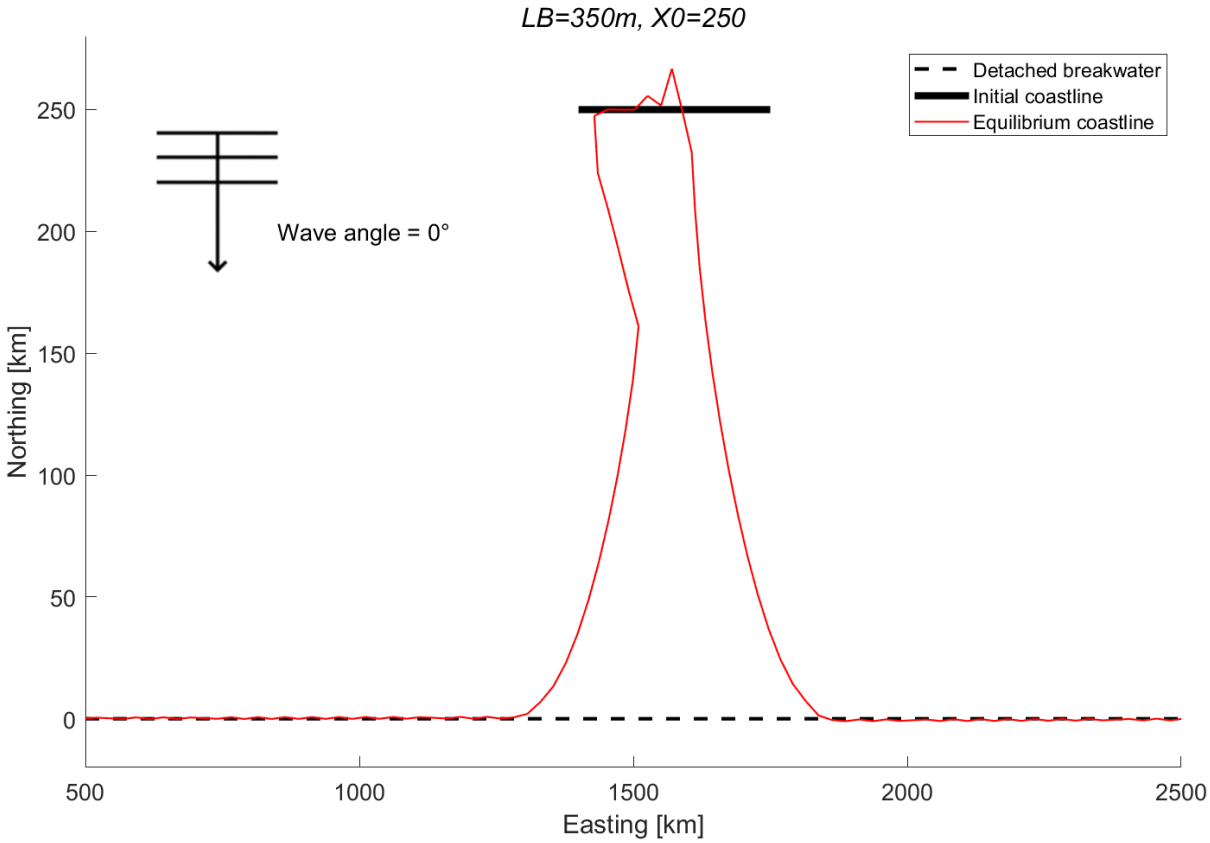
LB=350m, X0=250
Detached breakwater
Initial coastline
Equilibrium coastline
Wave angle = 0°
Northing [km]
Easting [km]
0
50
100
150
200
250
500
1000
1500
2000
2500